An investigation into the mechanisms underpinning the pH-sensitivity of GLP-1 release from the enteroendocrine cells of the gut

Philippa Garbutt
Queen's College
Supervisors: Prof Heidi de Wet
and Prof Pawel Swietach

Submitted in fulfilment of the requirements for the degree of Master of Science by Research in
Physiology, Anatomy and Genetics

University of Oxford
Trinity Term 2023

Declaration

I, Philippa Garbutt, declare as follows:

1. That the work described in this thesis has not been submitted to the University of Oxford, or any other tertiary institution, for purposes of obtaining an academic qualification, whether by myself or any other party.
2. That I performed the entirety of the laboratory work presented as results in this thesis.
3. That the thesis I am submitting is entirely my own work except where otherwise indicated.



Philippa Garbutt Date: 03/10/2023

Intracellular mechanisms underlying pH-dependent GLP-1 release in GLUTag cells

Philippa Garbutt

Queens College

Master of Science by Research in Physiology, Anatomy, and Genetics

Trinity Term 2023

Abstract

GLP-1 is a gut hormone primarily secreted from the enteroendocrine L-cell in response to a meal. GLP-1 acts to potentiate insulin secretion from pancreatic beta-cells and suppress appetite through actions on POMC and NPY neurons in the PVN. Reports of a lower average gut pH in obese and diabetic patients, prompted a preliminary investigation into the pH dependence of GLP-1 release. Work from our laboratory has shown that GLP-1 secretion is pH dependent when using a non-physiological HEPES buffering system. To further dissect the underlying mechanisms of pH-dependent GLP-1 secretion, the pH sensitive ratiometric dye, cSNARF1, was used to visualize the extra- to intracellular pH relationship in GLUTag cells, a model L-cell line, I show that, comparable to other cell lines, pHi of GLUTag cells is slightly more acidic and directly responded to changes in pHo. Decreasing extracellular [Cl^-] or [HCO_3^-] resulted in significant intracellular alkalinisation, demonstrating a significant role of the proton-loading anion exchanger (AE) for pH regulation in GLUTag cells. Using a FRET-based and ELISA assay, the pH-dependence of GLP-1 secretion was confirmed in both CO_2/HCO_3^- buffered and HCO_3^--free (HEPES) media despite inconsistent pHi regulation. Furthermore, I show that, specifically, the rate of GLP-1 secretion is markedly lower in acidic conditions. Considering the multifactorial nature of multiple mechanisms for both intracellular pH regulation and GLP-1 secretion, more sophisticated methods will be required to robustly investigate in real time the underlying pH-dependent intracellular mechanisms which impact GLP-1 secretion from gut enteroendocrine cells.

Acknowledgements

I would like to give my utmost thanks to both my supervisors, Heidi de Wet and Pawel Swietach, for all their support and guidance that made all the work over the year possible. I would like to thank members of the Swietach lab, in particular Johanna Michl, who was extremely generous in providing me with technical training and significant assistance throughout my project. As well, I am grateful to Gosia Cyranka, a member of the de Wet lab, for sharing her extensive knowledge and work in GLUTag cells, of which this thesis has fundamentally depended on.

Table of Contents

Declaration ..... *ii*

Abstract ..... *iii*

Acknowledgements ..... *iv*

List of Figures ..... *ix*

List of Tables ..... *xi*

Abbreviations ..... *xii*

1 Introduction *1*

1.1 Enteroendocrine cells and gut hormones **1**

1.2 Gut hormones in health and disease **2**

1.4 Stimulation secretion coupling of GLP-1 ..... **6**

1.5 GPCR regulation of GLP-1 secretion **8**

1.6 Glucose-stimulated GLP-1 secretion **11**

1.7 Mechanisms of GLP-1 production **13**

1.8 Physiological variation in gut pH **15**

1.9 Gut pH and pathology **16**

1.10 Work preceding this study: **17**

1.10.1 Extracellular pH effects GLP-1 secretion 17

1.10.2 Role of ions for the pH-sensitivity of GLP-1 secretion 18

1.10.3 pH-sensitivity of GLP-1 exocytosis 21

1.11 Research hypothesis and aims **22**

2 Materials and Methods 23

2.1 Cell Culture of GLUTag cells 23

2.2 Coating tissue culture dishes with Poly-L-lysine 23

2.3 pH and condition specific medium 24

2.1 Table of secretion buffer recipes used in experiments. (a) CO_2/HCO_3^- based medium and (b) HEPES based medium 25

2.1.2 [HCO_3^-] required for target pH in CO_2/HCO_3^- based medium 26

2.4 Cell viability analysis using SRB 26

2.5 Glucagon-like peptide 1 (GLP-1) secretion experiments 26

2.6 Glucagon-like peptide 1 (GLP-1) detection 27

2.7 pH_i measurements 27

2.8 tPA-Dendra2 plasmid transformation and extraction 28

2.9 Plasmid sequencing 28

2.10 Plasmid transfection 29

2.11 Live cell imaging 29

2.12 Western blot 29

2.2 Antibodies used for Western Blot 30

2.13 Immunofluorescence 30

2.3 Antibodies used for immunofluorescence 31

2.14 Statistical Analysis 31

3 Regulation of intracellular pH in GLUTag cells 32

3.1 Introduction **32**

3.1.1 Acid-extruders **32**

3.1.2 Proton-loaders **34**

3.1.3 Cellular medium composition and pH regulation **34**

3.2 Methods **35**

3.3 Results **36**

3.3.1 Regulation of intracellular pH in GLUTag cells 36

3.3.2 Influence of extracellular HCO_3^- on pH regulation 37

3.3.2 Influence of extracellular Cl^- on pH regulation 38

4 Influence of pH on GLP-1 secretion from GLUTag cells 45

4.1 Introduction **45**

4.2 Results **47**

4.2.1 Standard [GLP-1] calibration 47

4.2.2 Extracellular pH influences GLP- 1 secretion 48

4.2.3 pH-dependence of total GLP-1 secretion 50

51

4.2.4 Influence of extracellular Cl^- on pH dependent GLP-1 secretion **51**

4.2.6 Rate of GLP-1 degradation is not affected by pH 54

4.2.7 Influence of mTOR signalling on pH-dependent GLP-1 secretion 55

4.2.8 Cell viability controls 56

4.3 Discussion **57**

5 Visualisation of intracellular GLP-1 in GLUTag cells 67

5.1 Live-cell imaging of intracellular GLP-1 with tPA-Dendra2 67

5.1.1 Plasmid transfection 70

5.1.3 Troubleshooting 74

5.1.4 GLP-1 assay of tPA-Dendra2 transfected cells 75

5.1.5 Sequencing tPA-Dendra2 plasmid 76

5.1.6 Co-localisation of tPA-Dendra2 with anti-GLP-1 76

5.2 Fixed-cell imaging of intracellular GLP-1 77

5.2.1 Method 78

5.2.1 Results 80

5.3 Discussion 81

6 General discussion and conclusion 85

Reference 91

Appendix 103

tPA-Dendra2 sequence 103

Supplementary Code 1: 109

List of Figures

Figure	Title	Page No.
Figure 1.1	Figures of gut epithelium localising enteroendocrine cells.	1
Figure 1.2	Summary of the metabolic effects of GLP-1.	5
Figure 1.3	Summary of L-cell lipid stimulated GLP-1 secretion.	8
Figure 1.4	Summary of L-cell protein stimulated GLP-1 secretion.	**9**
Figure 1.5	Summary of L-cell glucose stimulated GLP-1 secretion.	11
Figure 1.6	Physiological pH profile of the human GI tract.	14
Figure 1.7	GLP-1 secretion from GLUTag cells and murine *ex vivo* primary gut crypt cultures is pH-dependent.	16
Figure 1.8	pH-dependent GLP-1 secretion from GLUTag cells is independent of extracellular Na^+ and dependent on extracellular Cl^-.	18
Figure 3.1	Diagram of the sensors and regulators of intracellular pH homeostasis.	30
Figure 3.2	Representative image of GLUTag cells loaded with SNARF-1 imaged with Cytation plate reader.	33
Figure 3.3	GLUTag cell intracellular pH regulation in CO_2/ HCO_3^--based media.	34
Figure 3.4	Intracellular pH regulation in HCO_3^--free (HEPES-based) media.	35
Figure 3.5	Intracellular pH regulation in CO_2/ HCO_3^--based media where gluconate ions replace osmolarity regulating excess Cl^-.	36

Figure 4.1	GLP-1 concentration standard curve for FRET-based assay	43
Figure 4.2	pHo dependence of active GLP-1 secretion from GLUTag cells in CO_2/ HCO_3^--based media and HCO_3^--free (HEPES-based) media.	45
Figure 4.3	pHo dependence of total amidated (active and inactive) GLP-1 secretion	46
Figure 4.4	pHo dependence of total amidated GLP-1 secretion in CO_2/ HCO_3^--based media where gluconate ions replace osmolarity regulating excess Cl^-.	48
Figure 4.5	pHo dependence of the rate of active GLP-1 secretion	50
Figure 4.6	pHo dependence of the rate of GLP-1 degradation	51
Figure 4.7	Influence of mTOR signalling.	52
Figure 4.8	GLUTag cell viability following incubation in various conditions.	53
Figure 5.1	tPA-Dendra-2 photoconversion from green to red in GLUTag cells.	66
Figure 5.1.2	Relative change in tPA-Dendra2 fluorescence intensity in 561nm (red) and 488 nm (green) excitation regions	68
Figure 5.1.3	cAMP-stimulated GLP-1 secretion from tPA-Dendra2 transfected GLUTag cells	70
Figure 5.1.4	Fixed cell imaging of tPA-Dendra2 transfected GLUTag cells with anti-GLP1 immunolabelling.	71

Figure 5.2.1	Fixed cell imaging of GLUTag cells with anti-GLP1 immunolabelling and example of quantified immunofluorescence intensity output	73
Figure 5.2.2	Quantified fluorescence intensity of anti-GLP-1 from GLUTag cells	74
Figure 6.1	Summary of pH sensing mechanisms and glucose-stimulated GLP-1 secretion in L cells.	83

List of Tables

Table	Title	Page No.
Table 2.1	Table of secretion buffer recipes used in experiments.	22
Table 2.1.2	[HCO_3^-] required for target pH in CO_2/ HCO_3^--based medium.	23
Table 2.2	Antibodies used for Western Blot.	27
Table 2.3	Antibodies used for immunofluorescence.	28

Abbreviations

AE	Anion exchanger
BMI	Body mass index
cAMP	Cyclic adenosine monophosphate
CA	Carbonic anhydrase
CaSR	Ca^{2+}-sensing receptor
cSNARF1	Carboxy SNARF-1
DMEM	Dulbecco's Modified Eagle Medium
EEC	Enteroendocrine cell
FFA	Free fatty acid
fsk	Forskolin
Gcg	Preproglucagon gene
GRPP	Glicentin-related polypeptide
GI	Gastrointestinal
GLP-1	Glucagon-like peptide 1
GLP-1R	Glucagon-like peptide 1 receptor
GIP	gastric inhibitory polypeptide
GPCR	G-coupled protein receptor
HTRF	Homogeneous Time-Resolved Fluorescence
IBD	Inflammatory Bowel Disease
IP_3	Inositol triphosphate
K_{ATP}	ATP-sensitive potassium channels

LDCV	Laser scanning confocal microscopy
LSCM	Large dense core vesicle
PAFP	Photoactivatable fluorescent protein
PC	Prohormone convertase
PDE	Phosphodiesterase
pHi	Intracellular pH
pHo	Extracellular pH
PLC	Phospholipase C
NBC	Na^+-coupled HCO_3^- transporters
NHE	Na^+/ H^+ exchangers
SCFA	Short chain fatty acids
SGLT-1	Na^+-coupled glucose co-transporter
SNARE	Soluble N-ethylmaleimide–sensitive factor attachment protein receptor
SNAT2	Na^+-dependent neutral amino acid transporter 2
TAS1R3	Takeda G protein-receptor-5
TGR5	Taste receptor type 1 member 3
TIRF	Total internal reflection fluorescence
T2D	Type-2 diabetes
tPA	Tissue-type plasminogen activator
TGN	Trans Golgi Network
V-ATPase	ATP-dependent proton pump

1 Introduction

1.1 Enteroendocrine cells and gut hormones

Enteroendocrine cells (EECs) are specialised cells found scattered across the gastrointestinal (GI) tract, accounting for 1% of the gut lining epithelial, Fig1.1[5]. EECs are responsible for the production and release of gut hormones in response to meal-related stimuli[6] - including the quantity and composition of nutrients. The actions of gut hormones are system-wide, and gut hormone activated receptors are expressed in a large variety of tissues and organs, both within and outside the gastrointestinal tract[7]. Generally, the actions of gut hormones involve energy regulation and metabolic homeostasis, such as blood glucose regulation[8], controlling food intake[9], modulating gut motility[10], and gall bladder contraction[11].

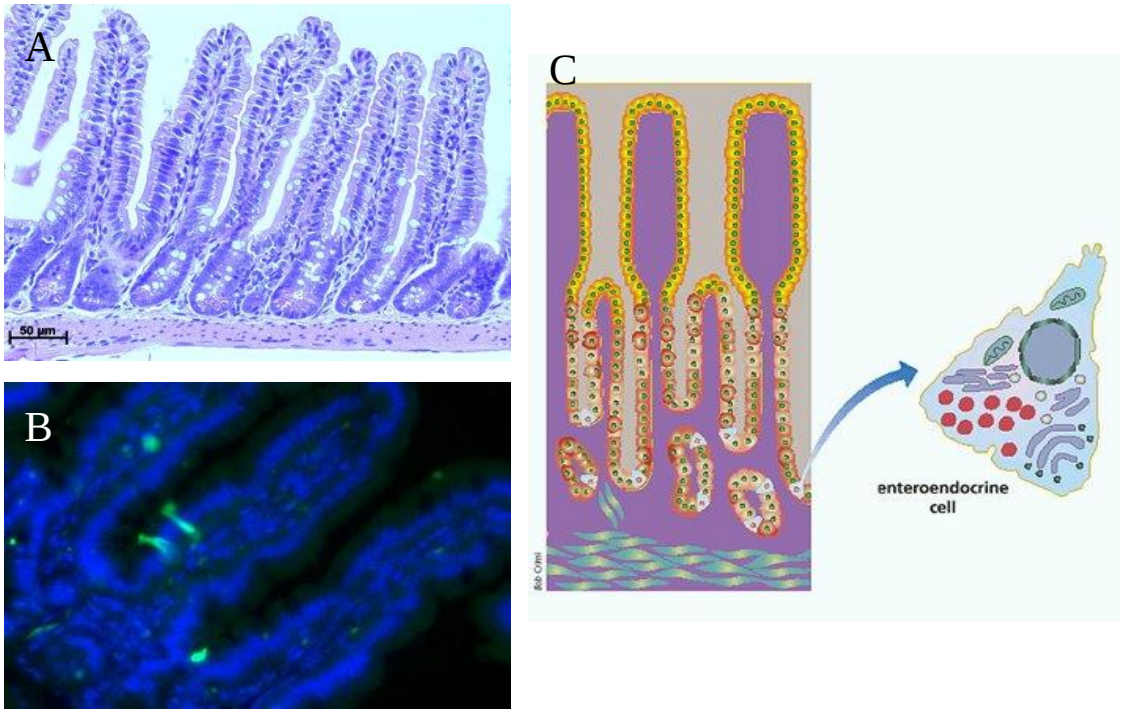


Figure 1.1 Gut epithelium of the small intestine, with visualized L-cells. A) A longitudinal section of murine small intestine epithelium, H&E staining. B) small intestine epithelium of GLUVenus mice, expressing YFP under transcriptional control of the preproglucagon promoter, showing L-cells in green. C) schematic diagram of enteroendocrine cells within the gut epithelium. Images from the de Wet laboratory.

At least 12 subtypes of EECs have been identified, and over 30 genes encoding gut hormones are known to be expressed[12]. The initial 'one cell type, one hormone' idea was found to be incorrect following the advent of single cell sequencing technologies, which demonstrated that EEC gut hormone expression is fluid[13]. Nevertheless, cell-types are generally associated with recognizable peptide secretion patterns and subpopulations characterised by their location along the GI tract[13].

1.2 Gut hormones in health and disease

Obesity is a chronic disease and a major public health concern, costing the NHS over £6 billion annually[14]. Obesity is clinically classified as an individual with body mass index (BMI) ≥ 30 kg/m^2, and qualitatively defined by the World Health Organization as 'abnormal or excessive fat accumulation that may impair health'[15]. The development of obesity is fundamentally caused by a chronic imbalance between energy intake and expenditure[15]. Although the mechanisms underlying obesity are not completely understood, a complex interaction between genetic, environmental, and psychological factors are thought to influence an individual's predisposition to developing the disease[15]. Inflammatory and metabolic pathophysiology changes associated with excessive adipose tissue hypertrophy dramatically increases an individual's risk of developing many non-communicable diseases[16]. This includes Type-2-diabetes mellitus (TD2M), with 90% of T2DM adults classified as overweight or obese[14]. Fundamentally caused by the dysregulation of glucose homeostasis[16], the disease can progress to life-threatening complications, such as cardiovascular disease, blindness, kidney failure and amputation[17]. It is well known that abnormalities of insulin secretion and/or action underlie the hyperglycaemic profile of TD2M patients[16]. However, treatment strategies remain

challenging, mostly attributable to suboptimal patient adherence to antidiabetic therapies (e.g. weight loss and exercise programmes) and therapeutic inertia[18].

Insulin is a key regulatory hormone for glucose homeostasis, acting to decrease blood glucose levels by promoting glucose uptake and glycogenesis in muscle and adipose tissue[19]. In pancreatic β-cells, insulin secretion occurs directly in response to plasma glucose via mitochondrial ATP production causing inactivation of the ATP-sensitive K^+-channel (K_{ATP}) and subsequent depolarisation[20]. Additional regulation of β-cell function is provided by stimuli such as other nutrients, hormones and neurotransmitters[21]. These stimuli mostly act via G-coupled protein receptors (GPCR). For example, the GLP-1 receptor (GLP-1R) is a $G_{s\alpha}$-coupled receptor, which when activated potentiates insulin release via cAMP-dependent pathways, such as modulating K_{ATP} channel activity and cytoplasmic Ca^{2+} levels via endoplasmic reticulum release[21]. Interestingly, insulin secretion following oral glucose administration is significantly greater than secretion following intravenous glucose administration[22]. This finding demonstrates the importance of GI tract glucose detection, stimulating the release of insulin-regulating stimuli, such as incretin hormones. Specifically, a significant role of gastric inhibitory polypeptide (GIP) and glucagon-like peptide-1 (GLP-1) has been identified following infusion of synthetic hormone analogues shown to augment insulin responses to intravenous glucose in human subjects[23]. However, unlike GIP, the insulinotropic effect of GLP-1 is shown to be preserved in patients with T2DM, thus has been identified as a potential therapeutic target[24].

Despite some ambiguity, dysregulation of hormones and downstream signal transduction cascades involved in energy and glucose metabolism are thought to play a key part in the

metabolic disturbances seen in obesity. Individuals who suffer from obesity tend to display irregular pre- and postprandial gut hormone regulation[9]. However, interpretation of this data is complicated by findings contradicting classical understandings of most gut hormones. For example, when assessing plasma levels of the hunger-stimulated gut hormone, ghrelin, obese individuals, who often report feeling hungry all the time, had lower fasting levels compared to lean subjects[25]. However, the pathophysiology of the anorexigenic gut hormone investigated in this study, glucagon-like-peptide 1 (GLP-1), in obesity seems clearer. GLP-1 is an incretin hormone released in response to the arrival of digested food in the duodenum. Although best known for its role as an incretin hormone which potentiates post-prandial insulin release, the hormone has many direct and indirect effects on metabolism, as outlined in Fig1.2. Crucially, GLP-1 acts to suppress appetite, via stimulation of the hypothalamic anorexigenic neuronal population (POMC/CART neurones)[22].

Evidence has shown the GLP-1 response to oral glucose is reduced in pre-diabetic and obese individuals[26]. Furthermore, the significant metabolic improvements of patients who undergo bariatric surgery, such as gastric bypass, sleeve gastrectomy, and gastric band, is in part attributed to GLP-1 plasma increases[27]. Such findings paved the way for significant progression of drug therapy for weight loss and T2D. GLP-1 receptor (GLP-1R) agonists have repeatedly shown significant weight loss and improved glucose homeostasis in obesity and T2D patients[28,29]. The STEP1 clinical trial testing the latest GLP-1 analogue, semaglutide, reported that obese participants lost on average 12% more of their body weight compared to placebo[30]. In fact, the drug was recommended in the 2023 NICE guidelines as an option for weight management. Furthermore, semaglutide has shown cardioprotective effects exceeding those of dietary weight loss, such as improving

cardiometabolic profile, cardiac structure and cardiac function[31], reported in the SELECT trial to reduce major adverse cardiovascular events by 20%[32]. However, anti-obesity agents, such as semaglutide, have many adverse effects, such as nausea, constipation and gallstones[33], and regarding weight loss are non-comparable to bariatric surgery[34].

1.3

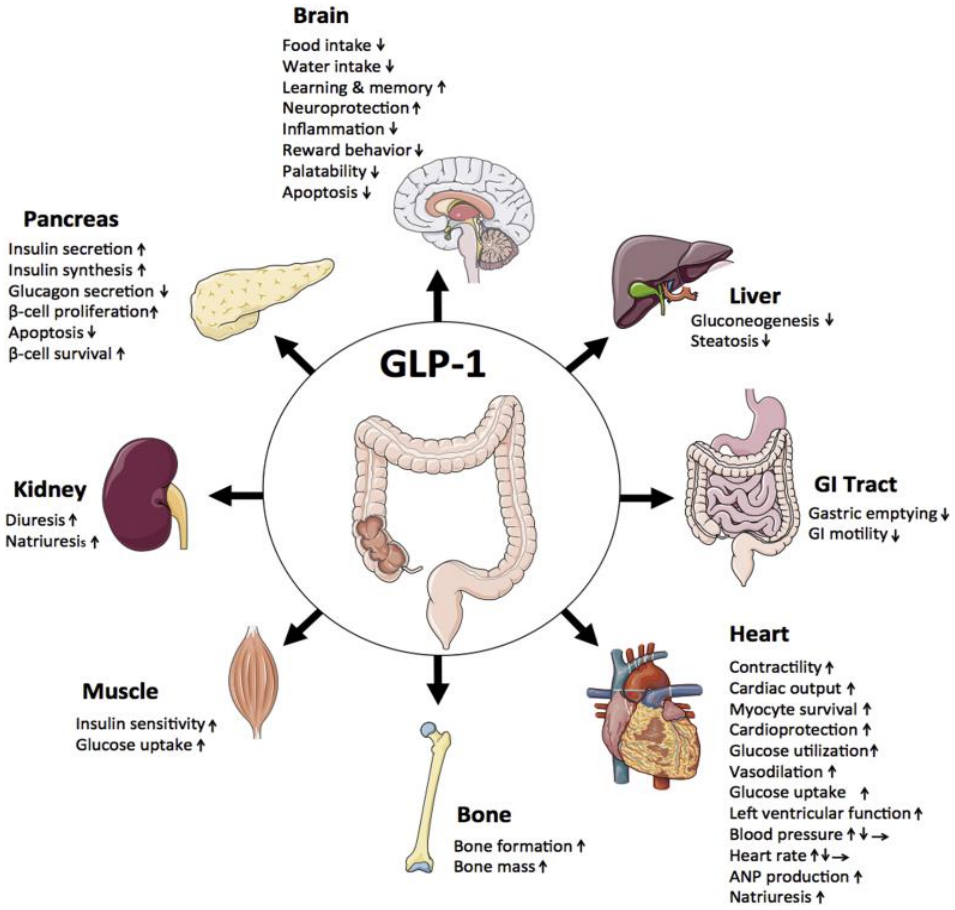


Figure 1.2 Summary of the metabolic effects of GLP-1
Taken from Muller, T.D., *et al.* Glucagon-like peptide 1 (GLP-1). *Mol Metab* **30**, 72-130 (2019).[1]

Physiology of GLP-1 secretion

The enteroendocrine L-cell is associated with the production and secretion of hormones expressed by the preproglucagon gene (*Gcg*)[22], including GLP-1[35]. L-cells are predominantly located at the distal part of the small intestine and colon, making up approximately 14% of the EEC population in the rectum[6]. They are described as cone-

shaped, open-type epithelial cells, with micro-villi protruding the apical surface facing the gut lumen. They directly detect post-prandial increases of nutrients, triggering GLP-1 secretion at the basal end in close proximity to neurones and intestinal microvasculature[36-38] (Fig 1.2). More recent work using 3D electron microscopy has shown that EECs are complex displaying features previously only attributed to neurones, including an axon-like feature, named a 'neuropod', shown to guide hormone secretion[39]. EECs appear to form direct connections to enteric glia with neuronal synapse characteristics (clear secretory vesicles)[39], forming a neuroepithelial circuit with afferent and efferent nerve pathways[12]. As such, it is now recognised that bidirectional brain-gut axis connections may also play an important role for homeostatic gut function[12].

1.4 Stimulation secretion coupling of GLP-1

Several molecular mechanisms have been proposed to link nutrient exposure to GLP-1 secretion, including neural, endocrine, and paracrine[40,41]. Following food ingestion, as L-cells are predominantly located in the lower intestine, the initial rapid rise in GLP-1 is thought to be stimulated by a neural reflex or circulating factors[42,43]. In rats, it has been shown that nutrient triggered release of GIP in the proximal gut can trigger GLP-1 secretion via a pathway mediated by the vagus nerve[44]. However, there is uncertainty about the physiological significance of the GIP-GLP-1 axis in humans. In healthy and T2D individuals, intravenous infusion of GIP failed to stimulate GLP-1 secretion. It is now recognised in the human duodenum, L-cells are at a sufficient density to account for early postprandial GLP-1 release[45]. Nonetheless, the close proximity of L-cells to enteric neurons and microvasculature supports a potential role of neuronal and endocrine regulation[36,37]. Furthermore, activation of cholinergic and β-adrenergic receptors was

shown to stimulate GLP-1 secretion in isolated perfused rat intestines[46-48] and human NCI-H716 cells (L-cell line)[47]. A potential paracrine relationship exists between L-cells and the somatostatin secreting D-cells, as speculated by the expression of the somatostatin receptor *Sstr5* in GLP-1 immunoreactive cells[49]. However, the enteroendocrine system is recognised to have functional redundancy[50]. Various gut hormones can activate receptors specific to others with low efficacy[50], and combined with the metabolic flexibility and complexity of endocrine, autocrine, and paracrine gut hormone signalling, makes data traditionally generated by single cell or isolated organoids, such as islets, difficult to interpret. Taken the proven system wide effect of gut hormones, future work should focus on whole organisms and integrated physiological systems, if we are to make progress in understanding the complexities of GLP-1 secretion and pathophysiological impairments in obesity.

Nevertheless, once food has reached the distal GI tract, direct sensing of nutrients from *Gcg* expressing EECs, such as L-cells, is thought to drive the prolonged, second phase release of GLP-1 into circulation[51,52]. Previous studies have identified a wide variety of secretagogues that are capable of stimulating GLP-1 secretion from L-cells, including sugars, amino acids and lipids from dietary sources[53]. In human subjects, sugar and protein ingestion was shown to stimulate a circulating GLP-1 peak at 30-60 mins, whereas a later and prolonged increase was observed following lipid intake[42]. Results demonstrate the presence of multiple stimulation-secretion pathways for L-cells to regulate postprandial GLP-1 circulatory levels.

1.5 GPCR regulation of GLP-1 secretion

For most nutrients other than glucose, specific G-coupled protein receptors (GPCR) at the apical surface of L-cells directly sense increases in the GI lumen, triggering downstream signalling, such as Ca^{2+} and/or cyclic adenosine monophosphate (cAMP) pathways[54]. Mostly at the basolateral side of the L-cell, metabolites of nutrients, such as lipids and proteins, are detected following epithelial absorption[55].

A wide range of short and long chain free fatty acids (FFA) have been shown to induce GLP-1 secretion in *in vitro*[56] and *in vivo*[57] studies. Interestingly, in healthy and T2D individuals, studies have reported GLP-1 responses were higher after ingestion of meals high in unsaturated fatty acids (olive oil) compared to saturated fats (butter), suggesting a relationship between fatty acid composition and the incretin response[58,59]. Multiple FFA receptors have been identified in GLP-1 secreting EECs, such as GPR43, GPR120 and GPR40[56]. Induction of GLP-1 secretion by FFA seems to occur via a Ca^{2+} dependent

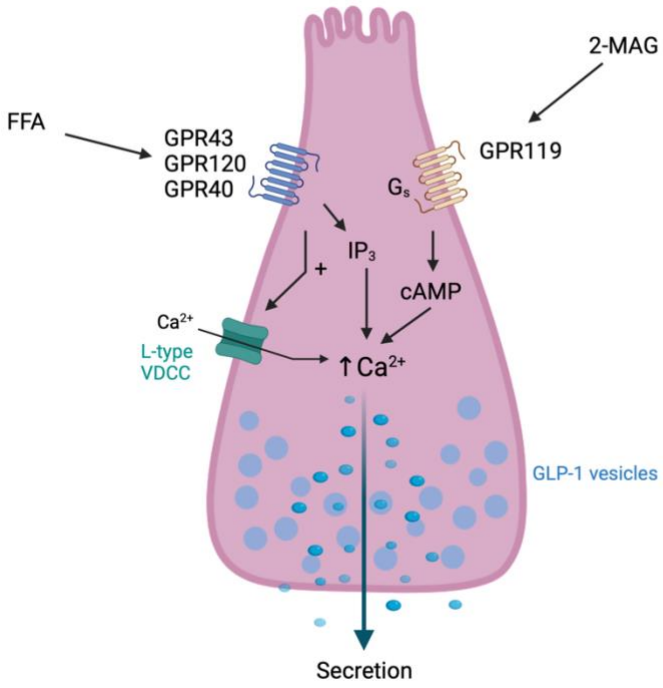


Figure 1.2 Summary of L-cell lipid stimulated GLP-1 secretion.

pathway[60], with receptor activation inducing an increase in intracellular Ca^{2+} influx via cell-surface Ca^{2+} channels[56]. Another triglyceride metabolite, 2-MAG, has also been shown to stimulate GLP-1 secretion by activation of the G_s-coupled GPR119 receptor[61,62] (Fig1.2)

The significant role of protein and amino acid stimulation for GLP-1 secretion is well established in L-cell cultures[63,64] and in *in vivo* murine[65] and human[66] studies. This stimulatory effect has been observed with a number of proteins, including whey, casein[64], and gluten[67], and amino acids such as glutamine[68], glycine[69] and leucine[64]. One study reported observations of protein-sensing pathways for GLP-1 secretion in L-cells, mediated by the proton-coupled peptide transporter-1 (PEPT1) and activation of the Ca^{2+}-sensing receptor (CaSR)[70]. Amino acids and small peptides have even been reported to directly activate CaSR signalling to stimulate GLP-1 secretion[71]. Belonging to GPCR family C group 2, CaSR induces increases of intracellular Ca^{2+} via signalling pathways, such as phospholipase C (PLC) and inositol triphosphate (IP3), stimulating GLP-1 exocytosis[72].

Whilst CaSR appears to be more sensitive to L-aromatic amino acids[72], the closely related GPCR family C group 6 subtype A (GPRC6A) binds to basic amino acids, such as L-arginine, L-lysine, and L-ornithine, stimulating GLP-1 secretion via a similar G_q coupled receptor signalling pathway[73]. (Fig1.3) As a major product of protein digestion, robust evidence supports the role of glutamine to trigger and potentiate GLP-1 secretion. In primary murine colonic cultures, glutamine is shown to elevate both cAMP levels and cytosolic Ca^{2+} in L-cells[68]. However, whilst removal of extracellular Na^{+} attenuated the Ca^{2+} response, the glutamine-triggered cAMP rise was not prevented. Microelectrode measurements have recorded glutamine-triggered membrane depolarisation[74], proposed to

be driven by Na^+-coupled electrogenic uptake via the sodium-dependent neutral amino acid transporter 2 (SNAT2, SLC38 family)[68]. The precise molecular mechanism of L-glutamine-induced increases in cAMP has not fully been elucidated, thought recent findings suggest that the GPCR taste receptor type 1 member 3 (TAS1R3) may be important[75]. Nonetheless, the glutamine-mediated GLP-1 response appears to compromise two components: increased cAMP signalling and increased cell excitability (Fig1.3).

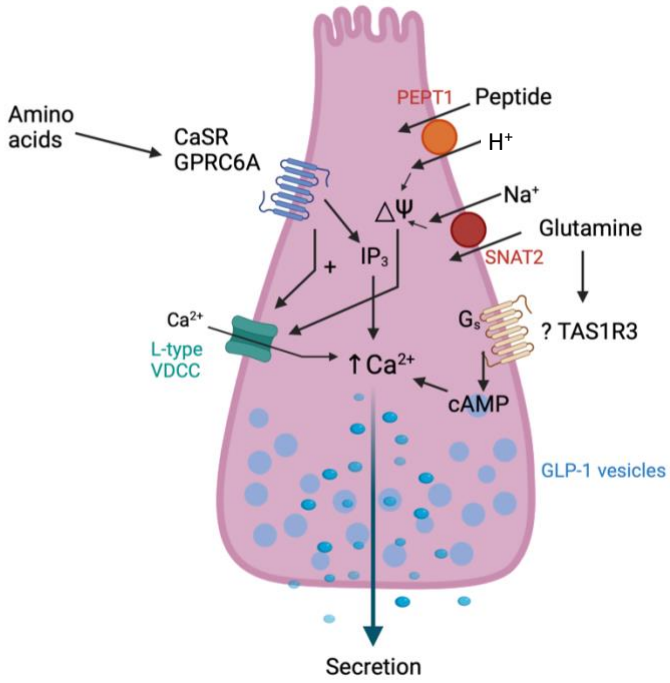


Figure 1.3 Summary of L-cell protein stimulated GLP-1 secretion.

Other stimulation-secretion loops have also been identified to regulate L-cell function. Bile acids have been recognised to stimulate GLP-1 secretion from L-cells via activation of the Takeda G protein-receptor-5 (TGR5)[76]. Immunofluorescence co-staining showed significant co-localisation of GLP-1 and TGR5 in the rat intestine[77], as well as treatment of a TGR5 agonist in murine increasing GLP-1 secretion[78].

Recent investigations have also shed light on the potential significance of the gut microbiota in shaping the function of enteroendocrine cells, including GLP-1 secretion regulation[79]. The gut microbiome's impact on gut peptides is thought to primarily involve the production and signalling of microbial metabolites which activate enteroendocrine GPCRs[80]. For instance, the Coriobacteriaceae population has been identified as a facilitator of GLP-1 secretion through the synthesis of bile acid metabolite agonists to TGR5[81]. Additionally, short-chain fatty acids (SCFA), generated through bacterial fermentation of fibre, have been revealed to modulate GLP-1 secretion via the activation of cell surface receptors[79].

Crucially, an expanding body of research implicates imbalances in the gut microbiota in the onset of metabolic disorders, including obesity[79,82]. Nevertheless, transformations in specific gut microbiota profiles following obesity or T2D treatment interventions, such as bariatric surgery or pharmacological agents[82], are believed to play a contributory role in elevating GLP-1 levels and ameliorating obesity-induced insulin resistance. Consequently, unravelling the intricacies of how the gut microbiota impacts GLP-1 secretion holds promise for gaining valuable insights into broader mechanisms underlying metabolic diseases, such as T2D and obesity.

1.6 Glucose-stimulated GLP-1 secretion

Whilst collectively, many dietary nutrients contribute to the GLP-1 secretory response, glucose appears to be one of the most effective stimuli for proglucagon-derived peptides in humans and rodents[83]. Similar to pancreatic β-cells[19], direct glucose-sensing in L-cells involves transepithelial transport of glucose into the cells[84]. Several molecular mechanisms responsible for glucose-stimulated GLP-1 secretion have been identified, including K_{ATP}-

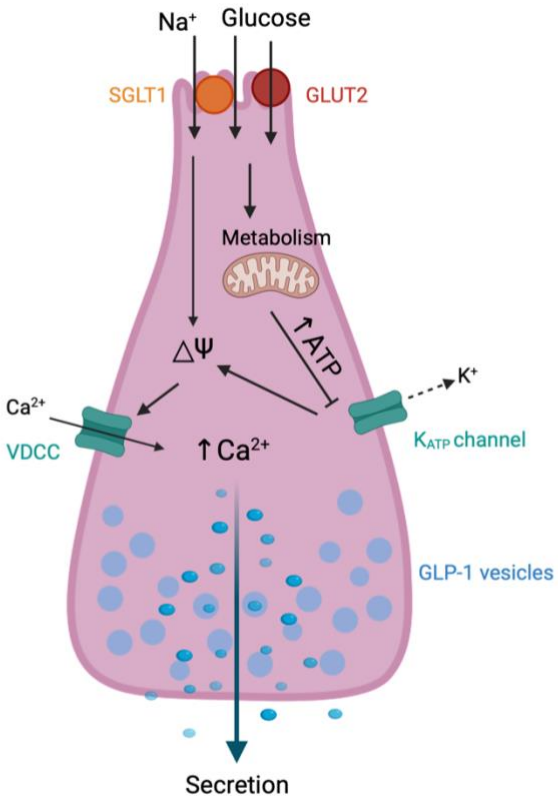


Figure 1.4 Summary of L-cell glucose stimulated GLP-1 secretion.

dependent pathways and taste receptors[40,85-87]. However, the Na^+-coupled glucose co-transporter, SGLT-1 (SLC5A1 family), accounts for a large proportion of glucose-stimulated GLP-1 secretion as shown in both *in vitro* cell lines[88,89] and *in vivo* rat[90,91] and human[92] intestine tissue preparations.

The SGLT-1 couples glucose exposure to GLP-1 secretion via the electrogenic uptake of Na^+ with glucose causing membrane depolarization (Fig 1.4) This consequently opens voltage-gated L-type Ca^{2+} channels causing a transient rise in intracellular Ca^{2+} and triggering GLP-1 vesicular exocytosis[40]. Increases in glucose metabolism and intracellular ATP/ADP ratio has also been linked to membrane depolarization in GLP-1 secreting cells through closure of the ATP-sensitive potassium (K_{ATP}) channels. Glucose uptake in L-cells is mediated by the SGLT-1 and the electroneutral glucose transporter, GLUT2[40]. However, whilst the presence of SGLT-1 inhibitors abolishes intestinal glucose-stimulated GLP-1

secretion, inhibition of GLUT2 only attenuates secretion[90]. It is thought the electrogenic activity of SGLT1 is crucial for glucose-stimulated GLP-1 secretion, with K_{ATP}-channel closure enhancing the response[90].

1.7 Mechanisms of GLP-1 production

The preproglucagon gene (*Gcg*) encodes a number of peptide hormones, including glucagon, glicentin, oxyntomodulin, glicentin-related polypeptide (GRPP), GLP-1 and GLP-2[93]. *Gcg* expression has been identified in pancreatic islets, the GI tract and brain neuronal populations, each demonstrating cell-type specific expression regulation[94]. Within the GI tract, nutrients, including amino acids, fatty acids and glucose, have been shown to upregulate *Gcg* expression[95-98]. Although the precise downstream signalling pathways regulating expression are yet to be confirmed, intestinal *Gcg* expression is thought to mostly be under cAMP control[99].

Following transcription, protein variations of the preproglucagon peptide are processed in a tissue-specific manner via site-specific cleavage by prohormone convertase (PC)[100]. Intestinal endocrine cells express high levels of PC1/3, which are responsible for the cleavage of the proglucagon peptide into active GLP-1 in L-cells[101,102]. Evidence confirms that GLP-1 is processed via PC1/3 cleavage in GLUTag cell, a L-cell model[100,103]. PC1/3 is first synthesised as a 99 kDa preform, undergoing autocatalytic processing first in the endoplasmic reticulum (ER) to generate the mature 87kDa form. In the Trans Golgi Network (TGN), the mature protein undergoes autocatalytic maturation to a truncated 74kDa form then the highly active 66kDa form within dense core secretory granules[104,105]. Within these secretory granules, PC1/3 is co-stored with its prohormone substrates where processing is localised[104]. Active GLP-1 either occurs in an amidated (7-36 amide; 80%)

or glycine-extended (7-37; 20%) form, with the latter predominantly secreted from the ileum[106]. However, the significance of each form is currently unknown.

In response to a physiological stimulus, a series of granular maturation steps ultimately results in the exocytosis of the large dense core vesicle (LDCV), this mechanism is generally referred to as the regulated secretory pathway[105,107]. Electron microscopy has shown the presence of homogenous LDCV at the basolateral side of L-cells[108], as well as secretory granules in GLUTag[87] and NCI-H716 cell lines[109]. Prior to exocytosis, vesicular maturation involves acidification via the ATP-dependent proton pump (V-ATPase)[105,107]. Bafilomycin A1 inhibition of V-ATPase in GLUTag cells was shown to suppress secretagogue-stimulated L-glutamate secretion, which is thought to be stored in secretory granules and secreted with GLP-1[110]. The pump is also associated with regulating insulin secretion in the pancreatic β-cell, as demonstrated by mice with null mutations of the enzyme's α3 isoform displaying attenuated glucose-stimulated secretion responses[111]. It is recognised intracellular pH of organelles are a critical factor for vesicular trafficking and hormone secretion[112]. Collapsing the pH gradient across Golgi membranes was shown to impair posttranslational modifications and processing of secreted proteins, misdirect cargo, and compromise organelle integrity[112]. However, no specific study has investigated the pH of pathway organelles in L-cells for GLP-1 secretion.

Due to their physiological similarities, L-cell GLP-1 secretion is often compared to pancreatic β-cell insulin. Both hormones follow a biphasic secretion pattern[113], with the 1st peak at 1-6 minutes and the 2nd at 7-12 minutes in GLUTag cells following glucose stimulation[114]. β-cell insulin release is characterised by a series of steps, involving vesicular docking, priming and fusion. Exocytosis of insulin secretory granules is mediated

by soluble N-ethylmaleimide–sensitive factor attachment protein receptor (SNARE) protein complexes. Attached to the complex is the calcium-sensor, synaptotagmin-7, which once bound to Ca^{2+} triggers modulatory changes in SNARE-complex proteins (VAMP, syntaxin and SNAP23/25) leading to exocytotic fusion[115]. Expression of synaptotagmin-7 and multiple isoforms of VAMP, syntaxin, SNAP25 were reported in GLUTag cells[114], suggesting a role in GLP-1 secretion. Furthermore, forskolin-induced GLP-1 exocytosis was significantly impaired in L-cells of syn1α knockout mouse, further supporting the importance of SNARE proteins for GLP-1 exocytosis[116].

1.8 Physiological variation in gut pH

In healthy human subjects, the use of radiotelemetry, swallowable capsules with pH sensors revealed real-time variation of luminal pH throughout the GI tract[3]. Reported fasted pH values of parts of the tract are shown in Fig1.5. In proximal areas of the GI tract, it is well-established that alterations of the luminal pH occur following meal intake. Within the stomach, pH is very acidic whilst fasting and increases following nutrient load (up to pH 5), whereas less dramatic alterations are seen in more distal segments of the GI tract (up to pH 8)[117]. Moreover, meal content has been shown to influence pH changes of the GI tract. In rats, increased dietary fibre intake increased the pH of the small intestines[118], as well as increasing pancreatic secretion of bicarbonate[119]. Furthermore, microbes throughout the gut can produce short-chain fatty acids from easily fermentable carbohydrates, which may have local influences on luminal pH[117].

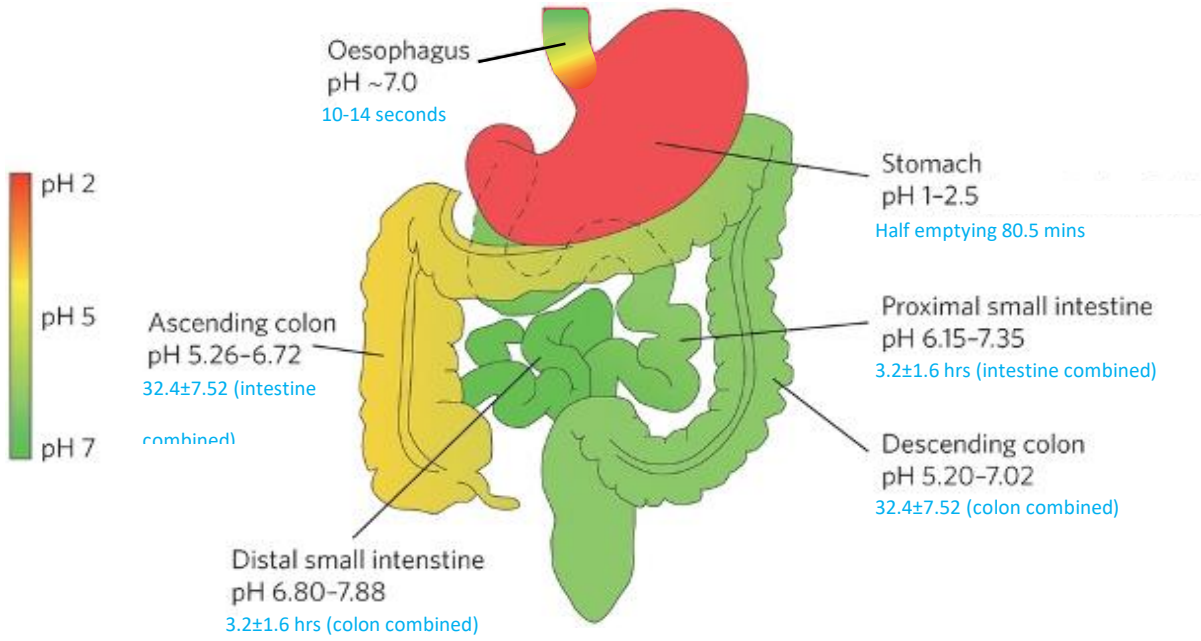


Figure 1.5 Physiological pH profile of the human GI tract. In blue are the transit times at difference parts of the tract. Adapted from Khutoryanskiy, V.V. Supramolecular materials: Longer and safer gastric residence. *Nat Mater* **14**, 963-964 (2015) and Kozelek, M., *et al.* Investigation of pH and Temperature Profiles in the GI Tract of Fasted Human Subjects Using the Intellicap((R)) System. *J Pharm Sci* **104**, 2855-2863 (2015)[2,3]

1.9 Gut pH and pathology

Studies utilizing radiotelemetric measurements have identified pathologically associated variation in GI pH, for example reduced colonic luminal pH in patients with Inflammatory Bowel Disease (IBD)[120]. The phenotype was attributed to reduced mucosal bicarbonate secretion, increased mucosal and bacterial lactate production as well as impaired SCFA absorption and metabolism[120]. Recently, reports have emerged identifying an association between alterations of the gut pH with diabetes and obesity[121]. Specifically, a lower median pH was observed in the small intestine of individuals with obesity compared to normal weight in the fasted (median pH: 6.68 ± 0.13 and 7.15 ± 0.13, respectively: p=0.02) and fed state (median pH: 6.71 ± 0.13 and 7.33± 0.13, respectively: p = 0.003)[121]. Furthermore, increases in pH levels of the stomach and distal gut were observed in

individuals following bariatric surgery[122]. Whilst the significance of post-surgery pH for treatment success has been attributed to changes in gut microbial communities, currently, no published work has investigated a potential relationship between luminal pH and functions of EECs of the lower GI tract.

1.10 Work preceding this study:

1.10.1 Extracellular pH effects GLP-1 secretion

Within the upper GI tract low luminal pH is important for nutrient digestion[123]. Early experiments have shown that acidification stimulates the secretion of multiple gut hormones associated with EEC populations within the stomach and duodenum, including secretin[124], somatostatin[125], vasoactive intestinal peptide[126] and motilin[127]. For example, exposure of the enteroendocrine M-cells to acidic extracellular pH (pH 5.0) caused an increase in secretion of the gut hormone, motilin, correlating with transient membrane depolarisation and action potential firing, likely mediated by the influx of Ca^{2+}. In contrast, alkaline solutions did not alter Ca^{2+} kinetics nor motilin secretion. Whilst the acute M-cell response to low pH (pH-induced currents) was largely attributed to the acid-sensing ion channels (ASIC1-4), blockage of the channel did not inhibit motilin secretion, suggesting other mechanisms may be involved[128].

Preliminary data from our laboratory showed that the secretion of GLP-1 is also pH dependent - double the amount of hormone was detected in the secretion media at alkaline pHo 7.6 compared to pHe6.5 in glucose-stimulated conditions. This effect was visible in both a model L-cell line (GLUTag cells, Fig1.5a) and *ex vivo* crypts (Fig1.5b). Here, results from GLUTag cells show over a 2-fold induction of GLP-1 secretion with glucose

stimulation compared to basal conditions (0mM glucose) at pHe7.4, demonstrating the effectiveness of the secretagogue in *in vitro* settings[88,89].

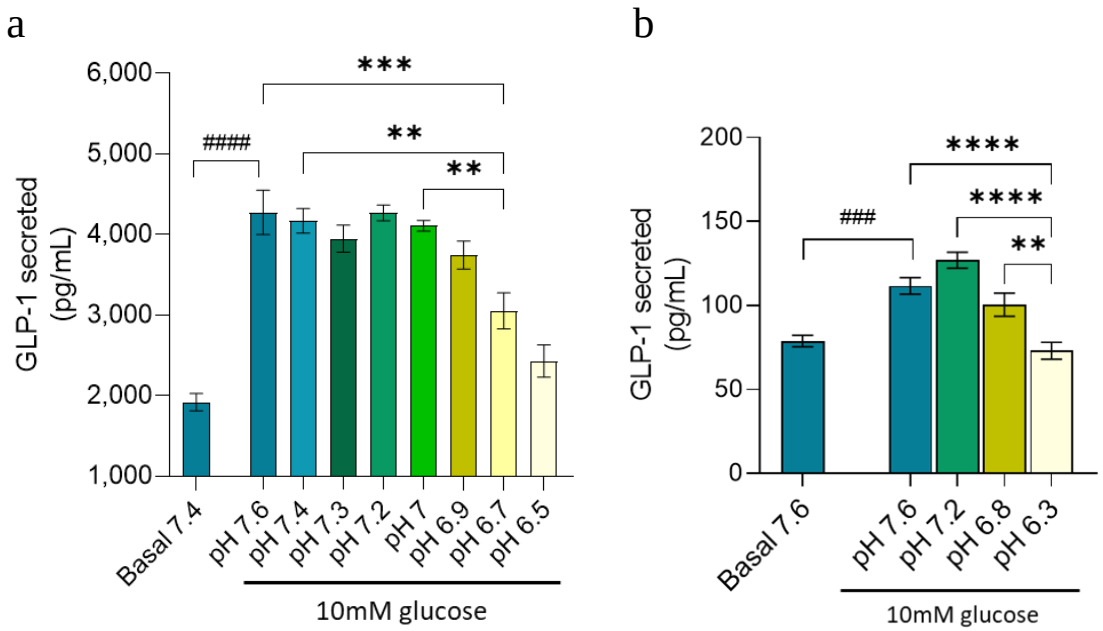


Fig 1.5 GLP-1 secretion from (a) GLUTag cells (n=6) and (b) murine *ex vivo* primary gut crypt cultures (n=3) is pH-dependent. The statistical comparison was made to either the Basal secretion at pH 7.4 (#) or 10mM glucose-stimulated secretion (*). Each bar graph represents mean±SEM. Significant values depicted as *p<0.05, **p<0.01, ***p<0.001, ****p<0.0001, (one-way ANOVA with Tukey's post hoc test). Data from Gosia Cyranka, reproduced with permission.

1.10.2 Role of ions for the pH-sensitivity of GLP-1 secretion

L-cell uptake of Na^+ primarily occurs through the co-transport of glucose, via the SGLT1, and voltage-dependent Na^+ channels[129,130]. Expression of the SGLT1 transporter has been confirmed on the apical surface of GI epithelial cells[131] and non-polarised GLUTag cells[88]. Evidence has shown SGLT1 kinetics is subject to pH-dependent alterations[132]. In the presence of Na^+, at more acidic pHo the transporter exhibits a lower glucose affinity but higher transport capacity[132]. It is thought the pH-dependence of the transporter's kinetics may coincide with fluctuations of pH within the GI tract. However, preliminary

experiments in our laboratory, where Na^+ was replaced with the non-permeable cation $NMDG^+$, 30mM KCl depolarisation and subsequent stimulation still triggered pH-dependent GLP-1 secretion with results comparable to that in the presence of Na^+ (Fig. 1.6a). These results confirm that the effect of pHo on GLP-1 exocytosis likely involves a pathway downstream of membrane depolarization.

Furthermore, our laboratory showed that removal of Cl^- from the incubation media attenuates the glucose-triggered GLP-1 response from GLUTag cells (Fig 1.6b). A similar dependence has been identified for insulin release from pancreatic β-cells[133]. The importance of Cl^- for pancreatic β-cell insulin release is attributable to Cl^--channels (ClC-3) on vesicle membranes, which appear to play an essential role for granule acidification, acting to counter the large electrical gradient from ATP-dependent H^+ accumulation[134]. Supporting this, ClC-3 KO mice display impaired insulin secretion, with the β-cells of KO mice storing higher amounts of proinsulin suggesting impaired post-translational processing[135]. Given the similarities of the regulated secretory pathway, it is plausible to suggest a similar Cl^--dependence for GLP-1 secretion in L-cells. RNAseq confirmed GLUTag cells express a variety of genes encoding Cl^-- channels associated with plasma and vesicular membrane localisation, including CLC-3 (*Clnc3*).

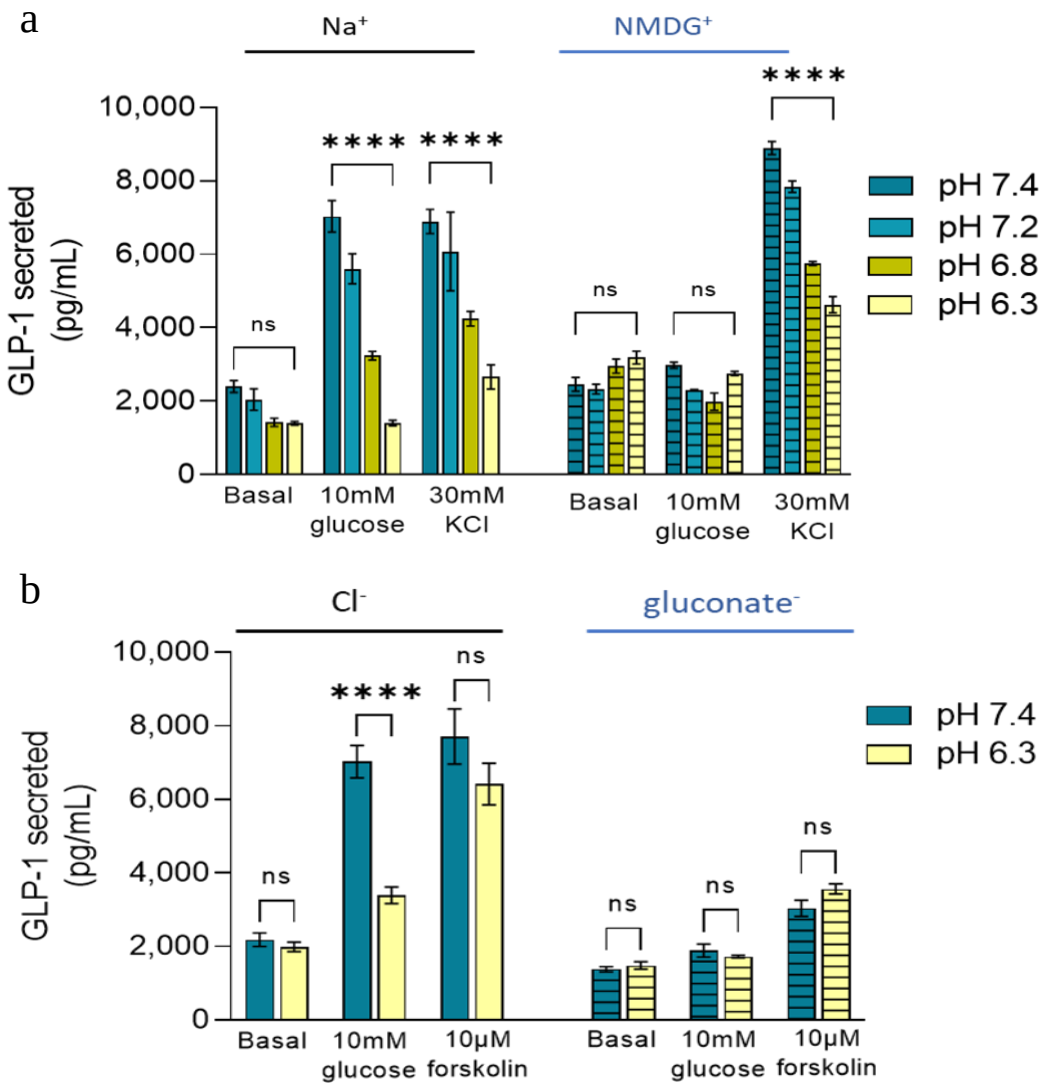


Figure 1.6 pH-dependent GLP-1 secretion from GLUTag cells is independent of extracellular Na^+ and dependent on extracellular Cl^-. **(a)** GLP-1 secretion stimulated by 10mM glucose or 30mM KCl in standard secretion buffer or with Na^+ removed and replaced by non-membrane permeable cation ($NMDG^+$) from n=3. **(b)** GLP-1 secretion stimulated 10mM glucose or 10μM forskolin in standard secretion buffer or with Cl^- removed and replaced by non-membrane permeable anion (gluconate) from n=6. Each bar graph represents mean±SEM. Data were analysed by two-way ANOVA and statistical significance shows the multiple comparison Tukey's test where *p<0.05, **p <0.01, ***p<0.001, ****p <0.0001, ns – not significant. Data from Gosia Cyranka, reproduced with permission.

1.10.3 pH-sensitivity of GLP-1 exocytosis

Prior to exocytosis, secretory granules in the regulated pathway undergo maturation, involving vesicular acidification via the ATP-dependent proton pump (V-ATPase)[105,107]. The activity of the pump is directly regulated by cytoplasmic pH[136]. Preliminary results from our laboratory found reducing pHo to 6.8 caused a similar effect on reducing glucose-stimulated GLP-1 secretion as the addition of the V-ATPase inhibitor, bafilomycin A1, at pH 7.4. It is thought vesicular proton gradients are important for the priming of granules and fusion to the target membrane via SNARE proteins[105,107,134,137]. Thus, results could suggest changes in intracellular pH influence the V-ATPase activity, impairing pre-exocytosis acidification and GLP-1 secretion.

Further supporting this suggestion, results from preliminary experiments show extracellular pH does not affect overall production of active GLP-1 but does influence retention. From whole cell lysates, the amount of active GLP-1 was not different following 2-hour incubation in pHe6.3 or 7.4. However, a higher amount of active GLP-1 was found in the secretory granules of acidic pHe6.3 versus physiological pHe7.4 (227±22pg/µg protein vs 169±10pg/µg protein, p=0.02, paired Student t-test). These results suggest decreases in GLP-1 secretion at low extracellular pH may be due to influences on exocytosis mechanisms.

1.11 Research hypothesis and aims

We hypothesise that GLP-1 secretion is influenced by changes in extracellular pH through a process dependent on subsequent changes in intracellular pH. We know that gut lumen pH is perturbed in human pathology, and the pH dependence of GLP-1 release may therefore have significant implications in both health and disease. In this study, I aim to further investigate the underlying cellular mechanisms of the pH-dependency of GLP-1 secretion. The preliminary work done on the pH dependence of GLP-1 release have two major caveats. (1) All previous work used a non-physiological buffer system (Krebs-HEPES buffer) and (2) established a link between extracellular pH and GLP-1 release. In other words, changes in intracellular pH were not assessed in these experiments.

The 3 main aims of this study were to:

- (1) Characterise the extra- to intracellular pH relationship in a L-cell model cell line, GLUTag cells to unequivocally establish the relationship between extracellular and intracellular pH in this model system.
- (2) Confirm the pH-sensitivity of GLP-1 secretion in physiological CO_2/HCO_3^- buffered systems.
- (3) Further investigate the pH-sensitivity of intracellular mechanisms that directly or indirectly influence GLP-1 secretion, such as ionic transport and exocytosis machinery.

2 Materials and Methods

2.1 Cell Culture of GLUTag cells

The GLUTag cells are widely used and specific for the study of GLP-1 secretion[138]. The cell line was originally derived from the colonic tumour of transgenic mice expressing SV40 large T antigen under the control of the *proglucagon* promoter[87]. Cells were grown in low glucose (1g/L) DMEM (cat.no.: 21885085, Gibco) with sodium pyruvate, GLUTamax and phenol red. This mixture was supplemented with 10% in-house heat inactivated FBS, foetal bovine serum (F7524-500mL, Sigma) and 1x Penicillin-Streptomycin (10,000units/mL of penicillin and 10,000µg/mL of streptomycin, cat.no.: 15140122, life technologies). Cells were routinely grown in vented flasks T75cm^2 (430641U-SP, Corning) without coating in 15ml DMEM media. For seeding/maintaining GLUTag cells, they were rinsed once with warm Dulbecco's phosphate-buffered saline (DPBS) without calcium and magnesium (cat.no.: 14190094, Life Technologies) and trypsinised with Trypsin-EDTA (0.05% cat.no.: 25200-072, Gibco) solution for 2 – 3min at 37°C, 5% CO_2. Cells were thoroughly pipetted up-and-down until single-cell suspension was achieved, which was confirmed under the light microscope and cells were resuspended in the appropriate volume of growth media. For maintenance, cells were split at 70-80% confluence once every 3-4 days in a 1:5 ratio.

For all experiments, cells were counted electronically using the Life Technologies Countess II Automated Cell Counter and re-seeded to the desired density into cell culture dishes coated with Poly-L-lysin (P4707-50mL, Sigma). In 96-well plates, cells were seeded at 1.5 x 10^5cells/well, 24-well plates at 3 x 10^5cells/well, 6-well plates at x 10^5cells/well. As specified in each experiment, cells were allowed to grow for either 48hr or 72hr. At all instances GLUTag cells were grown at 37°C, 5% CO_2.

2.2 Coating tissue culture dishes with Poly-L-lysine

All dishes for GLUTag experiments were coated with Poly-L-Lysin. Compared to other coatings (eg Matrigel, Fibronectin, Laminin), cells grew as a flat monolayer with sufficient adhesion so Poly-L-lysin was the most suitable for imaging and experiments requiring multiple media changes. The volumes of Poly-L-lysin solutions used were as follows:

1ml/well for 6-well plates, 0.2ml/well for 24-well plates, 0.1ml/well for 96-well plates. Dishes were coated with Poly-L-lysin and left at RT for 10 minutes, then the coating was removed, and dishes washed with deionised water. Cells were then seeded immediately.

2.3 pH and condition specific medium

Medium was made up in solution using deionized water, with added 1% Pen/Strep (Table 2.1a). In CO_2/HCO_3^- buffered media, pH was set by adjusting [HCO_3^-] (Table 2.1b), achieved by mixing various ratios of stocks containing 44 and 0mM of $NaHCO_3$ or pH 7.7 and 6.2, respectively. Previous work from our laboratory standardised the [HCO_3^-] for cell culture medium required to attain a target pH in a 5% CO_2 incubator[139]. To account for differences in osmolarity, 44mM NaCl or gluconate ($NaC_6H_{11}O_7$) was added to 0mM HCO_3^- solutions. For the latter, increases in $CaCl_2$ were necessary to compensate for gluconate interactions (chelating) with Ca^{2+} in solution. Alternatively, cells were treated with HEPES buffered media (2.3.2 Table b) and pH adjusted with NaOH, accurately determined using a pH meter at 37°C. In HEPES buffered media, cells were incubated at 37°C.

Glucose was the primary secretagogue used to stimulate GLP-1 secretion. 'Standard secretion media' refers to the CO_2/HCO_3^- buffered solution with added osmolarity regulating NaCl, containing 10mM glucose. Additives were added to the media as indicated in the legends to the figures and text. The following volumes of secretion buffer (unless stated otherwise for specific experiments) were used: 1ml/well for 6-well plates, 0.25ml/well for 24-well plates, 0.2ml/well for 96-well plates. 0.2ml/well for 12-well µ-Slide ibidi coverslips.

2.1 Table of secretion buffer recipes used in experiments. (a) CO_2/HCO_3^- based medium and (b) HEPES based medium

a

Ingredients	0mM glucose			10 mM glucose			
	pH 7.7 (mM)	**pH 6.2 (mM)**	**pH 6.2 (Gluconate) (mM)**	**pH 7.7 (mM)**	**pH 6.2 (mM)**	**pH 6.2 ($NaC_6H_{11}O_7$) (mM)**	**pH 7.4 Ca^{2+} free (mM)**
$CaCl_2$	1.8	1.8	3.188	1.8	1.8	3.188	-
$Fe(NO_3)_3 \cdot 9H_2O$	0.248	0.248	0.248	0.248	0.248	0.248	0.248
$MgSO_4$	0.811	0.811	1.003	0.811	0.811	1.003	0.811
KCl	5.4	5.4	5.4	5.4	5.4	5.4	5.4
NaCl	117.5	161.5	117.5	117.5	161.5	117.5	139.5
NaH_2PO_4	0.908	0.908	0.908	0.908	0.908	0.908	0.908
D-Glucose		-	-	10	10	10	10
$NaHCO_3$	44	-	-	44	-	-	22
$NaC_6H_{11}O_7$ Sodium gluconate	-	-	44	-	-	44	-
EGTA	-	-	-	-	-	-	0.5

b

Ingredients	0mM glucose	10 mM glucose	
	pH 7.4 (mM)	**pH 7.4 (mM)**	**pH 7.4 High KCl (mM)**
NaCl	135	140	95
HEPES	20	20	20
KCl	4.5	4.5	44.5
$MgCl_2$	1	1	1
$CaCl_2$	1	1	1
D-Glucose	10	-	10

2.1.2 [HCO_3^-] required for target pH in CO_2/HCO_3^- based medium

Target medium pH	[HCO_3^-] mM at 5% CO_2
6.3	1.65
6.5	2.75
6.8	5.5
7.1	11
7.4	22
7.6	33

2.4 Cell viability analysis using SRB

To confirm cell viability was not compromised by condition-specific media, a sulforhodamine B (SRB) assay was taken after incubation to determine cell density. Cells were fixed using 10% trichloroacetic acid (TCA) at 4°C for at least 60 mins. Afterwards, they were washed with H_2O four times, left to dry, and stained with SRB (0.057% in 1% acetic acid) for 30min. SRB was aspirated, washed four times with 1% acetic acid and left to dry. SRB was then dissolved in 10 mM Tris base for 30minutes. Absorbance was read at 520nm using the Cytation 5 imaging plate reader (Biotek).

2.5 Glucagon-like peptide 1 (GLP-1) secretion experiments

To quantify GLP-1 secretion, supernatant samples were taken from GLUTag cell cultures seeded in dishes coated with Poly-L-Lysin and grown for 48hr at 37°C, 5% CO_2. After incubation, media was aspirated and replaced with experimental specific secretion buffer (table 2.1a). Supernatant samples were taken at the 2hr end-point, or where the rate of GLP-1 secretion was investigated, supernatant samples were collected every 30mins for up to 2hr and replenished with fresh media to maintain volume of the incubating media. In each assay experiment, 100µL of supernatant sample was collected from each well. Apart from GLP-1 degradation rate, 0.5ml supernatant samples were collected from GLUTag cells incubated in 1ml bicarbonate buffered media for 1hr. Supernatant was stored in 24-well plates, and every 30mins, 0.05ml samples collected for quantification.

Samples were collected in Eppendorf tubes pre-loaded with the concentrated mixture of detergents 0.5% Triton-X and 0.4% Tween-20 (w/v) in ultrapure water. This was diluted 10-fold with the secretion supernatant. This approach was suggested to avoid GLP-1 sticking on tubes and tips and improve the stability and recovery of GLP-1 for future measurements. Harvested samples were stored on ice until all samples were collected. After this point, Eppendorf tubes were then spun at 4°C, 300 x g for 5mins to remove floating cells and debris, and either, 0.05ml supernatant harvested into fresh Eppendorf tubes and stored at -80°C until further processing, or supernatant was used immediately for [GLP-1] quantification. Remaining cell monolayer was washed with DPBS and fixed with 10% TCA for SRB protein quantification.

2.6 Glucagon-like peptide 1 (GLP-1) detection

The amounts of active GLP-1 (7-37 and 7-36-NH_2) secreted by GLUTag cells were measured in secretion medium by FRET-based HTRF assay (Active GLP-1, Cisbio) according to manufacturer's protocols. Final concentrations of secreted GLP-1 were calculated from the standard curve generated by active GLP-1 peptide standard provided by the manufacturer and presented as pg/mL. GLP-1 stock solution at 2800 pg/mL was prepared in ultrapure water and serial dilutions were made in experimental secretion buffer. Where stated, the Multi Species GLP-1 Total ELISA kit was also used to measure and quantify total (active plus inactive) supernatant [amidated GLP-1] according to manufacturer's protocols (catalog #EZGLP1T-36K; Millipore, Burlington, MS).

2.7 pH_i measurements

Intracellular pH was measured using carboxy SNARF-1 (cSNARF1) in cells identified by particle analysis of fluorescence centred around nuclei visualized using the DNA-binding stain Hoechst-33342. In black wall, flat coverslip bottom µ-plate 96-well plates, cells were seeded in triplicated at 1.5 x 10^5cells/well and grown for 48hr. For experimentation, growth media was aspirated and replenished with 0.2ml/well pH specific bicarbonate or HEPES media. After a 2-hour incubation period, cells were then incubated in media supplemented with cSNARF1-AM (5 mg/mL, Molecular Probes) and the nuclear stain Hoechst-33342 (10 mg/mL, Molecular Probes), for 15 mins. Media was then aspirated, washed twice and

replenished with 0.2ml/well pre-incubated pH specific medium. Plates were imaged using the Cytation 5 imaging plate reader (Biotek) and measurements performed in an atmosphere of 37°C, and either 0% CO_2 in HEPES or 5% CO_2 in bicarbonate buffer. Hoechst-33342 fluorescence was detected by 377nm excitation and 447nm emission, and cSNARF1 fluorescence excited by 531nm and simultaneously collected at 590nm and 640nm. Further analysis of the population distribution of pH data was performed with a MATLAB script[139].

2.8 tPA-Dendra2 plasmid transformation and extraction

tPA-Dendra2 was a gift from Janis Lochner (Addgene plasmid # 82636). Competent bacteria cells transformed with tPA-Dendra2 were streaked onto a LB agar [Sigma] plates with 100 μg/mL Ampicillin and incubated overnight at 37°C. A single colony was selected and grown overnight in sterile LB broth in a shaking incubator at 37°C. Plasmid extraction from the overnight liquid culture was carried out using the QIAGEN Plasmid Maxiprep Kit [cat.no.: 12181] according to the manufacturer's instructions. The DNA concentration of the extracted plasmid was determined using the NanoDropTM ND-1000 Spectrophotometer.

2.9 Plasmid sequencing

Initial primers were synthesised by Life Technologies according to the 5' and 3'sequencing primer of the tPA-Dendra2 plasmid provided by Addgene (Plasmid #82636). To obtain a complete sequence, new primers were synthesised from end portions of sequencing result until the 5' and anti-parallel 3' sequence results aligned.

Primers for sequencing are as follows:

5′ sequencing primer: GGT GAC ACT ATA GAA TAA CAT CCA CTT TGC

Second 5' sequencing primer: ATG GTG TGA CTT ACC GTG GC

3′ sequencing primer: GAG TTT GGA CAA ACC ACA ACT AGA ATG CAG

Second 3′ sequencing primer: GCC CAA CTT GTT TAT AGC

Sequencing was performed by Source Bioscience. The sequences obtained were compared to sequences provided by addgene and depositing laboratories using SerialCloner 2.6.1 multiple sequence alignment.

2.10 Plasmid transfection

GLUTag cells were plated onto Poly-L-lysin plates at a density of 3 x 10^5cells/well in 4-well ibidi plates, or 1.5 x x 10^5cells/well in 12-well ibidi plates. Cells were grown for 48 to 72hours and then cells were transfected with tPA-Dendra2 using a 1:3 ratio of DNA to Lipofectamine 2000 (100014469, Life Technologies) according to manufacturer's instructions. Cells were kept in the transfection mixture for 6 hours before being replaced by DMEM media. After 2 days of recovery, transfection was confirmed using the Zeiss confocal microscope and cells were used for further experimentation.

2.11 Live cell imaging

Cells were transfected as described above in 4-well u-slide ibidi coverslips. After transfection, cells recovered for 48 hours prior to further experimentation. For imaging, media was aspirated and replenished with 500ul of HEPES buffered solution (10mM glucose, pH7.4) or if using a CO_2 chambre, bicarbonate buffered media (10mM glucose, pH7.4). Imaging was performed using the Zeiss Laser Scanning Confocal Microscope.

2.12 Western blot

Immunoblotting Samples were prepared by lysing the cells using radioimmunoprecipitation assay (RIPA) buffer (cat.no.: 20-188) containing proteinase and phosphatase inhibitors. Samples were then spun on a rotating wheel for 10mins then centrifuged at 13,000 RPM for 10mins at 4°C. Protein concentration in the samples was measured using bicinchoninic acid (BCA) protein assay kit and adjusted using deionised water. Samples were heated at 70°C for 5mins, and loaded onto a 10% acrylamide gel. The gel was run at 90 V for 15mins and at 120 V for 90mins. Afterwards, membrane transfer was performed at 90 V for 90mins. Primary antibodies were diluted in 5% milk TST-T and incubated at 4°C overnight. Unbound antibodies were washed off 3x 10mins in TBS-T

before membranes were incubated in HRP-conjugated goat anti-rabbit secondary antibody in 5% milk TST-T for 1 hour at room temperature (1:5000). Membranes were washed 3x 10mins in TBS-T again and visualized using horseradish peroxidase. Proteins were detected using SuperSignal™ West Pico PLUS Chemiluminescent Substrate (cat.no.:34580) according to the manufacture's instructions.

Antibody binding of b-Actin protein was used as a loading control. Western blot signals were quantified using the ImageJ Gel Analysis tool.

2.2 Antibodies used for Western Blot

	Target	**Manufacturer and Catalogue Number**	**Species raised in**	**Dilution**
Primary antibodies	P-S6	Cell signalling Technologies 4858	Rabbit	1:500
	P-S6K (Thr421/Ser424)	Cell signalling Technologies 9204	Rabbit	1:500
	HRP-conjugate Beta actin	Protein tech 66009	Rabbit	1:1000
Secondary antibodies	HRP-conjugated anti-Rabbit IgG	Invitrogen G21234	Goat	1:5000

2.13 Immunofluorescence

After incubation, media was aspirated, and cells immediately fixed with 4% paraformaldehyde in PBS. Wells were then washed 2x with PBS and permeabilised with 0.2% Triton X-100 in PBX for 10mins. Wells were then washed again 3x with PBS and blocked with 3% BSA in PBS for 1 hour at room temperature. Cells were incubated with primary antibody in 3% BSA for 2 hours, then washed 3x with PBS for 5 mins each wash. Cells were incubated with the secondary antibody for 1 hour at room temperature wrapped in tinfoil. Following this, cells were washed 3x with PBS, 5 mins each wash, and stained

with Hoechst-33342 (10 mg/mL, Molecular Probes) in PBS for 1min. Cells were washed 3x in PBS for 5 mins. Slides were then mounted using SlowFade Diamond Antifade Mountant with DAPI (S36964, Life technologies) and High Precision 170um coverslip (cat.no.:10811). Slides were imaged immediately or the following day.

2.3 Antibodies used for immunofluorescence

	Target	**Excitation and Emission (nm)**	**Catalogue number and Manufacturer**	**Species raised in**	**Dilution**
Primary antibody	GLP-1	-	Abcam Ab22625	Rabbit	1:500
Secondary antibodies	Rabbit IgG	493/518	Invitrogen A32731	Goat	1:1000
	Rabbit IgG	631/650	Invitrogen A21070	Goat	1:1000

2.14 Statistical Analysis

All statistical analysis and graph generation was performed using GraphPad Prism 9. For comparing variables within one sample, one-way analysis of variance test (ANOVA), or comparing two or more samples, two-way analysis of variance test (ANOVA) with a Tukey's multiple comparison test was used.

3 Regulation of intracellular pH in GLUTag cells

3.1 Introduction

Generally, for most cell types under physiological conditions, intracellular pH (pHi) (~7.2) tends to be slightly more acidic than extracellular pH (pHo) (~7.4)[4]. Many mechanisms, such as the regulated secretory pathway and ATP synthesis, are pH-sensitive due to the influence of protonation on protein function and electrochemical gradients[4]. As such, membrane bound organelles, including the nucleus, endoplasmic reticulum and Golgi apparatus, have various optimal pH conditions which largely depends on cytoplasmic pH[4]. As changes in pHo directly influence pHi[139], systems to sense and regulate fluctuations of pH are ubiquitous and necessary for all cell types[4].

Acute challenges to pHi are initially counteracted by an intracellular pH buffering system. The total buffer capacity (β_{total}) consists of intracellular weak acid and bases ($\beta_{intrinsic}$), such as side chains of amino acids and phosphate groups, and the equilibrium reaction (β_{HCO3-})[4]:

$$CO_2 + H_2O \rightleftharpoons H^+ + HCO_3^-$$

However, β_{total} is a finite buffering system and has limited regulation. As protons are consistently accumulated from metabolic acid equivalents and the negative transmembrane electrical potential, mechanisms to continuously extrude protons are required. Thus, transmembrane transporters (proton-extruders and proton-loaders) regulate long-term pHi homeostasis, Fig3.1[4].

3.1.1 Acid-extruders

Acid extrusion generally refers to a process that aims to raise pHi. Across cell types, this is typically achieved by the extrusion of H^+ or accumulation of weak bases (HCO_3^-). Considering the former, the Na^+/ H^+ exchangers (NHE, SLC9A family) are well-

established regulators of pHi attributable to the transporters' intracellular H^+ modifier site for allosteric regulation of activity[4]. At low pHi, the transporters' activity increases at a steep rate, minimising acidification exposure and cellular injury[4]. Whereas, at pHi values above 7.2, the transporters' activity rapidly decreases, preventing an alkaline overshoot[4]. The SLC9A family of transporters are expressed ubiquitously across cell types[4], including both pancreatic β-cells[140] and human intestinal enteroids[141] where Na^+-dependent alkalinisation is crucial for pH recovery[141].

Cellular uptake of HCO_3^- is another means to counteract cytosolic pH decreases[4]. Increasing the cytosolic concentration of the anion would shift the CO_2/HCO_3^- equilibrium and increase production of membrane-permeant CO_2 and H_2O via carbonic anhydrase (CA)[4]. Predominantly, the uptake of HCO_3^- is coupled with Na^+ transport. The Na^+-coupled HCO_3^- transporters (NBC, *SLC4A* family) consist of both electroneutral (NBCn, $1Na^+$: $1HCO_3^-$) and electrogenic (NBCe, $1Na^+ : 2HCO_3^-$ and $1Na : 3HCO_3^-$) isoforms[4]. As such, the driving force and transport activity of the isoforms are differentially regulated by the transmembrane potential and electrochemical gradients of Na^+ and HCO_3^-. NBCs are

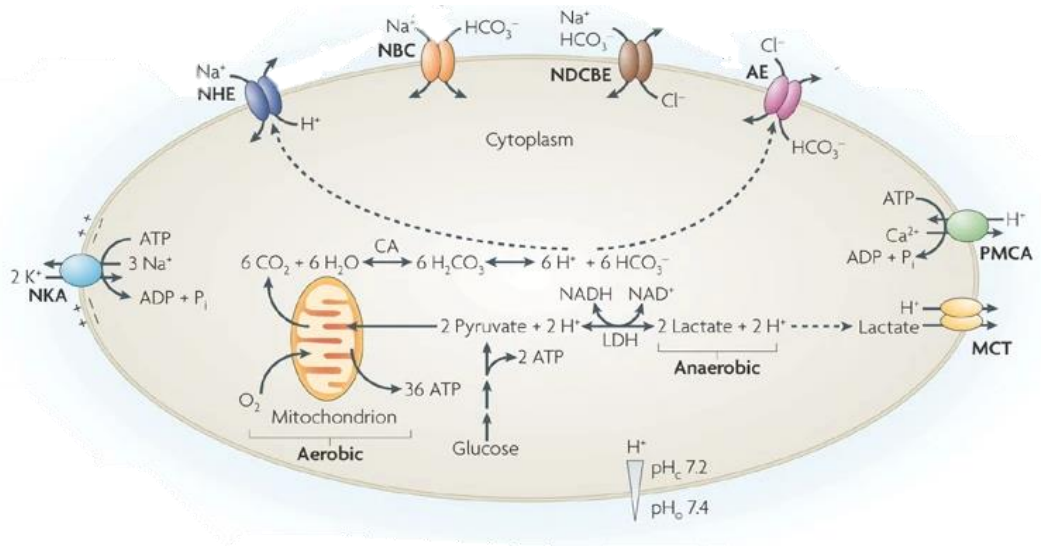


Figure 3.1 Diagram of the sensors and regulators of intracellular pH homeostasis.
Adapted from Casey, J.R., Grinstein, S. & Orlowski, J. Sensors and regulators of intracellular pH. *Nat Rev Mol Cell Biol* **11**, 50-61 (2010)[4].

essential for pH regulation across many cell types[4], including pancreatic β-cells[140], and the presence of HCO_3^- in the extracellular media was shown to significantly alter pHo/pHi dynamics[142].

3.1.2 Proton-loaders

Counterbalancing proton extruders, cells also possess acid-importing transport mechanisms, enabling a tight regulation of cytoplasmic pH. This is primarily attributed to Cl^- coupled exchangers, including the anion exchanger (AE), SLC4A, and the SLC26A protein family, consisting of electrogenic and electroneutral Cl^-/HCO_3^- exchangers[4,143]. The steep inward concentration gradient of Cl^- is the main driving force for HCO_3^- extrusion, consequently causing a shift in the CO_2/HCO_3^- equilibrium to favour the production of intracellular protons[4]. Accordingly, extracellular [Cl^-] is known to influence pHi; for example, in pancreatic β-cells Cl^--free media induced a similar increase in intracellular pH as exposure to extracellular media of pH 8.3[144].

In GLUTag cells, RNAseq results from our laboratory confirmed the expression of genes encoding proton extruders, NHE (SLC9A family), NBC (SCL4A5, SCL4A7, SCL4A10) and NDCBE (SCL4A8); and proton loaders, AE (SLC4A2 and SLC4A3) and SLC26A family[145]. However, the role of these individual transmembrane transporters for pHi regulation in GLUTag cells is currently unknown.

3.1.3 Cellular medium composition and pH regulation

An important consideration when investigating cellular pH regulation is the ionic composition and buffering regime in the medium. Altering the ionic concentration of the extracellular medium may influence the kinetics of pH regulating transporters outlined in

Fig3.1[139]. As well, the physiological CO_2/HCO_3^- buffering system is volatile, meaning the weak acid/base can evaporate as a gas (CO_2 (g)). This can cause experimental difficulties as the pCO_2 largely influences the equilibrium position and, as a result, pH. However, the use of non-volatile buffers (e.g., HEPES) for cell culture medium can produce non-physiological conditions[139]. For example, non-volatile buffers often do not contain HCO_3^-, inactivating transporters which influence the pHo/pHi relationship leading to artefacts or misinterpretation of data[139].

Therefore, investigations assessing the response of an intracellular system to changes in extracellular pH must consider potential influences on pH regulation. As such, it is important to standardise the extra- to intracellular pH relationship under a CO_2/HCO_3^- buffering regime, where pCO_2 is carefully controlled. From this, the effect of altering superfusate composition on pHi can be considered when evaluating observations of the cellular response investigated.

3.2 Methods

Intracellular pH can be investigated using cSNARF-1, a cell-permeant dye which undergoes pH-dependent shifts in emission from yellow-orange to red fluorescence in acidic and basic conditions, respectively[146]. Exciting the dye at 531nm generates inversely related signals at 590nm and 640nm which can be ratioed and converted to represent pH using a pre-established calibration curve[139]. The cSNARF-1 signal of individual cells can be identified using Hoechst-33342 nuclei staining (Fig3.2a,b) and used to calculate pHi of sample cells. An example generated in this study is shown in Fig3.2. The graph shown in Fig3.2f demonstrates that the ratio is independent on SNARF-1 fluorescence intensity. The

average pHi of cells incubated in a range of pHo can then be used to determine the extra- to intra- cellular pH relationship.

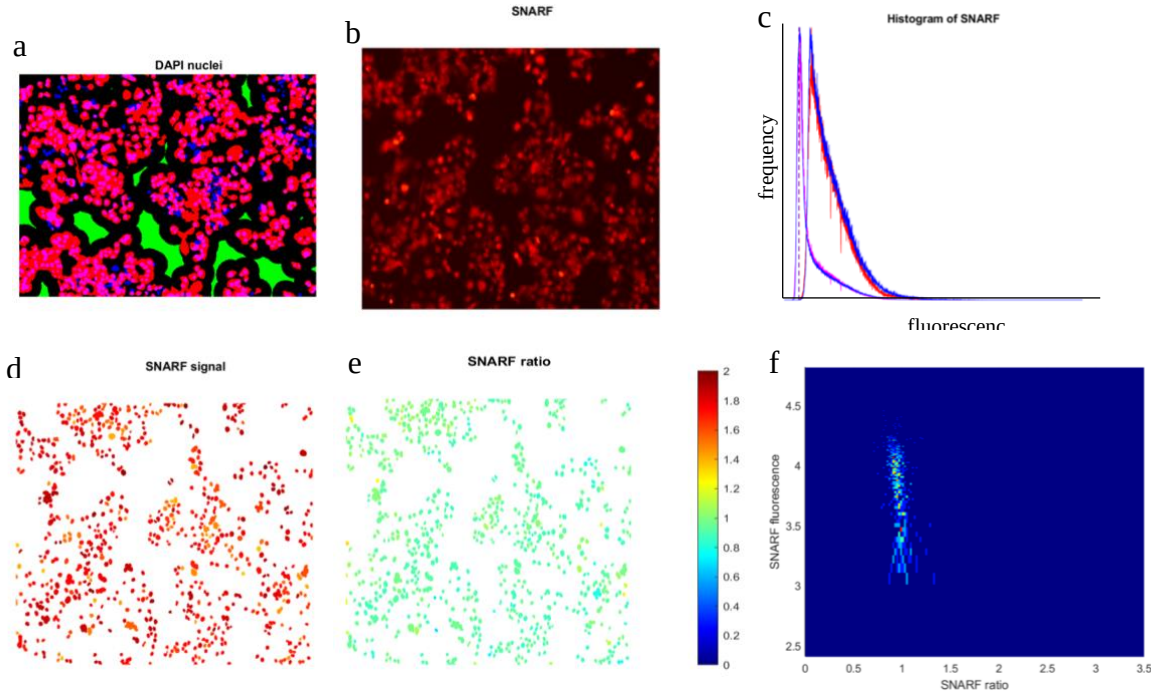


Figure 3.2 Representative image of GLUTag cells loaded with SNARF-1 imaged with Cytation plate reader. (a) and (b) respective Hoechst-33342 and cSNARF1 fluorescence maps (c) histogram of cSNARF-1 fluorescence distribution in background (left) and area occupied by cells (right) (d) identified cSNARF1 signal fluorescence intensity (e) ratio for individual cells used to calculate pHi (f) SNARF ratio and SNARF fluorescence

3.3 Results

3.3.1 Regulation of intracellular pH in GLUTag cells

In GLUTag cells, extracellular pH significantly alters intracellular pH in a linear relationship, Fig3.3 ($p<0.0001$). In bicarbonate buffered media, the presence or absence of glucose had no effect on pH regulation over the 2-hour incubation period ($p=0.4904$). At physiological pHo 7.4, pHi is slightly more acidic at pH7.155±0.041 in 10mM glucose and pH7.187±0.081 without glucose (mean±SEM). In GLUTag cells, an increase in pHo from 7.6 to 6.4 appears to affect pHi linearly, with a slope in 10mM glucose of 0.3003- and

without glucose of 0.3274-units pHi per unit pHo. Fig3.3b and Fig3.3c shows histograms of pHi in 10mM glucose and 0mM glucose conditions at pHo6.4, 7.1 and 7.6, representing cell-to-cell variation in pHi control. The standard deviation of pHi in both conditions is comparable; in 10mM glucose 0.140 and in 0mM glucose 0.144.

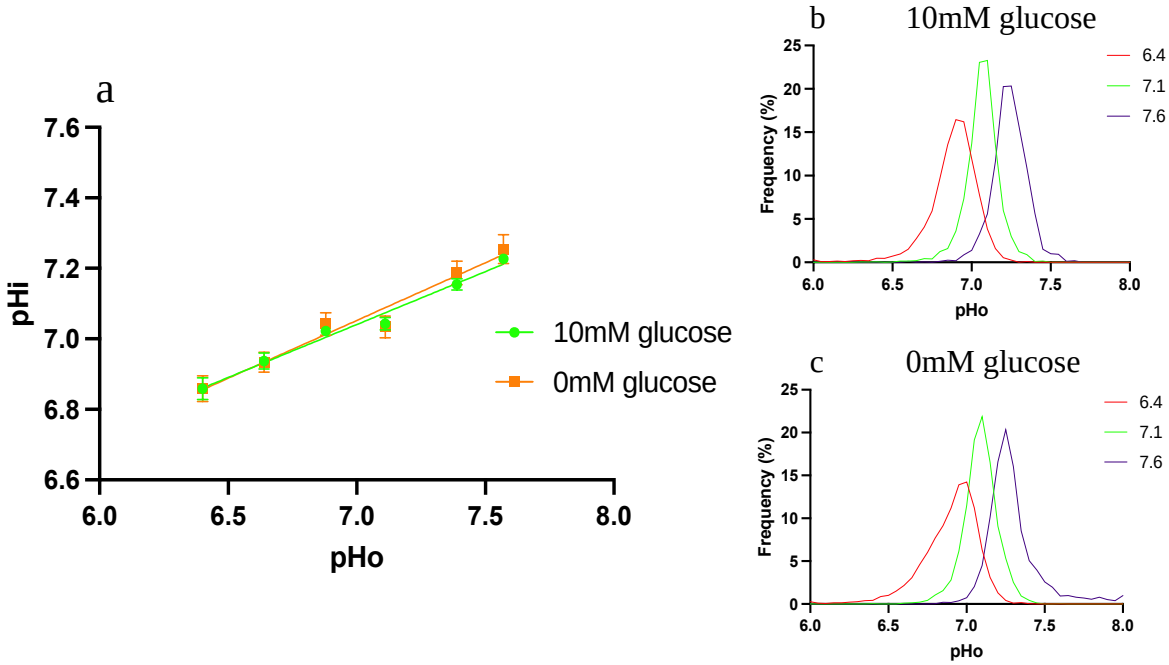


Figure 3.3 GLUTag cell intracellular pH regulation in CO_2/ HCO_3^--based medium. Intracellular pH relative to extracellular pH measurements across extracellular pH 6.4 - 7.6 in either 10mM glucose or 0mM glucose conditions. All measurements were taken at 37°C in 5% CO_2. a) pHi-pHo relationship, each bar represents mean±SEM from **n=7**. b,c) Histograms of pHi measured at pHo6.4, 7.1 and 7.6 in 10mM glucose and 0mM glucose as labelled.

3.3.2 Influence of extracellular HCO_3^- on pH regulation

As shown in Fig3.4, use of the non-volatile HCO_3^--free buffer (HEPES) had a significant effect on intracellular pH dynamics ($p<0.0001$, two-way ANOVA). In all extracellular pH conditions, intracellular pH is significantly higher in HCO_3^--free media compared to CO_2/HCO_3^- buffer media (standard secretion media) ($p<0.01$, two-way ANOVA), with an average difference of 0.138±0.025 pH units (mean±SEM) between these two buffering

systems. Importantly, at physiological pHo 7.4, pHi in HCO_3^--free media is significantly higher than CO_2/HCO_3^- buffered media (7.324±0.045 vs 7.158±0.011, $p<0.0001$). Although the difference between best-fit line elevations' are strongly significant ($p<0.0001$), there appears to be no significant difference between the slopes of HCO_3^--free compared to CO_2/HCO_3^- buffered media (0.3193 vs 0.2914, $p=0.3474$ respectively, simple linear regression).

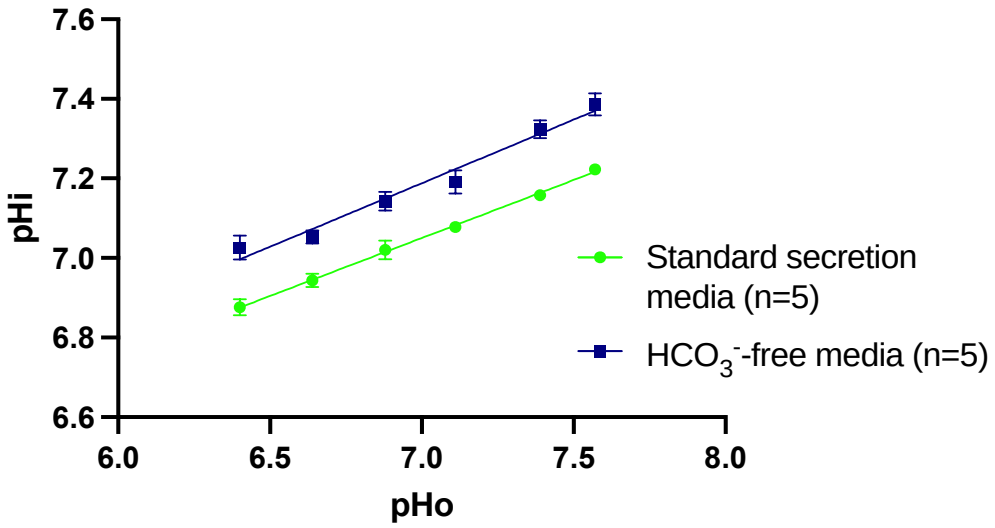


Figure 3.4 Intracellular pH regulation in GLUTag cells in HCO_3^--free (HEPES-based) media. Intracellular pH relative to extracellular pH, across extracellular pH 6.3 - 7.6 in 10mM glucose. All measurements taken at 37degC and either 5% CO_2 in bicarbonate buffer or 0% CO_2 in HEPES-buffered conditions. Each bar represents mean±SEM from **n=5.**

3.3.2 Influence of extracellular Cl^- on pH regulation

In the standard secretion media, to generate specific pHo values using a CO_2/HCO_3^- buffering system, medium [HCO_3^-] is adjusted. However, as HCO_3^- influences osmolarity, additional NaCl is required to regulate pH-dependent media osmolarity differences. This means lower pH or [HCO_3^-] medium would have higher [Cl^-]. In order to rule out any confounding effect directly related to the availability of Cl^- ions, Cl^- excess of the standard 117.5mM NaCl in CO_2/HCO_3^- buffered media were replaced with gluconate ions.

Accordingly, in this CO_2/HCO_3^- buffered media, across all pHo values, $[Cl^-]$ is constant, thus named 'constant $[Cl^-]$ media'. The difference in $[Cl^-]$ across pHo values between the standard CO_2/HCO_3^- buffered media and constant $[Cl^-]$ media is outlined in Fig3.2b by the red dotted line. Results show the pHo-pHi relationship is significantly influenced by pHo-dependent changes in $[Cl^-]$ ($p=0.0001$, two-way ANOVA) and the slopes between standard secretion and constant $[Cl^-]$ media are significantly different (0.2975 vs 0.2068, $p=0.0174$ respectively, simple linear regression). However, differences in steady-state pHi between standard secretion and constant $[Cl^-]$ media are only significant at pHo 6.4 (pHi 7.020±0.043 and 6.867±0.028 (mean±SEM), $p=0.0013$ respectively) where there is the largest difference in media $[Cl^-]$. Noticeably, at pHo 6.4, the increase in pHi in constant $[Cl^-]$ media is comparable to the pHi in HCO_3^--free media (7.027±0.060).

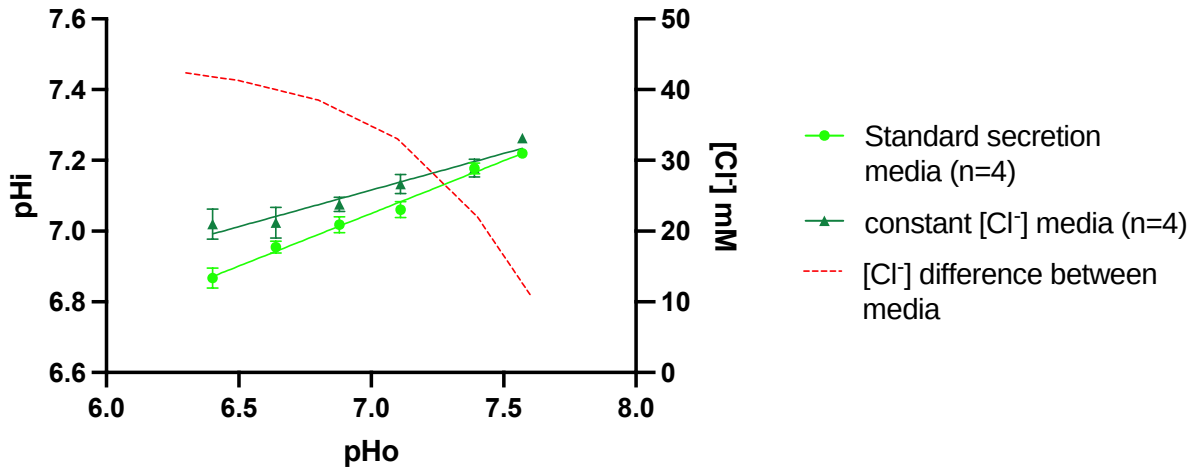


Figure 3.5 Intracellular pH regulation in GLUTag in CO_2/ HCO_3^--based media where gluconate ions replace osmolarity regulating excess Cl^-. Intracellular pH relative to extracellular pH, across extracellular pHo6.3 - 7.6 in 10mM glucose. The red line indicates the difference in extracellular $[Cl^-]$ between media. All measurements taken at 37degC and 5% CO_2 in bicarbonate buffer. Each bar represents mean±SEM from **n=4**

3.4 Discussion

Results presented here are the first to describe the relationship between extracellular pH and intracellular pH in GLUTag cells. As expected, changes to pHo have a direct effect on pHi. Similar to reports in other cell types[4], in GLUTag cells, steady-state pHi tends to be slightly more acidic (around 7.2) than physiological pHo 7.4[139]. The sensitivity of the pH regulatory system is also comparable, where the pHo-pHi slope from GLUTag cells (around 0.3) is near average compared to other cancer cell lines (ranging from 0.18 to 0.5)[147]. Furthermore, compared to other cancer cell lines (ranging from 0.05 to 0.18), GLUTag cells appear to have relatively high pHi standard deviation at around 0.14 in CO_2/ HCO_3^- buffered media. It has been suggested that greater intra-variation of pHi may facilitate a greater evolutionary capacity for cellular pHi regulation[147], however differences in pHi-regulatory phenotype have also been linked to stochastic variation, such as transient changes in transporter activity[147]. Nonetheless, given the slope and standard deviation of pHi regulation in GLUTag cells falls within the range generated from other cancer cell lines[147], GLUTag cells appear to exhibit a standard cellular pH regulation system in CO_2/ HCO_3^- buffered media.

As well, results presented here show the concentration and presence of Cl^- and HCO_3^- in the extracellular media influences pH regulation in GLUTag cells (Fig3.4, Fig3.5), suggesting the presence of pH regulating Cl^- and HCO_3^--dependent transporters. Importantly, results show for the first time that incubation in HEPES-buffer (HCO_3^--free media) has a significant effect on GLUTag cell pH regulation. On average, at the same pHo, pHi was increased by over 0.1 units when incubated in HCO_3^--free media compared to CO_2/ HCO_3^- buffered media (Fig3.4). This means to achieve physiological pHi of 7.2, in HCO_3^--free media GLUTag cells would need to be exposed to pHo 0.5 units lower than if

cells were incubated in CO_2/ HCO_3^- buffered media (pH6.9 vs pH7.4, respectively). This could amount to considerable impacts on intracellular physiology and cause misleading inferences from experiments where GLUTag cells are incubated in what is thought to be 'physiological' conditions of pHo 7.4 in HEPES buffer[4].

The steepness of the pHo-pHi slope represents the capacity of the system to maintain intracellular pH at physiological levels[148]. Fundamentally, the slope's steepness depends on the balance between the rate of acid influx (proton loading) and acid efflux (proton extrusion)[148]. For example, a lower pHo would decrease the driving force and rate for acid-extruders, shifting steady-state pHi to more acidic unless matched by an equal decrease in acid loading. As such, the rate at which changes in pHo influence pHi depends on the capacity of acid-loaders and acid-extruders to modulate their activity to maintain an equilibrium. Specifically, for GLUTag cells in physiological CO_2/ HCO_3^- buffered media, the capacity of the pH regulatory system amounts to one unit increases in pHo causing around a 0.3 unit increase in pHi.

Acid-loading in cells predominantly results from the accumulation of metabolically generated H^+ [148]. Previously it has been shown cytosolic pH is regulated by glucose metabolism[149]. However in pancreatic islet cells, glucose-induced changes in pH appear to be rapid (observed between 7-30mins) and reversible[150]. In contradiction to beta-cells, results here show pH regulation in GLUTag cells is independent on the presence of glucose. Thus, it can be assumed over the 2-hour time course of experiments influences of glucose metabolism on intracellular pH has minimal effects on steady-state pHi.

Preliminary results from our laboratory confirmed the expression of two well-established acid extruders[4], NHE (SLC9A family) and NBC (SCL4A5, SCL4A7, SCL4A10) in

GLUTag cells. However, it was interesting to find that despite a consistent increase in steady-state pHi across the pHo range, removing HCO_3^- from the incubation media did not change the pHo-pHi slope of GLUTag cells. This suggests HCO_3^--independent acid loaders, NHEs, are the predominant pH sensing mechanism in GLUTag cells, rather than HCO_3^--dependent acid loaders, NBCs. In many other cellular systems, including pancreatic β-cells[140], HCO_3^- uptake has been identified as crucial for pH regulation[4]. As such, the direction and magnitude of the effect of removing [HCO_3^-] from the incubating media is thought to be cell-type dependent[139]. For example, in other cancer cells lines, pHi showed a greater sensitivity to changes in pHo in CO_2/HCO_3^-free media buffered, such that the pHi/pHo relationship was steeper[139]. Thus, the finding presented here is unexpected and suggests in GLUTag cells pH regulation does not involve pH-dependent modulation of NBC activity. However, the significant role of NHEs, and not NBCs, for GLUTag cell pHi homeostasis will require further confirmation, such as pharmacological inhibition of NHE (eg amiloride) and NBCs and re-assessment of pH sensitivity impairment.

As removing HCO_3^- did not change the pHo/pHi slope but shifted the steady-state pHi higher at each pHo value, this likely demonstrates the presence of a HCO_3^- dependent acid-loader in GLUTag cells with consistent activity over the pHo range investigated. Multiple HCO_3^- -dependent pH regulatory transporters are blocked when using a HEPES-based buffering system[4]. However, removing HCO_3^- caused an increase rather than a decrease in pHi, suggesting the presence of the proton-loading anion exchanger (*SLC4A2*) in GLUTag cells. Indeed, expression of the AE2 and AE3 isoforms (SLC4A2 and SLC4A3, respectively) are confirmed from RNAseq analysis[145]. Furthermore, recently, it has been identified that cancer cells are able to increase pHi by inactivating the anion exchangers,

AE2[147]. It is plausible to suggest that GLUTag cells also possess this adaptation mechanism. This means in physiological conditions, activity of the AE draws HCO_3^- out of the cell, usually acting to decrease intracellular pH. However, by removing HCO_3^-, the AE is inactivated and consequentially an increase in pHi is seen. Again, this suggestion should be further investigated by inhibiting AEs with pharmacological agents or KO models and assessing the impairment of GLUTag cell pH regulation.

Furthermore, in CO_2/ HCO_3^- buffer media where gluconate ions replaced excess, osmolarity-regulating Cl^- ions, there appears to be a change in the extra- to intracellular pH relationship. Unsurprisingly, differences were greater at more acidic pHo where there is a larger difference in the [Cl^-] of the standard secretion and constant [Cl^-] media. Noticeably, at pHo 6.4, the difference in [Cl^-] has a meaningful impact on steady-state pHi, suggesting significant alteration of the activity of pH regulatory Cl^--dependent transporters. As incubation in constant [Cl^-] media raises pHi, results suggest the presence of a Cl^- dependent acid loader in GLUTag cells. Corroborating with findings using HCO_3^- free media, it is likely these results also reflect the activity of the AE, which uses the concentration gradient of Cl^- to drive HCO_3^- extrusion[4,143]. Thus, decreasing the exchanger's driving force by lowering extracellular [Cl^-] would result in the alkalinisation of the cell, disrupting pHi homeostasis.

The results obtained here describe the extra- to intracellular pH relationship in GLUTag cells. These findings can be used alongside further investigation to dissect the influence of changes in extracellular pH to GLP-1 secretion from GLUTag cells. Importantly, findings presented here disclose the significant impact alterations of the incubation media composition (such as [Cl^-] and [HCO_3^-]) can have on pH regulation in GLUTag cells.

Thus, should be taken into consideration when investigating the pH-sensitivity of an intracellular system to avoid misleading observations and experimental artefacts[139]. The CO_2/HCO_3^- buffering system with consideration of pCO_2 (using an incubator) is the most replicable of physiological systems, thus, is best suited to investigate the response of an intracellular system to changes in extracellular pH.

4 Influence of pH on GLP-1 secretion from GLUTag cells

4.1 Introduction

Glucagon-like peptide 1 (GLP-1) is a gut hormone released in response to direct sensing of nutrients[35], acting to repress appetite and potentiate pancreatic insulin secretion[22]. Evidence suggests the action of GLP-1 is impaired in obese subjects, with some studies reporting reduced postprandial levels in obese compared to lean subjects[151]. Currently, the cause of this observed reduced GLP-1 levels is unknown[152].

Inspired by reports of a lower average gut pH in obese and diabetic individuals[121], preliminary work from our laboratory has shown GLP-1 secretion is pH-dependent, with around double the amount secreted at pHo7.6 compared to pHo6.5. Together, this may suggest alterations of luminal pH underlie the pathophysiological derangements of GLP-1 secretion.

Preliminary experiments used a Krebs-HEPES buffering system where NaOH and HCl was used to adjust pH of the secretion buffer. However, physiologically organisms rely on CO_2/HCO_3^- to buffer unwanted pH change. Systems are adapted to regulate pH according to the CO_2/HCO_3^- buffering regime, such as gaseous exchange of the weak acidic CO_2, or transmembrane transport of the weak base, HCO_3^- [139]. This work and previous studies have shown that incubating cells in non-bicarbonate buffer, such as HEPES, can significantly alter the extra- to intracellular pH relationship compared to a physiological CO_2/HCO_3^- buffer [139]. These changes in intracellular pH can have significant effects on intracellular mechanisms and processes[4], including the regulated secretion pathway. Furthermore, the first and second phase of insulin secretion from β-cell is thought to be evoked by different secretagogues, suggesting, as well as total amount, the rate of

secretion is also under regulation[153]. Given the similarities between insulin and GLP-1 secretion, this is also likely true for L-cell GLP-1 secretion. Thus, the influence of pH on the rate of GLP-1 secretion will also be investigated in this chapter.

Many intracellular processes can directly and indirectly influence GLP-1 secretory dynamics[22]. As discussed in the introduction, GLP-1 secretion crucially depends on the transmembrane movement of key ions, and is therefore influenced by the ionic composition of the assay media. Na^+ is essential for glucose-stimulated GLP-1 exocytosis, both for the transport of glucose and membrane depolarisation[63,132]. Furthermore, glucose-triggered GLP-1 secretion depends on the opening of voltage gated Ca^{2+} channels[40]. As such, the influx of extracellular Ca^{2+} is crucial for GLP-1 exocytosis[154]. A novel finding from our laboratory showed that removal of Cl^- from the incubation media attenuates glucose-triggered GLP-1 response from GLUTag cells. Supporting this, a similar role of Cl^- for insulin secretion in β-cells has also been reported[134]. The impact of Cl^- on GLP-1 secretion must therefore also be considered and the composition of buffers used to ascertain pH-dependent exocytosis of hormones must be very carefully considered (eg pH-dependent $[Cl^-]$ variation in CO_2/HCO_3^- buffer media).

Furthermore, cellular processes such as growth, proliferation and protein synthesis have been shown to be influenced by decreases in pHo[155,156]. In relation to these findings, the mTORC1 signalling pathway, responsible for regulating cell metabolism, growth, and survival, was shown to be inhibited by acidification[157]. Significant decreases in mTORC1 signalling have been detectable after just 30 minutes after exposure to extracellular pH 6.2-6.6[157]. Interestingly, some evidence has suggested proglucagon mRNA expression is also regulated via Stat3-mTOR-dependent pathways in model L-cell lines[158]. Together, this

may also suggest pH-dependent influences on the mTORC1 pathway, and potentially cell viability, could affect GLP-1 secretion.

In this chapter I first aim to (1) validate the pH dependence of GLP-1 secretion from GLUTag cells in a physiological CO_2/HCO_3^- buffered system, while (2) taking into consideration the potential influence of different [Cl^-] across [HCO_3^-] and pH values in the media. Finally, I will investigate potential intracellular mechanisms underlying the pH-dependence of secretion.

4.2 Results

4.2.1 Standard [GLP-1] calibration

A Homogeneous Time-Resolved Fluorescence (HTRF) immunoassay was used to quantify active forms of GLP-1 (7-37 and 7-36-NH_2). Standard calibration curves of solutions with various pH were generated to confirm the HTRF signal was not affected by pH. Active GLP-1 gold standard peptide was used to prepare standard samples at a two-fold dilution range from 1400pg/mL to 43.8pg/mL in secretion buffer at pH 6.3, pH 7.4 and pH 7.6, Fig4.1. Two-way ANOVA results found the pH of the media was not a significant source of variation for the HTRF ELISA signal ($p=0.2486$).

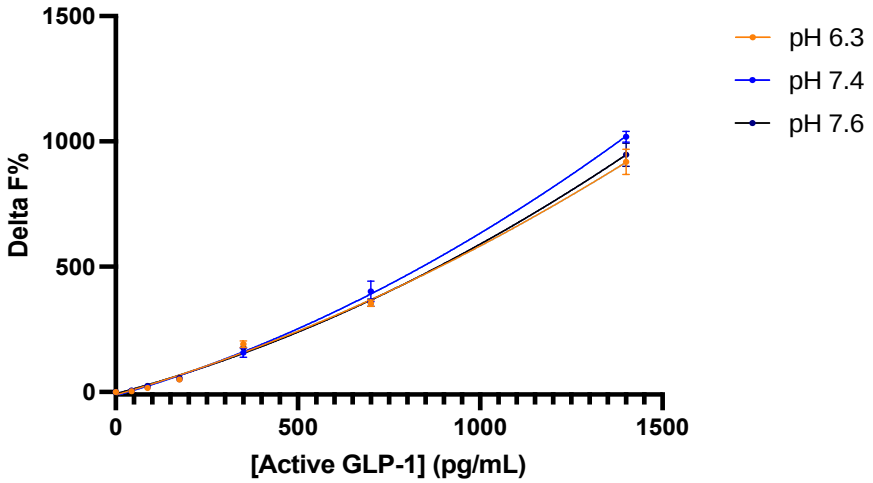


Figure 4.1 GLP-1 concentration standard curve for FRET-based assay**.** Generated from peptide gold standard provided by the manufacturer (Cisbio) at the stock concentration of 56ng/mL. GLP-1 standard was diluted as per instruction to 1400pg/mL and further two-fold until 43.8pg/mL in BC buffer (+) glucose, pH 7.4. Signal plotted as delta F%, which reflects the signal to background of the assay**.** Each point represents mean±SEM from **n= 5**

4.2.2 Extracellular pH influences GLP- 1 secretion

The experimental protocol established for the preliminary work was repeated with CO_2/HCO_3^- buffer to confirm pH-dependence of GLP-1 secretion. GLUTag cells were incubated in acidic (pH6.4), physiological (pH7.4) and alkali (pH7.6) medium. Results from Fig4.3a show glucose-stimulated GLP-1 release is pH dependent (p=0.0002, one-way ANOVA). Decreasing pHo from pH7.4 to pH6.4 resulted in a significant decrease in stimulated GLP-1 secretion (p=0.0019, one-way ANOVA). Whereas no effect was observed following alkalinisation from pHo7.4 to pH7.6 (p=0.5730, one-way ANOVA). Furthermore, the influence of glucose on GLP-1 secretion was significant (p=0.002, two-way ANOVA) with the pH-dependence of secretion lost in the absence of glucose (p=0.4707, one-way ANOVA). Interestingly, there was a trend for glucose to stimulate GLP-1 secretion at pHo7.4 and 7.6 (p=0.0623 and p=0.0531, respectively), whereas this appears to be lost at pHo6.4 (p=0.7461, two-way ANOVA).

To assess whether the buffering regime of the incubation media affects the pH-dependence of GLP-1 secretion, GLP-1 secretion in standard CO_2/HCO_3^- buffer media (green) and HCO_3^-free (HEPES) buffer media (blue) (10mM glucose) was compared, Fig4.3b. Results show the buffering regime does not significantly influence glucose-triggered GLP-1 secretion (p=0.3653, two-way ANOVA). A similar dependence of pH on GLP-1 secretion is found in both media, decreasing the pHo from 7.4 to 6.4 decreased section 1.3-fold in CO_2/HCO_3^- media (p=0.0002, one-way ANOVA) and 1.2-fold in HCO_3^-free media (p=0.0331, one-way ANOVA). When cross-comparing results, no significant difference was found between incubation in CO_2/HCO_3^- or HCO_3^--free media at each pHo value (pH6.4: p=0.9590; pH7.4: p>0.9999; pH7.6: p>0.9995, two-way ANOVA). Thus, the stimulated GLP-1 secretion response to pH is independent of HCO_3^-.

Ca^{2+} is known to play a pivotal role for GLP-1 vesicle exocytosis[40], and as expected, removing Ca^{2+} from the secretion media markedly attenuated GLP-1 secretion (p=0.0078, paired student t-test. From the literature, much evidence has shown cAMP-dependent pathways stimulate GLP-1 secretion[154]. Pharmacologically, intracellular cAMP levels can be increased by the drugs forskolin (fsk), a potent activator of adenylate cyclase[159], and IBMX, a competitive non-selective inhibitor of phosphodiesterase (PDE)[160]. Exposure of the cAMP activators induced a significant increase in GLP-1 secretion, around 3-fold of 10mM glucose alone (p=0.0015, paired student t-test), Fig4.3c. Results demonstrate the range of GLUTag cell GLP-1 secretion from basal (Ca^{2+}-free conditions) to cAMP-stimulation (fsk/IBMX).

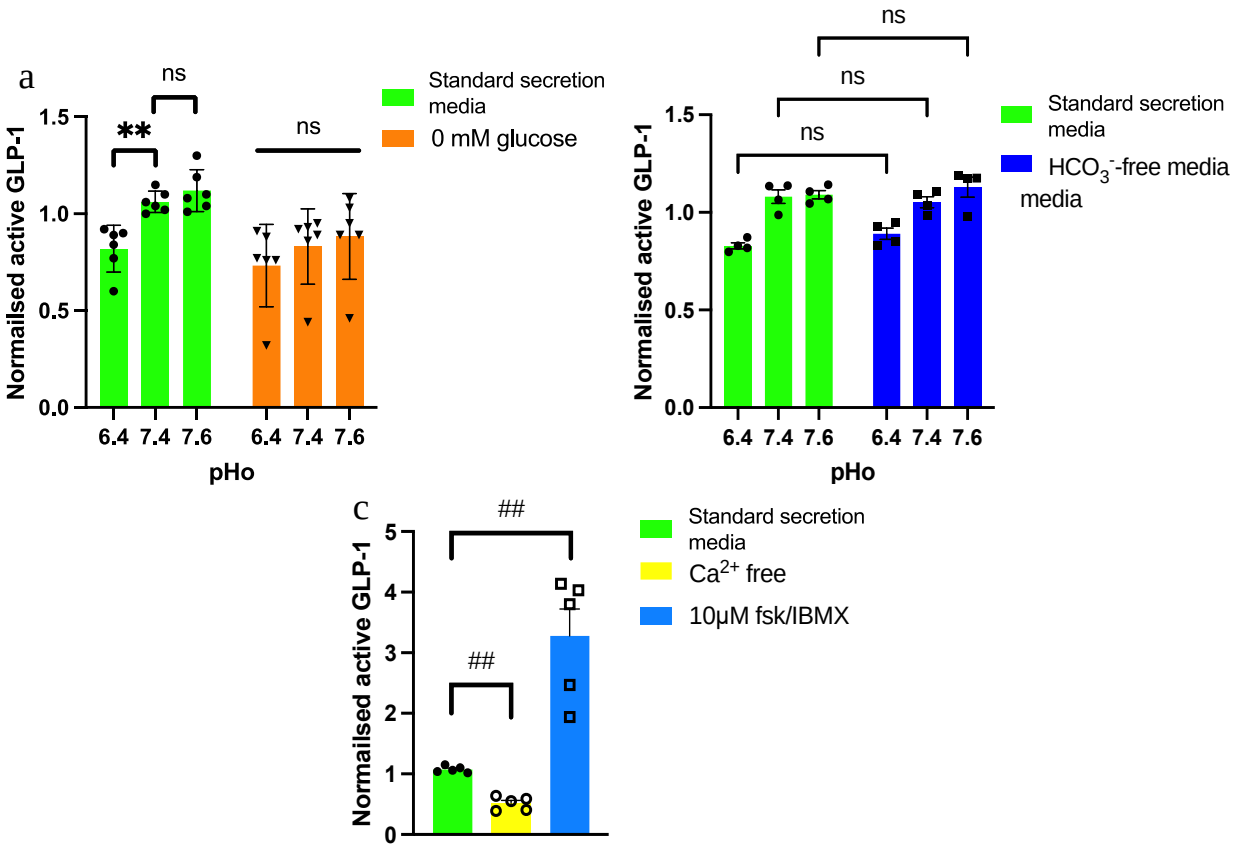


Figure 4.2 pHo dependence of active GLP-1 secretion from GLUTag cells in a) CO_2/ HCO_3^--based media and b) HCO_3^--free (HEPES-based) media. Measurements taken after 2hr incubation at pHo6.4, 7.4 and 7.6 in standard secretion media (10mM glucose) or in a) 0mM glucose where labelled. Or c) in standard secretion media at pHo7.4 without Ca^{2+} ions or with 10µM fsk/IBMX. Secretion was normalized to the average GLP-1 secretion in 10mM glucose pHo6.4, 7.4 and 7.6 measured in parallel on the same day. Each bar represents mean±SEM from a) **n=6**, b) **n=5** and c) **n=5.** ns depicts not significant, **p <0.01 a) two-way ANOVA with Tukey's multiple comparisons test and b) one-way ANOVA with Tukey's multiple comparisons test and ## p < 0.01 (paired

4.2.3 pH-dependence of total GLP-1 secretion

Total amidated GLP-1, active (7-36) and inactive (9-36) forms, as opposed to active GLP-1 only, was also ascertained, Fig4.4, using the ELISA-based assay kit. Corroborating active GLP-1 results, pH significantly influenced glucose stimulated total GLP-1 secretion (p=0.0002, one-way ANOVA). Acidification of the media from pHo7.4 to pH6.4 decreased GLP-1 secretion (p=0.0069); however, it is interesting to also report an effect of

alkalinisation from pHo7.4 to pH7.6 on GLP-1 secretion (p=0.0496). In the absence of glucose, GLP-1 secretion was attenuated, and the pH effect lost (p=0.9008, one-way ANOVA). As well, it seems the glucose stimulatory effect on GLP-1 secretion is only present at more alkali conditions (pHo6.4, p=0.9966; pHo7.4 p=0.0890; pHo7.6, p=0.0092, two-way ANOVA).

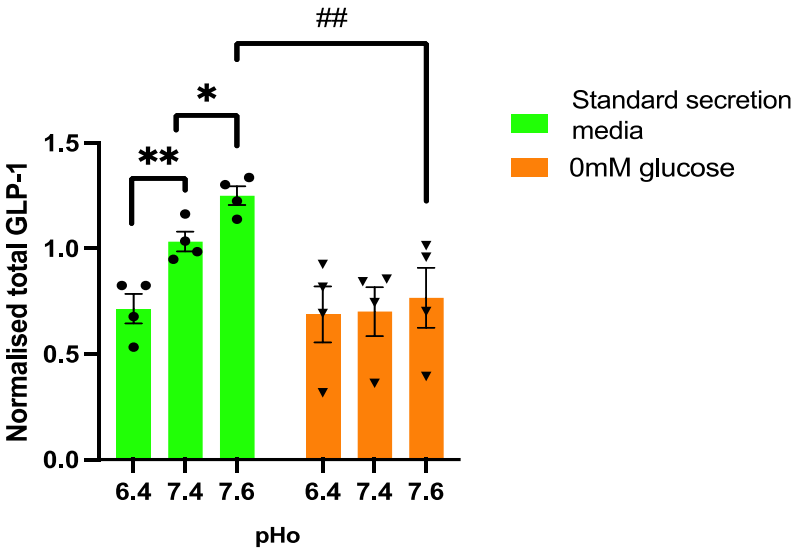


Figure 4.3 pHo dependence of total amidated (active and inactive) GLP-1 secretion. Measurements taken after 2hr incubation in CO_2/ HCO_3^-based media at pHo6.4, 7.4 and 7.6 in standard secretion media (10mM glucose) or 0mM glucose. Secretion was normalized to the average [GLP-1] of 10mM glucose secretion from pHo6.4, 7.4 and 7.6 measured in parallel on the same day. Each bar represents mean±SEM from **n=4.** Significant values depicted as **p <0.01 (one-way ANOVA with Tukey's multiple comparisons test) and ## p < 0.01 (two-way ANOVA with Tukey's multiple comparisons test)

4.2.4 Influence of extracellular Cl^- on pH dependent GLP-1 secretion

To control for altered Cl^- levels at lower [HCO_3^-] and pHo, excess osmolarity regulating Cl^- was replaced with gluconate ions so across pHo values [Cl^-] is constant (constant [Cl^-] media) Fig4.5. Compared to the standard secretion media, replacing excess Cl^- with gluconate did not influence GLP-1 secretion (p=0.8731, two-way ANOVA). Although no significant difference was identified at each pHo value when cross-comparing results (pH6.4, p=0.5213; pH7.4, p=0.9717; pH7.6, p=0.5969, two-way ANOVA), the influence

of pH on GLP-1 secretion appears to be insignificant when assessing results from constant [Cl^-] media (p=0.2679, one-way ANOVA). Nonetheless, in line with what had been observed previously, there was a clear pH dependent trend, and the data was most likely skewed by one anomalous result at pHo6.4 (boxed in red). Upon further investigation, this result was not statistically defined as an outlier (Grubbs method alpha = 0.05), however it most likely influences the results. Robust statistical analysis is limited by the low n numbers in this case, and these experiments were clearly underpowered. Unfortunately, we were unable to perform further experiments as all the GLP-1 assay kits had run out. These kits are prohibitively expensive, and my laboratory were unable to purchase a replacement kit at this point in time. We are currently awaiting funding decision outcomes to proceed with this work.

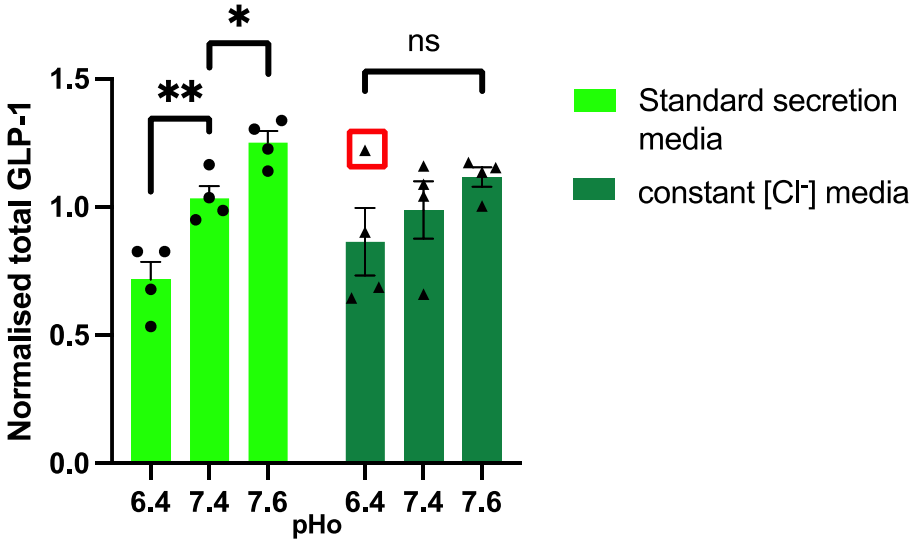


Figure 4.4 pHo dependence of total amidated GLP-1 secretion in CO_2/ HCO_3^--based media where gluconate ions replace osmolarity regulating excess Cl^-. Measurements taken after 2hr incubation at pHo6.4, 7.4 and 7.6 in 10mM glucose**.** Secretion was normalized to the average [GLP-1] of 10mM glucose secretion from pH 6.4, 7.4 and 7.6 measured in parallel on the same day. Each bar represents mean±SEM from **n=4.** Significant values depicted as *p<0.05, **p <0.01 (one-way ANOVA with Tukey's multiple comparisons test)

4.2.5 Influence of pH on GLP-1 secretion rate

To investigate the effect of pH on the rate of GLP-1 secretion, samples were collected every 30mins up to 2 hrs for GLP-1 quantification from the secretion media. The average individual time course for each pHo value in each condition investigated are outlined in Fig4.6a-c. Initial rate of GLP production was measured from the slope of an exponential best fitting the time course data: one-phase association: y = a*(1-exp(-x/b)), Fig4.6d. With glucose stimulation, the rate of GLP-1 secretion was significantly influenced by pH ($p=0.0020$).

The rate was shown to increase with alkalinisation of the secretion media; rate at pHo7.6 was over 2.5-fold higher than pH6.4 ($p=0.0015$, one-way ANOVA), and there was a trend for rate to increase from pHo6.4 to pH7.4 and pHo7.4 to pH7.6 ($p=0.727$ and $p=0.0656$, one-way ANOVA, respectively). The dashed line in Fig6.4d is the average secretion across pHo in Ca^{2+}-free conditions, representing basal GLP-1 secretion. Removal of glucose or Ca^{2+} significantly influenced GLP-1 secretion ($p=0.0002$ and $p<0.0001$, respectively, two-way ANOVA), and secretion between glucose- and Ca^{2+}-free conditions was not significant ($p=0.2974$, two-way ANOVA). Accordingly, the pH-dependence of GLP-1 secretion was lost in 0mM glucose and Ca^{2+} free conditions ($p=0.2795$ and $p=0.8224$, respectively, one-way ANOVA). Glucose and Ca^{2+} appear to have a significant effect on stimulation at pH7.4 ($p=0.0440$ and $p=0.0103$, respectively) and pH7.6 ($p<0.0001$ and $p<0.0001$, respectively), however, this effect is lost in pH6.4 ($p=0.8748$ and $p=0.9930$, respectively, two-way ANOVA). Results provide further evidence that stimulated GLP-1 secretion is inhibited at acidic pHo values.

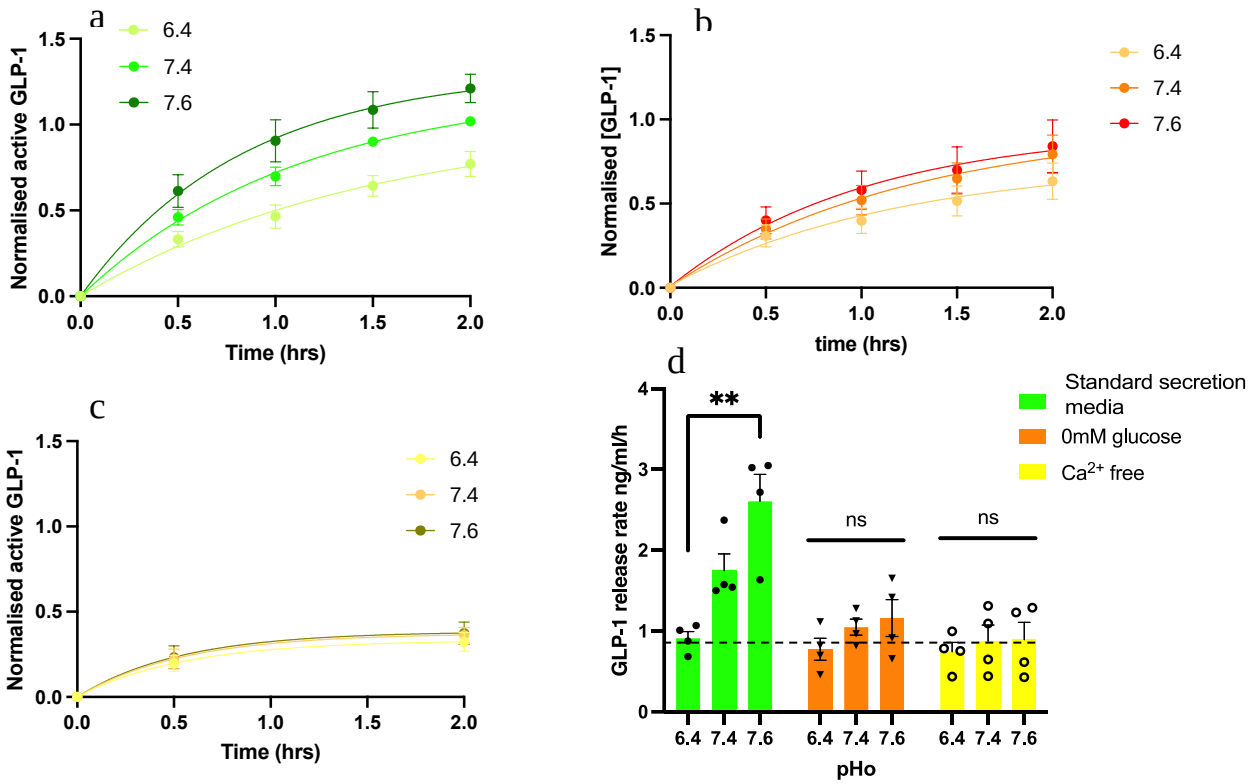


Figure 4.5 pHo dependence of the rate of active GLP-1 secretion. Measurements taken after 2hr incubation in CO_2/ HCO_3^--based media at pHo6.4, 7.4 and 7.6 in a) standard secretion media (10mM glucose) b) 0mM glucose or c) Ca^{2+} free conditions. 0.1ml samples were collected and replenished at regular 30mins intervals from each 0.25ml well. Secretion was normalized to the average [GLP-1] of 10mM glucose secretion from pHo 6.4, 7.4 and 7.6 at 2hrs measured in parallel on the same day. a,b,c) Time course of GLP-1 secretion in labelled conditions with the best fit line to the exponential equation y = a*(1-exp(-x/b)) and d) initial rate of GLP-1 secretion at pHo6.4, 7.4, 7.6.. Each point/bar represents mean±SEM from **n=4.** Significant values depicted as **p <0.01 (one-way ANOVA with Tukey's multiple comparisons test)

4.2.6 Rate of GLP-1 degradation is not affected by pH

To determine if the rate of GLP-1 degradation is affected by pH, supernatant samples of secretion buffer were taken 1hr after incubation with GLUTag cells (Fig4.2). Supernatant samples were incubated at 37degC, 5% CO_2, and at 0.5hr intervals samples were taken for [GLP-1] assay quantification. For all pH values, there was a significant decrease (between

-23 and -31%) in active [GLP-1] over the 2 hours ($p<0.0001$). However, GLP-1 degradation was not influenced by pH ($p=0.5181$, two-way ANOVA), and no significance was found between pH values at each time. Furthermore, fitting the graph to the best fit exponential curve: one-phase decay: y = a*(1-exp(-x/b)), although there appears to be a trend, the rate of degradation as a % change of [GLP]-1] per minute was not significantly different between pH values ($p=0.2476$, one-way-ANOVA).

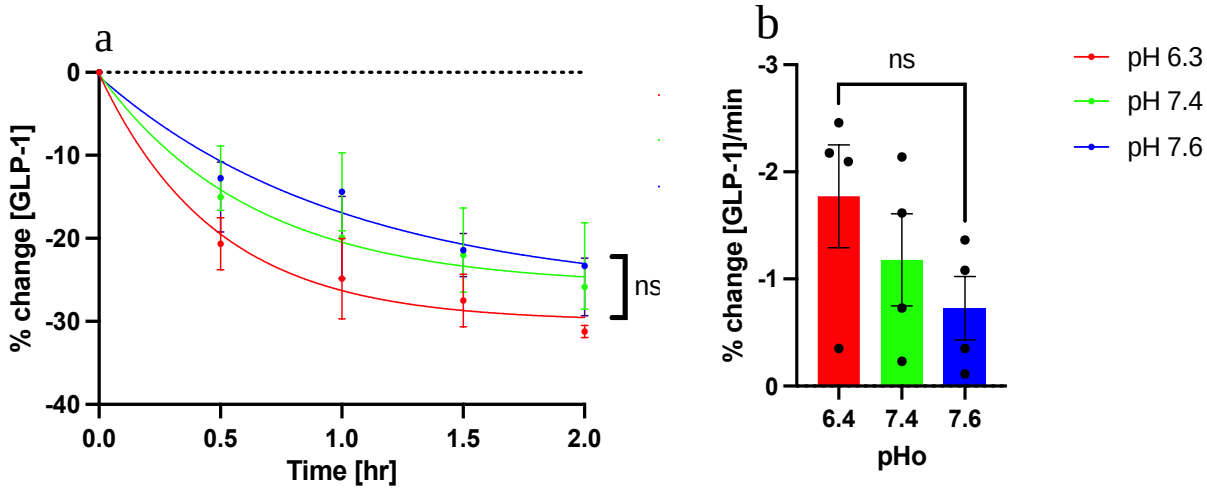


Figure 4.6 pHo dependence of the rate of GLP-1 degradation. Supernatant samples of secretion buffer were taken 1hr after incubation with GLUTag cells, samples were incubated at 37degC, 5% CO_2 and at 0.5hr intervals samples were taken for GLP-1 quantification. a) shows the % change of [GLP-1] in the samples relative to the initial reading at 0hr with the best fit line to the exponential equation y = a*(1-exp(-x/b)) and b) shows the initial rate of GLP-1 degradation. Each point/bar represents mean±SEM from **n=4**. ns depicts not significant (a) Two-way ANOVA and (b) One-way ANOVA with Tukey's multiple comparisons test.

4.2.7 Influence of mTOR signalling on pH-dependent GLP-1 secretion

Previous work from our laboratory found the amount of GLP-1 was higher in secretory granules, but the same in whole cell lysates, following 2-hour incubation in acidic pHo6.3 compared to pHo7.4. However, other studies have identified mTOR signalling as pH-dependent, inhibited at lower pH[157], and has been shown to regulate GLP-1 production[158]. Thus, the potential influence of mTOR signalling on the pH-dependence of GLP-1

secretion was assessed. Compared to the standard secretion media, the addition of 10nM rapamycin (mTOR inhibitor) significantly influenced active GLP-1 secretion (p=0.0002, two-way ANOVA). With rapamycin, the pH-dependence of GLP-1 secretion was lost (p=0.9410, one-way ANOVA), Fig4.7a. However, the pH dependence of GLP-1 secretion was still present with the mTOR activator, MHY-1485 (p=0.0002, one-way ANOVA). Results suggest pH-dependent mTOR inhibition does not solely underly the pH sensitivity of glucose-stimulated GLP-1 secretion.

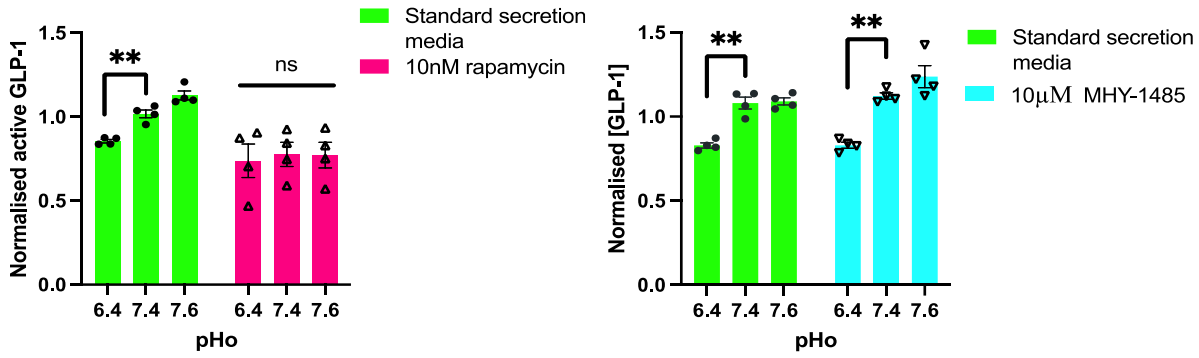


Figure 4.7 Influence of mTOR signalling. Measurements taken after 2hr incubation at pHo6.4, 7.4 and 7.6 in standard secretion media with a) 10nM rapamycin or b) 10μM MHY-1485 where labelled. Secretion was normalized to the average [GLP-1] of 10mM glucose secretion from pH 6.4, 7.4 and 7.6 measured in parallel on the same day. Each bar represents mean±SEM from **n=4**. Significant values depicted as **p <0.01 (One-way ANOVA with Tukey's multiple comparisons test)

4.2.8 Cell viability controls

To determine if cell viability is compensated when using different pH and superfusate composition, sulforhodamine B (SRB) assays were performed for every experiment. SRB assays were performed after 2-hour incubations. 520nm absorbance readings were corrected by subtracting background absorbance, and results are shown in Fig4.8. One-way ANOVA with comparison to the mean of pH 7.4 standard secretion media found there was no significant difference to the mean of each condition presented in Fig4.8 (p values

shown on graph) and cell viability was not compromised by any of the experimental conditions used in this study. Two results were statistically defined as outliers (circled red) and not included in statistical analysis (Grubbs method alpha = 0.05).

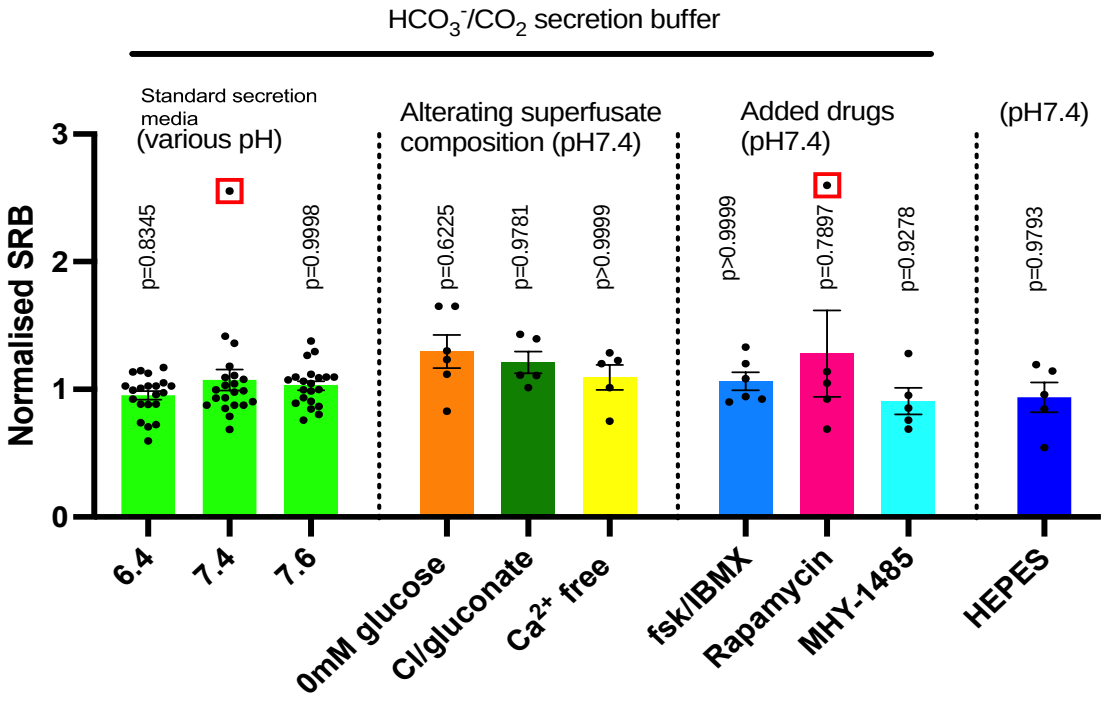


Figure 4.8 GLUTag cell viability following incubation in various conditions. Measured from protein biomass (sulforhodamine B (SRB) assay) at the end of the 2-hour incubation period. Results are normalized to the average SRB 520nm absorbance of 10mM glucose pHo6.4, 7.4, 7.6 measured in parallel on the same day. The statistical comparison was made to pHo7.4 standard secretion media (10mM glucose) (one-way ANOVA with Tukey's post hoc test).

4.3 Discussion

Preliminary data from our laboratory found that GLP-1 secretion from GLUTag cells is pH-dependent, with lower secretion seen when exposed to acidic extracellular pH. Here, I present results that support preliminary findings, confirming GLP-1 secretion is influenced by pH in physiological CO_2/HCO_3^- buffered media.

In preliminary results using HEPES buffer, the magnitude of the effect of pH on GLP-1 secretion appears to be greater than the results shown here. Using the same FRET-based assay kit, preliminary data showed a 2-fold increase in secretion at pH 7.6 compared to pH

6.5, whereas in CO_2/HCO_3^- buffered media a 1.3-fold increase was observed. However, these differences may reflect variability of GLUTag cell physiology. For example, glucose-stimulated GLP-1 secretion in GLUTag cells follows a dose-dependent increase, with maximal stimulation observed at 10mM glucose[88]. However, in the literature there is a large degree of variation of GLP-1 secretion at 10mM glucose, ranging from 1.5-fold[154] to 3.5-fold[85] compared to 0mM glucose media. Previous studies have even reported a total loss of glucose-responsiveness for unknown reasons, which has also been observed in our laboratory for some GLUTag cells when re-established from frozen stocks[161]. In this study using CO_2/HCO_3^- buffered media the glucose stimulatory effect on GLP-1 secretion was also markedly lower than preliminary data generated in HEPES buffer. At pH 7.4 GLP-1 secretion in 10mM glucose media was around 1.3 to 1.5-fold greater than 0mM glucose, whereas in preliminary findings over a 2-fold difference was consistently reported. Limited understandings of the physiology of GLUTag cells likely underlies the large variation of secretion results. One study has claimed that GLP-1 secretion is influenced by passage number, with more consistent results reported after passage 13-15[161]. Indeed, results collected at a later passage number (P15-18, Fig.4.4) appear to show greater glucose- and pH-dependent GLP-1 responsiveness than earlier experiments (P12-15, Fig. 4.3). Potential physical and molecular damage of cryopreservation on cells may underly these secretary impairments[162]. Furthermore, research has shown different cryopreservation protocols, such as optimal cooling and thawing rates, and the type and concentration of cryoprotectants can improve post-cryo viability and function in a cell-specific manner[162,163]. As well, secretagogue-stimulated GLP-1 secretion in GLUTag cells appears to follow a circadian pattern[164], which could also contribute to secretory response variation. Thus, for future experiments it may be worth investigating the influence of

cryopreservation on the integrity of GLUTag cells to stabilise physiology and increase the reproducibility of results.

Nonetheless, comparable to preliminary data generated in HEPES buffer, GLP-1 secretion CO_2/HCO_3^- buffered media at pH 6.4 decreased by a similar degree as incubating cells in 0mM glucose, suggesting the stimulatory effect of 10mM glucose is attenuated at acidic pH. As mentioned previously, non-physiological buffers can have significant effects on pH regulation. Cellular systems are adapted to accommodate a CO_2/HCO_3^- buffering regime (e.g. gaseous exchange of CO_2 (g) and transmembrane transport of HCO_3^-)[139] which may become particularly relevant when studying the response of an intracellular system to extracellular pH[4]. However, results from Fig4.3b appear to suggest the influence of extracellular pH on GLP-1 secretion is independent of the buffer used and the presence of HCO_3^-. Crucially, the pH dependence of GLP-1 release was reproduced by different researchers, in two different labs, using two different buffer systems. Both studies show that GLP-1 secretion from GLUTag cells is pH-dependent, with differences between the two studies likely representing variation of the GLUTag cell batch, rather than the buffering regime of the media.

Several factors could influence the pH-dependence of GLP-1 secretion. One of these factors could be pH-dependent degradation of GLP-1. GLP-1 is subject to rapid degradation by the proteolytic enzyme, dipeptidyl peptidase-4 (DPP-4), which cleaves active GLP-1 (7-36amide and 7-37) into its truncated inactive form, GLP-1 (9-36amide and 37)[165]. In GLUTag cells, mRNA expression and secretion of DPP-4 has been confirmed[166] likely acting on active GLP-1 in the secretion buffer. However, although active GLP-1 appeared to degrade on average -25% over a 2-hour period, despite a trend,

the pH of the secretion buffer did not significantly affect the rate of degradation (Fig4.2). Furthermore, as the optimum activity of DPP-4 is at pH 7. 8[167], it can be assumed any influence of pH on the rate of GLP-1 degradation is insufficient to significantly effect results.

The role of pH for the amidation of GLP-1 was also considered. In physiological systems, active GLP-1 occurs in an amidated (7-36 amide; 80%) and glycine-extended (7-37; 20%) form. The amidated form is predominantly secreted from the pancreas and glycine-extended from the ileum and hypothalamus[106]. System-wide actions of the two peptides are comparable[168], however, the amidated form appears to have a longer half-life in plasma[169]. The majority of GLP-1 is amidated by the peptidyl-α-hydroxyglycine α-amidating lyase (PAM), with optimal activity at pH 5.0[170]. The FRET-based assay used in this study detects only the active forms of GLP-1, amidated and glycine-extended. Whereas the sandwich ELISA detects only the amidated forms of GLP-1, active and inactive. Results from the sandwich ELISA appear to show a similar pH dependence as observed with the FRET-based assay and GLP-1 secretion is attenuated at low pH. Further investigations could be informative of the pH-dependence of GLP-1 amidation, however, requires immunoassay detection kits with lower cross-reactivity and greater sensitivity to each GLP-1 form.

As alterations of intracellular pH effect a large variety of cellular processes[155,156], it is also worth considering pathways that may indirectly influence GLP-1 secretion. For example, intracellular acidification (around 0.3-0.4 pH units) has been recognised to precede apoptosis in cells[171] and trigger acidic stress signalling in the mitochondrion and endoplasmic reticulum. However, effects of acidic exposure on cell viability appear to only be significant after 24hrs[172]. Furthermore, SRB assay results demonstrate GLUTag

cell viability was not compensated by incubation in acidic media over the time course of these experiments. Thus, it is unlikely this impacted the pH-dependent response of GLP-1 secretion.

It has also been recognised that mTOR signalling, responsible for regulating cell metabolism, growth and survival, is pH-dependent[157] and influences GLP-1 production[158]. Results here show that in the presence of the mTOR inhibitor, rapamycin, GLP-1 secretion is inhibited and there is a loss of pH-dependence. However, mTOR signalling is known to influence multiple pathways[173], thus inhibition likely has many indirect impairments to GLP-1 secretion. As well, in the presence of the mTOR activator MHY-1485, pH-dependent secretion is still observed. However, whilst the pH sensitivity of GLP-1 secretion isn't dependent on alterations of the mTORC1 pathway, we cannot disregard a potential influence. Furthermore, previously, the influence of mTOR signalling on GLP-1 secretion has only been investigated over longer time periods (minimum 24hr), with rapamycin-dependent inhibition detectable after 12hr of exposure[174]. Within this study Western Blots for the mTOR activity surrogate markers, phospho-S6 (pS6) and S6, were taken, however results were inconclusive due to nonspecific antibody binding (results not shown). Thus, before further assessment of the acute influence of pH-dependent changes in mTOR signalling on GLP-1 secretion, confirmation that mTOR signalling is in fact altered by pH within the 2hr time course is required.

As well as total amount of GLP-1 secreted, results shown here demonstrate that the rate of GLP-1 secretion from GLUTag cells is also dependent on pH (Fig4.6). Interestingly, the effect of pH on rate is markedly greater than the effect on total GLP-1 secretion at 2hrs. At pH 7.6 compared to pH 6.4, rate was increased around 2.5-fold, whereas total production around 1.3-fold. This points to a pH-sensitivity of the exocytotic mechanisms which

underlies the pH-dependence of GLP-1 secretion within the 2hr experimental time window. Supporting this, much evidence suggests an important role of intracellular pH for protein transport[112,175]. Intraorganellar pH is regulated by the vesicular membrane V-ATPase, with activity directly influenced by changes in cytoplasmic pH[136]. In fact, preliminary results from our laboratory found that the addition of the V-ATPase inhibitor, bafilomycin A1, at pH 7.4 reduced GLP-1 exocytosis to a similar level as lowering the pHo to 6.8. Similarly, in yeast, deficiency of V-ATPase activity was shown to disrupt membrane trafficking of proteins, with impairment rescued by increasing medium pH[136]. It is thought vesicular proton gradients are important for the priming of granules and fusion to the target membrane via SNARE proteins[105,107,134,137]. Indeed, preliminary results from our laboratory found the GLP-1 content is higher in the secretory granules from cells incubated in acidic pHo, hinting at GLP-1 vesicle retainment. Furthermore, specifically for the synthesis of GLP-1, the acidic pH of granules regulates the activity of PC1/3, responsible for the post-translational processing of proglucagon to active GLP-1[112,176]. Thus, it could be suggested that changes in intracellular pH influence the intraorganellar pH via alterations of V-ATPase activity, which in turn impacts rate-limiting secretory mechanisms. However, bafilomycin A1 treatment has been shown to acidify pHi in cancer cells[147], which could also underlie impaired GLP-1 secretion. As well, observations of the effects of bafilomycin A1 should be taken with caution as the agent is known to cause toxicity, impairing many cellular pathways and compromising viability[177]. Nonetheless, it is clear results demonstrate a significant sensitivity of GLP-1 secretion rate to extracellular pH, suggesting influences of exocytotic mechanisms.

There are several limitations to the method used to investigate GLP-1 secretion rate in this study. Firstly, RNA-sequencing has confirmed the expression of GLP-1 receptor (GLP-1R), demonstrating the presence of a feedback system[178]. Evidence has shown exposure of GLUTag cells to the GLP-1 mimetic, exendin-4, increases acute GLP-1 secretion in a positive feedback loop[179]. Here, the protocol used to investigate the rate of GLP-1 secretion involved taking and replenishing incubation media at regular intervals. These repetitive serial dilations may have disrupted paracrine/autocrine regulation of GLP-1 secretion. Secondly, GLP-1 secretion is known to follow a biphasic secretion pattern with the 1st peak at 1-6 minutes and the 2nd at 7-12 minutes in GLUTag cells[114]. In the pancreatic β-cells the 1st and 2nd phases of insulin secretion have been shown to have distinct regulation patterns[180]. In this study samples were collected every 30mins, thus it was not possible to further dissect influences of pH on the secretion pattern of GLP-1. However, the validity of results would have been compromised by reducing the incubation time between sample collections as removing cells from the 5% CO_2 incubator causes immediate alkalisation and pH fluctuations. As used in *ex vivo* and *in vivo* studies, ideally, a perfusion set up should be used to investigate live changes in GLP-1 secretion. However, for culture studies this would be challenging given GLP-1 secretion from cells in this set up would likely be out of range of the detection capabilities of kits currently available. The most robust method for studying GLP-1 secretory dynamics in GLUTag cells involves live-imaging and tracking of intracellular GLP-1. In the next chapter I will assess the use of a potential novel GLP-1 surrogate marker, tPA.

Alternatively, proton-dependent modification of ion-selective channels could be another influence of pH on GLP-1 secretion is. Preliminary data found that in the absence of Na^+, which would prevent the initial membrane depolarization of GLUTag cells via Na^+-

dependent- and glucose co-transporters, such as the SGLT1 and voltage gated Na^+ channels, GLP-1 secretion was still pH sensitive following membrane depolarisation by the addition of KCl. As such, it is reasonable to assume pH-dependent glucose-stimulated GLP-1 secretion is independent of glucose sensing via the SGLT1 and the pH sensitivity of secretion is driven by a mechanism downstream of membrane depolarisation. Furthermore, the sensitivity of GLUTag cells to pH does not depend on the transmembrane transport of Na^+, such as via the NHE or Na^+-coupled HCO_3^- transporters[141]. This suggests the response of GLP-1 secretion to extracellular pH is transduced via changes in intracellular pH independent of Na^+-dependent transporters or via surface-expressed H^+ sensors.

Ca^{2+}plays a crucial role for stimulant-triggered GLP-1 vesicle exocytosis[40]. Thus, unsurprisingly, in the absence of Ca^{2+}, total amount and rate of GLP-1 was significantly attenuated. Interestingly, preliminary results found a trend for extracellular [Ca^{2+}] to have a steeper dose-response curve for glucose-stimulated GLP-1 at pH 7.4 compared to pH 6.4. However, the multifactorial role of Ca^{2+}, from action potential generation[40] to exocytotic membrane fusion[115], makes observations difficult to evaluate. Nonetheless, findings from pancreatic β-cells showed extracellular pH significantly influenced glucose-stimulated [Ca^{2+}]i responses[181]. However, it was actually shown external acidification increases [Ca^{2+}]i levels with enhanced β-cell activity[182], opposing suggestive influences of acidification on the rate of GLP-1 secretion presented in this study. Within this study time limitations prevented further investigation, however, in the future it may be informative to use fluorescence Ca^{2+} indicators and dyes[183] to assess the real-time influence of extracellular pH on the glucose-stimulated Ca^{2+} response in GLUTag cells.

Previous results from our laboratory showed GLP-1 secretion was highly dependent on Cl^- with similar findings reported for insulin secretion from pancreatic β-cells[134]. It is hypothesised that Cl^- is important for GLP-1 secretion due to the role of ClC-3 on vesicle membranes, which acts to counter the electrical gradient of granule acidification during maturation[134]. However, Cl^--dependent membrane transporters are known to play a significant role for pH regulation[4,143], thus, complete removal of Cl^- can have a significant impact on intracellular pH[144] leading to misleading inferences of data. In this study, the use of a CO_2/HCO_3^- buffer meant media with lower $[HCO_3^-]$ had a higher extracellular $[Cl^-]$ to account for osmolarity differences. To investigate the influence of varying extracellular $[Cl^-]$ at different pHo values, osmolarity regulating excess Cl^- was replaced with gluconate. When conducting these experiments, low n numbers from financial constraints limited statistical analysis. As such, although there still appears to be a trend for pH-dependent GLP-1 secretion (Fig4.5), it is worth considering discussion points for both scenarios where a trend remains or is lost in constant $[Cl^-]$ media, where specifically, there is lower extracellular $[Cl^-]$ at acidic pHo compared to the standard secretion media. Importantly, results from Chapter 3 show pHi at pHo6.4 is significantly alkalinised (by around 0.1 pH units) in the constant $[Cl^-]$ media (Fig3.3). As such, if the trend is indeed correct, this could suggest, either the pH-dependence of GLP-1 secretion is independent of Cl^- or detected by surface-expressed H^+ sensors, or both. On the other hand, if the trend was lost, the opposite could be inferred, that the pH-dependence of GLP-1 secretion is dependent of Cl^- and/or detected by changes in pHi. Therefore, two main further investigations will be required to dissect the underlying mechanism of Cl^--dependent GLP-1 secretion. Firstly, current experiments will need to be repeated to strengthen statistical power and confirm if a similar pH-dependence of GLP-1 secretion is found or lost when using constant $[Cl^-]$

media compared to the standard secretion media. Secondly, whether the influence of extracellular Cl^- is mediated by a direct effect, such as influencing the rate of vesicular exocytosis via the ClC-3 transporter, or an indirect effect by altering pHi which in turn influences secretion. However, to investigate the latter, due to the multifactorial nature of Cl^- for pHi regulation and GLP-1 secretion, more sophisticated methods, such as ClC-3 KO model, will fundamentally be required.

In conclusion, results here confirm the pH sensitivity of GLP-1 secretion in GLUTag cells, irrespective of the use of non-physiological (HEPES) or physiological (CO_2/HCO_3^-) buffering system. As well as total GLP-1 secretion, it was also shown the rate of GLP-1 secretion is pH-dependent, which could be due to the pH sensitivity of ionic transport and/or exocytotic machinery. In future experiments, due to the independence of pH-regulation and GLP-1 secretion systems, a wider range of sophisticated experimental method will be required to further dissect the pH-sensitivty of GLP-1 secretion, such as, live-tracking of intracellular GLP-1, fluorescence Ca^{2+} indicators, and KO models of key ion channels.

5 Visualisation of intracellular GLP-1 in GLUTag cells

Currently, the influence of extracellular pH on an intracellular process, GLP-1 secretion, has been assessed using extracellular measurements (e.g., GLP-1 in the incubation media). As such, the use of alternative methods, such as cell imaging, can provide unique and novel insights into the responses of intracellular regulatory systems and protein dynamics. In this chapter I describe how GLP-1 secretion in GLUTag cells was visualized with the aim of confirming and further dissecting the pH-sensitivity of the system.

5.1 Live-cell imaging of intracellular GLP-1 with tPA-Dendra2

Investigations of intracellular GLP-1 dynamics would preferentially involve a fluorescent-tag for real time-visualisation of GLP-1. However, as GLP-1 is generated from post-translational processing of preproglucagon[100], direct labelling of the hormone is experimentally challenging and has not been achieved to date. Previous work from the Gribble group in Cambridge tried to overcome this issue by assessing the localisation of alternative fluorescent protein (FP)-tagged peptide hormones which is co-loaded with GLP-1into vesicles in GLUTag cells[184]. The group showed that transfection of GLUTag cells with a plasmid expressing tPA, tissue plasminogen activator, showed high co-localisation of tPA with GLP-1 containing vesicles[184]. Using Total Internal Reflection Fluorescence (TIRF) microscopy, the fluorescent dynamics of tPA-GFP-expressing vesicles could be observed live in GLUTag cells. L-ornithine application, a known secretagogue of GLP-1, was reported to induce sparks of fluorescent spots, described as rapid transient increases in fluorescence intensity which then dimmed. This was thought to represent single exocytotic events, demonstrating vesicular fusion causing a fast reduction in pH-dependent quenching of the fluorescent protein followed by its extracellular

release[184]. Furthermore, consistent with the observed ELISA measurements of GLP-1 secretion in the extracellular media, the co-administration L-ornithine signalling inhibitors significantly decreased the frequency of tPA-GFP fusion events. Supporting these results, using the same technique, another group observed increased spark frequency within 6 minutes of high K^+ exposure[185], which is known to significantly trigger GLP-1 secretion[114]. Results demonstrate the potential of FP-tPA to monitor GLP-1 secretory vesicles for live cell imaging.

Tissue-type plasminogen activator (tPA) is a serine protease, primarily responsible for catalysing the conversion of plasminogen to plasmin, subsequently dissolving fibrin clots in the vasculature[186]. Expression of tPA has also been identified in neuronal populations, including neuroendocrine cells of the hypothalamus[187], pancreas (somatostatin cell)[188] and adrenal medulla (chromaffin cell)[189], and is thought to be important for neuronal survival and synaptic plasticity[190]. Currently, the exact role of tPA in enteroendocrine cells in unknown.

No study has specifically investigated tPA secretion regulation in GLUTag cells. However, similar to GLP-1 secretion in GLUTag cells, tPA secretion is thought to be targeted to the regulated secretory pathway in neuroendocrine cells[191,192]. As well, in neuronal pre-synaptic terminals, tPA was found in large dense core vesicles (LDCV) localized in close proximity to VAMP2 positive vesicles[193]. Although there is current uncertainty to the reason why, in the neuroendocrine chromaffin cell, tPA was also found to be co-released in parallel with catecholamines in response to secretagogue stimulation[191]. tPA exocytosis was shown to increase in response to depolarisation (high K^+ exposure) and be abolished by Ca^{2+} channel blockers, similar to that seen for insulin and GLP-1[194]. Thus, together

with previous work confirming tPA co-secretes with GLP-1[184], fluorescently labelled tPA analogues appear to be a good surrogate marker to visualise GLP-1 exocytosis events.

Dendra2 is a photoactivatable fluorescent protein (PAFP) that switches from green to red fluorescent states in response to either visible blue or UV-violet light exposure[195]. The photoconversion is irreversible and can therefore be used to label proteins and track intracellular dynamics following activation at an experimental time zero. For example, in HeLa cells transfected with a Dendra2-tagged protein vector, the protein could successfully be photoactivated at specific intracellular sights (eg. the nucleus) and a red fluorescent signal detected[196]. By using a laser scanning confocal microscope to detect real-time changes of fluorescence signal intensity, at the sight of photoconversion, significant decreases in red fluorescence were recorded within 5 seconds[196]. The photoactivated red fluorescent protein appeared to diffuse throughout the cell, likely representing intracellular protein mobility[196].

The redistribution of Dendra2 could accurately be monitored, thus, presents a potential method to study intracellular protein dynamics in response to changes of extracellular conditions.

Taken together, data from the literature provide strong evidence for tPA-Dendra2 will be a useful tool for disentangling the secretory dynamics of GLP-1. In this chapter I investigated the use of tPA-Dendra2 for the live-imaging of GLP-1 in GLUTag cells with the aim to further dissect the pH-sensitivity of GLP-1 secretion regulation.

5.1.1 Plasmid transfection

GLUTag cells could successfully be transfected with tPA-Dendra2 and green fluorescence (488nm) was visualised (Fig5.1) Distinct regions of green fluorescence were observed, likely representing subcellular localisation to cytoplasmic vesicles. Negligible green signals in non-transfected control cells were seen (not shown). Using the Zeiss confocal microscope, in live cells successful photoconversion of tPA-Dendra2 could be achieved following 405nm exposure, represented by irreversible conversion from a green (488nm) to red (561nm) fluorescent state (Fig. 5.1). Hoechst staining was not included due to 405nm exposure likely interfering with the dye. The white circle in Fig5.1A is a representative example of a ROI used for analysis.

The optimal parameters for Dendra2 photoconversion and imaging can vary amongst tagged proteins and cell types[197]. Too-weak illumination can result in low conversion efficiency, but too-strong illumination can bleach the red signal and risk cellular damage[197,198]. Thus, to optimise activation conditions, different % laser intensity and durations of irradiation were tested. In each test conditions, intensity of the 488nm and 561nm fluorescence signal from 3 non-overlapping ROI of the same frame were averaged. A 40% laser intensity for 60x iterations was found to have the highest green to red photoconversion efficacy, thus will be used throughout the rest of this investigation.

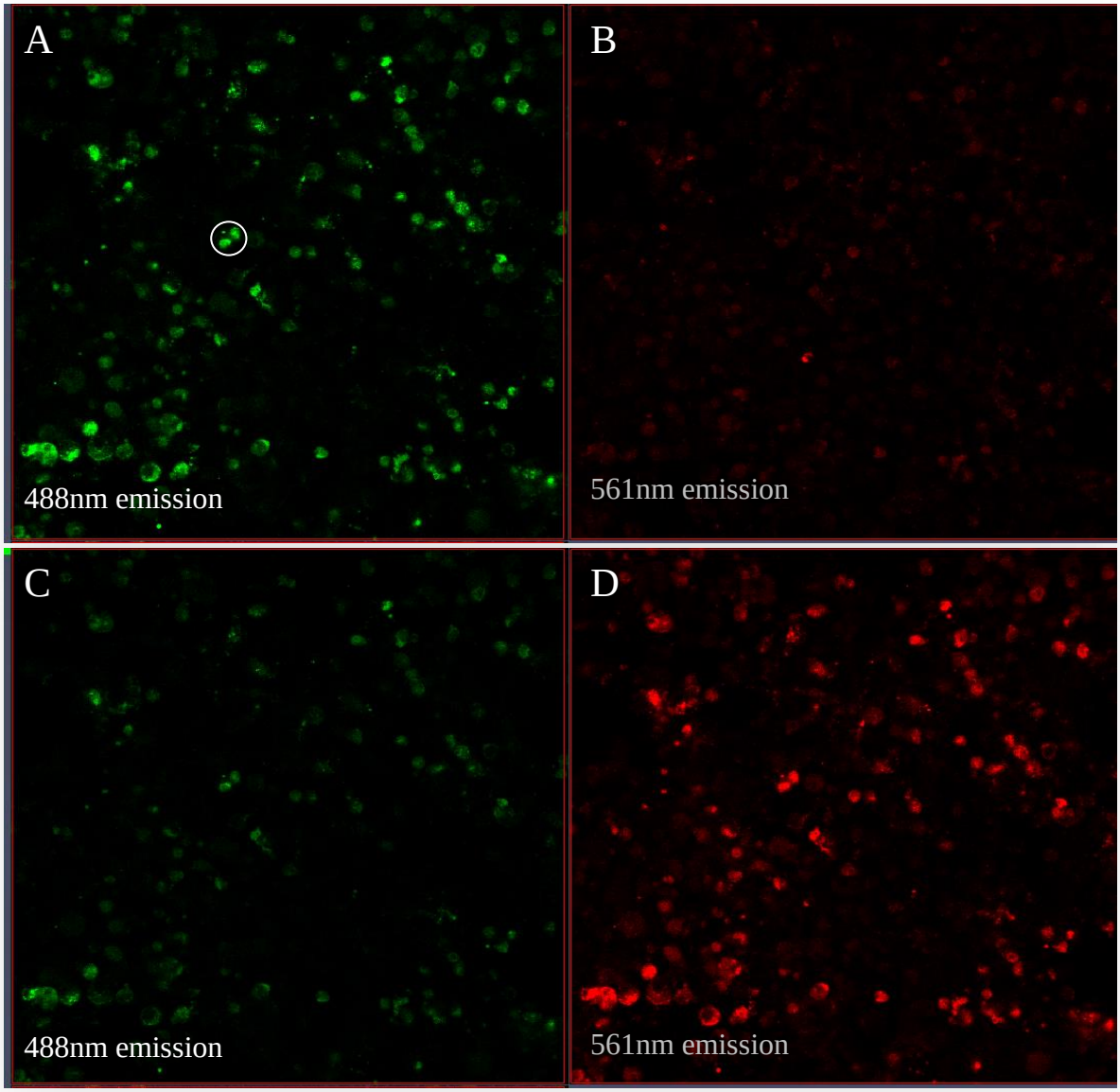


Figure 5.1 tPA-Dendra-2 photoconversion from green to red in GLUTag cells**.** Live cell imaging snapshots of GLUTag cells before and after exposure to 405nm light (60x iteration, 40% intensity). A, B) GLUTag cells pre-photobleach; C,D) GLUTag cells post-photobleach. The white circle in A) is a representation of a ROI used for analysis.

5.1.2 Initial recordings

If tPA-Dendra2 was successfully tracking intracellular GLP-1 secretory vesicles, following photobleach, it would be expected that red fluorescence levels will steadily decrease representing tPA-Dendra2 exocytosis. Whereas green fluorescence levels would stay

consistent or steadily increase dependent on the rate of production of novel tPA-Dendra2 protein.

In a single frame, Dendra2 was bleached by 405nm exposure, 40% intensity and 60x iterations. Initially, a CO_2 chamber was used to replicate physiologically relevant conditions. This meant cells could be incubated in standard bicarbonate buffer at 5% CO_2 and 37C.

Following photoconversion, visually there was no obvious change in the red signal. Furthermore, there was no significant change of the average intensity of the 488nm and 561nm fluorescence signal, Fig5.1.2), with fluctuations likely representing movement artefacts. Strong evidence has shown tPA[199] and GLP-1 secretion[40] is stimulated by cAMP-dependent pathways. However, recordings made following the addition of 10µM fsk/IBMX still observed no clear change in either green or red signal (data not shown).

The nature of the CO_2 chamber set up meant the effects of fsk/IBMX stimulation could only be investigated after the addition of the agents. As such, it was postulated the effects of fsk/IBMX on GLP-1 secretion were so rapid that changes in tPA-Dendra2 fluorescence were missed, occurring before the cells could be microscopically visualised. Thus, a perfusion set up was used to visualise tPA-Dendra2 fluorescence precisely at the moment when GLUTag cells are exposed to alterations of the superfusate composition. However, during the perfusion of 10uM fsk/IBMX media, no changes of red or green fluorescence were visually or quantitatively observed, Fig5.1.2. Furthermore, high extracellular K^+, known to instantaneously stimulate significant GLP-1 secretion in GLUTag cells[40], failed to induce changes to the fluorescence signal (data not shown).

NCI-H716 are another cell line widely used to study mechanisms underlying GLP-1 secretion. NCI-H716 cells are specifically a human L-cell line, derived from ascites fluid of a human with adenocarcinoma of the colon[200]. As an alternative L-cell line, the potential of tPA-Dendra2 to monitor intracellular GLP-1 protein dynamics was also assessed in NCI-H716 cells. At a high efficacy similar to GLUTag cells, NCI-H716 cells could successfully be transfected with tPA-Dendra2 and successful photoconversion of Dendra2 from green to red fluorescence observed (data not shown). However, no changes in green or red fluorescence were seen during live-imaging of NCI-H716 cells using a confocal microscope, even during the perfusion of fsk/IBMX and high K^+ (data not shown). Therefore, as no changes were observed following significant exogenous stimulation of GLP-1 secretion in both cell lines, GLP-1 exocytosis events could not be observed using tPA-Dendra2 as a marker with confocal laser scanning microscopy.

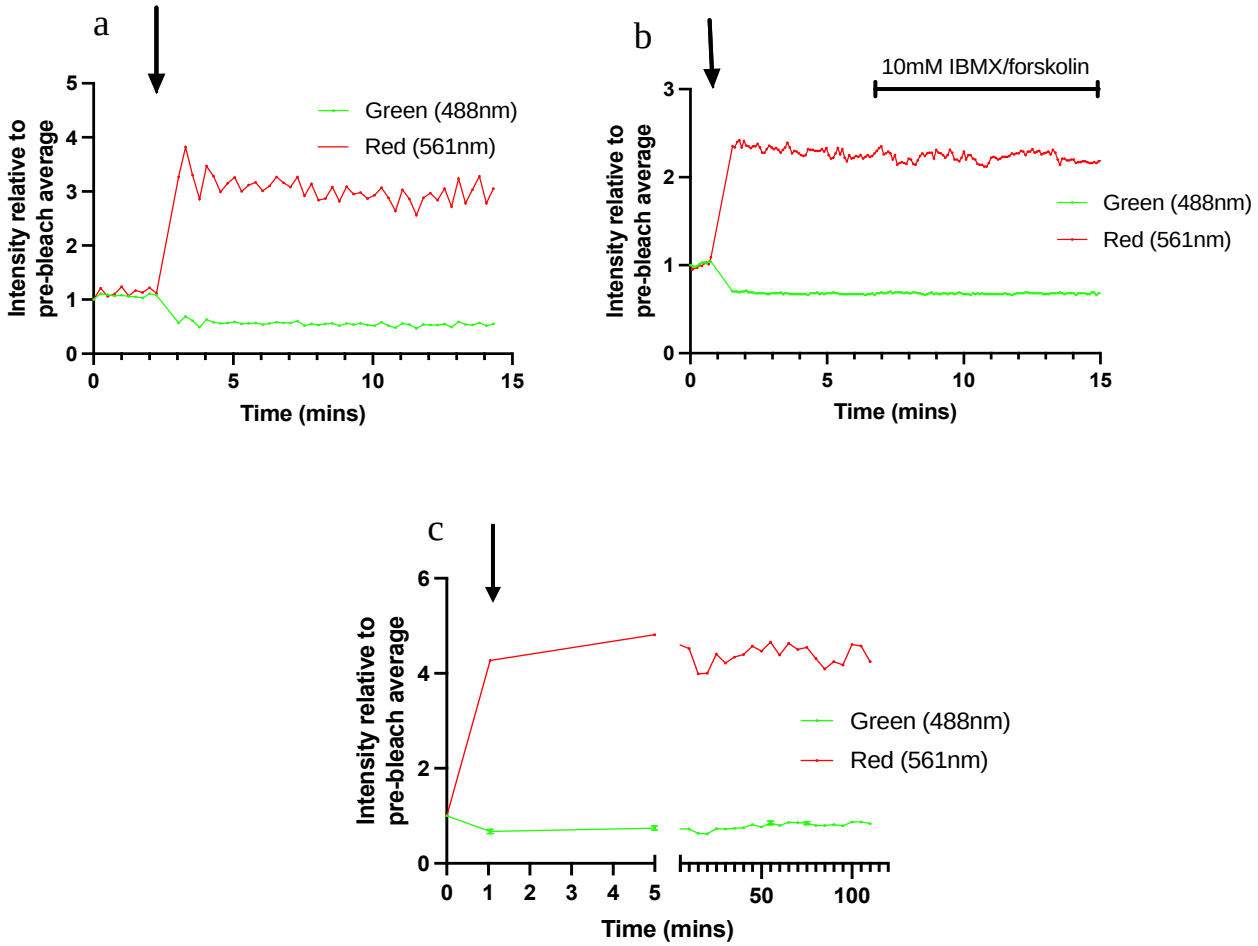


Figure 5.1.2 Relative change in tPA-Dendra2 fluorescence intensity in 561nm (red) and 488 nm (green) excitation regions after photoconversion at 405nm, 60x iterations and 40% intensity (arrow). Scans were taken every 30 seconds. All recordings were taken at 37C. Cells are in 10mM glucose, pHo7.4 a) bicarbonate buffer at 5% CO_2 or b,c) HEPES buffer with b) 10µM fsk/IBMX perfusion where labelled. Results show the average relative change of fluorescence intensity from 3 non-overlapping ROI in each frame.

5.1.3 Troubleshooting

Further experimental investigations were carried out to determine if the set up or imaging parameters being used were implicating exocytosis visualisation. For technical ease, tPA-transfected GLUTag cells were incubated in pH7.4 HEPES buffer solution in 10mM glucose.

Firstly, the potential cell damage of bleaching impairing secretory mechanisms was investigated[197,198]. Photoconversion from 405nm exposure at lower intensity (30%) and

iterations (5x) was used. However, no significant changes were observed, even in the presence of 10uM fsk/IBMX or high K^+ (data not shown). Even in the absence of photobleaching, following cAMP-dependent or depolarisation stimulation no decreases in green signal could visually or quantitatively be observed (data not shown).

To determine if a longer time frame was required to observe meaningful changes of Dendra2 fluorescence, a 2-hour time course was taken Fig5.1.2C. No obvious changes in red or green signal representing exocytosis were seen. The slope generated from the red emission did not significantly deviate from zero ($p=0.9668$), however, the green emission had a significant positive linear regression (slope = 0.001734, $p<0.0001$) which could represent the production of novel green emitting tPA-Dendra2.

5.1.4 GLP-1 assay of tPA-Dendra2 transfected cells

To determine if GLP-1 secretion is impaired in cells with tPA-Dendra2 transfection, a 2-hour secretion assay was performed. In standard bicarbonate buffer, 10µM fsk/IBMX induced a significant increase in GLP-1 secretion in tPA-Dendra2 transfected cells, however, stimulation was significantly lower compared to control cells ($p=0.0048$). This impairment is likely due to lipofectamine exposure and not transfection, as GLP-1 secretion is equally lowered with or without the presence of the plasmid ($p>0.9999$). Nevertheless, results demonstrate GLUTag cells maintain GLP-1 secretion following tPA-Dendra2 transfection.

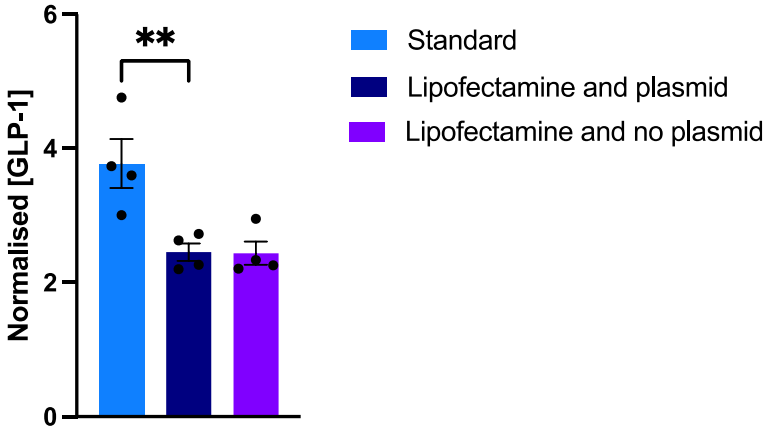


Figure 5.1.3 cAMP-stimulated GLP-1 secretion from tPA-Dendra2 transfected GLUTag cells. Measurements taken after 2hr incubation in standard secretion media (CO_2/HCO_3^- buffer with 10mM glucose), at pHo7.4 treated with 10uM fsk/IBMX. Results are normalized to secretion at 10mM glucose measured in parallel on the same day. Each bar represents mean±SEM from **n=4.** Significant values depicted as **p <0.01. One-way ANOVA with Tukey's multiple comparisons test.

5.1.5 Sequencing tPA-Dendra2 plasmid

As tPA-Dendra2 did not show the anticipated visualisation of secretion using confocal microscopy, we tested if the DNA sequence of the plasmid was correct. The partial sequence of the transformed tPA-Dendra2 plasmid is shown in Appendix 1. From the 2380-base length provided by Addgene for the partial sequence of tPA-linker-Dendra2, the obtained sequencing results had 99.72% similarity. Other sequenced portions of the plasmid (Dendra2-R, CMV-F and SV40pA-R) provided by Addgene were identified within sequencing results (see Appendix 1), all of which had >99% similarity.

5.1.6 Co-localisation of tPA-Dendra2 with anti-GLP-1

To confirm the co-localisation of tPA with GLP-1, transfected cells were immunolabelled for GLP-1. A secondary antibody with a non-overlapping excitation and emission spectra was used to distinguished signals. A representative image of co-stained cells is shown in Fig5.1.4. Results shown here appear to show tPA-Dendra2 does not overlap with

intracellular GLP-1, suggesting tPA is not co-loaded with GLP-1 vesicles in GLUTag cells.

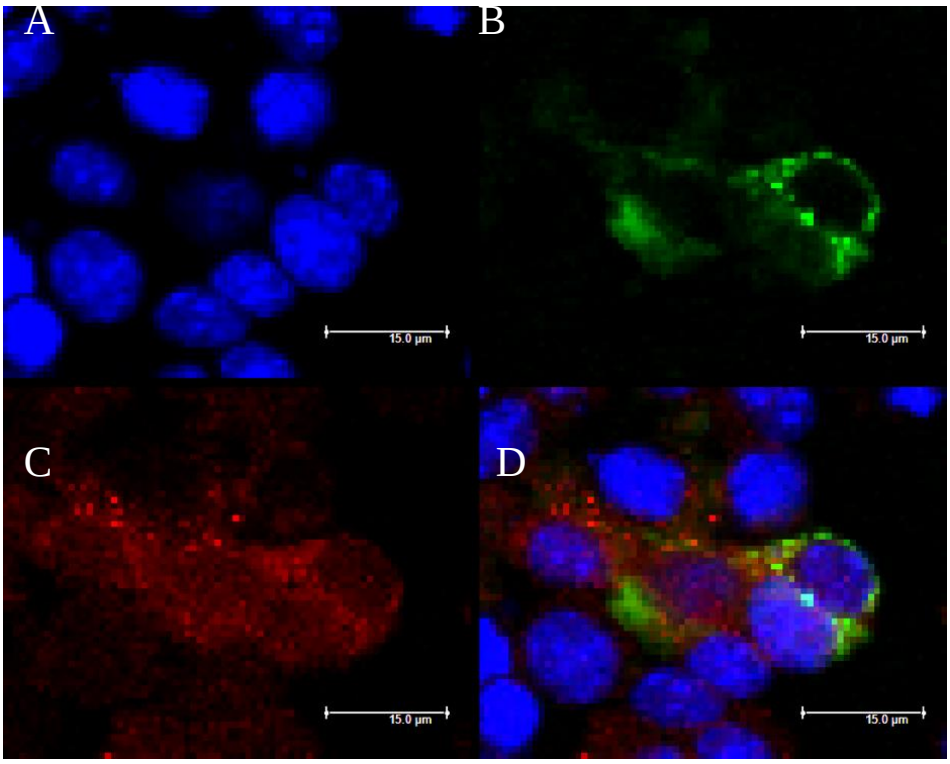


Figure 5.1.4 Fixed cell imaging of tPA-Dendra2 transfected GLUTag cells with anti-GLP1 immunolabelling. A) Hoechst nuclear staining B) tPA-Dendra2 imaging C) anti-GLP-1 immunolabelling D) overlay. Scale bar 15 um

5.2 Fixed-cell imaging of intracellular GLP-1

As the visualization of GLP-1 movement with tPA-Dendra2 was unsuccessful, alternative methods to image GLP-1 in GLUTag cells were explored. Immunofluorescence labelling allows detection and localisation of intracellular proteins. The technique permits the visualisation of target proteins through the combined use of specific antibodies and complementary fluorophores. Furthermore, the amount of protein at the time of cell fixation can be quantified using the intensity signal of the fluorescent probes[201]. Laser Scanning Confocal Microscopy (LSCM) allows high-resolution images of bright

fluorophores to be obtained, and with accurate optimisation, has the potential to detect differences in signal intensity[202]. Computational methods, here a MatLab code (see Supplementary code 1), can quantify the pixel density (representing the fluorescent signal) of a region of interest, such as a cell, to represent the intracellular concentration of a targeted protein.

Influences on protein secretion dynamics can also be assessed by analysing intracellular vesicular retention. For example, if exocytotic mechanisms are inhibited, such as secretory granule maturation and fusion, it may be expected that a larger quantity of the secreted protein is found within the cell (ie intracellular). Preliminary findings done in HEPES buffer showed that in GLUTag cells whole cell content GLP-1 was not pH dependent, but rather that a higher amount of active GLP-1 was retained in secretory granules following a 2-hour incubation in pH6.3 compared to 7.4. These results suggest decreases in GLP-1 secretion at low extracellular pH may be due to disrupted exocytotic mechanisms. I therefore attempted to use automated immunolabelling quantification to assess the influence of extracellular pH on GLP-1 vesicle retention in GLUTag cells.

5.2.1 Method

To investigate the influence of pH on GLP-1 production and retention, following a 1-hour pre-incubation at pHo7.4 in standard secretion media (CO_2/HCO_3^- buffer with 10mM glucose), GLUTag cells either remained in standard secretion media pHo7.4 or were exposed to acidic (pHo6.4) or alkali (pHo7.6) media with/out either 10µM fsk/IBMX or 10nM rapamycin. Cells were also incubated with 10mM bafilomycin and Ca^{2+}-free conditions, however, adhesive and/or cell viability complications meant an insufficient

number of cells could be imaged for analysis. At 1-, 2- and 4-hour intervals, cells were fixed for immunofluorescence staining and imaged using Laser Scanning Confocal Microscopy. A representative image of GLUTag cells with anti-GLP1 immunolabelling is shown in Fig5.2.1A-C. For each condition and time point, 3 distinct, non-overlapping images were taken from each well. A MatLab code (see Supplementary code 1) was generated to identify individual cells by particle analysis of Hoechst-33342 nuclei staining and quantify the pixel density of the green fluorescent signal for each cell. The raw quantified immunofluorescence intensity output from images of GLUTag cells incubated in 3 different conditions (pHo6.4, 7.4, and 7.6) is shown in Fig5.2.1D. Consistency of the cell area output (Fig5.1.2E) between conditions suggests the code can successfully distinguish individual GLUTag cells from input images.

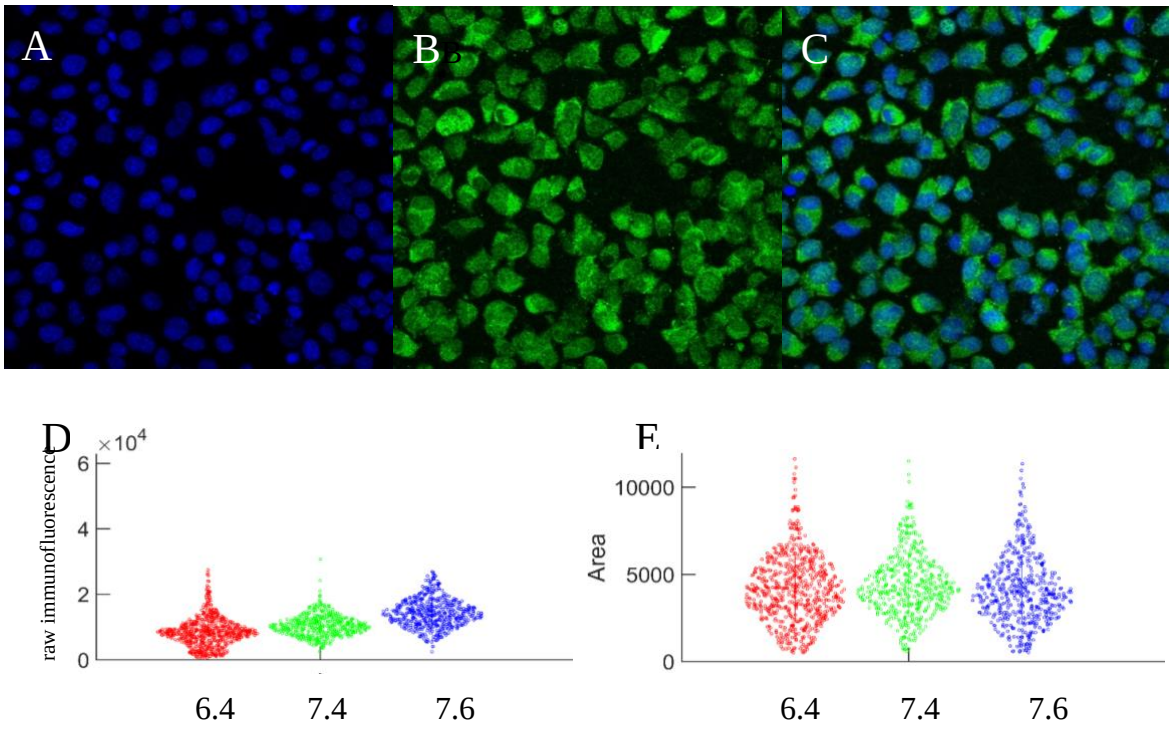


Figure 5.2.1 Fixed cell imaging of GLUTag cells with anti-GLP1 immunolabelling and example of quantified immunofluorescence intensity output. Images were taken after 2-hour incubation in standard secretion media at pHo7.4. A) Hoechst nuclear staining B) anti-GLP-1 immunolabelling C) overlay. Confocal microscopy x40 objectification. Example of quantified immunofluorescence intensity output form the matlab code D) raw immunofluorescence intensity at pH 6.4, 7.4 and 7.6 E) calculated cell area.

5.2.1 Results

The mean fluorescence intensity of cells from each condition and time point were used for further analysis with results shown in Fig5.2.2. However, even after normalising each test repeat to the average fluorescence intensity of pH 6.4, 7.4 and 7.6 in 10mM glucose at 2 hours measured in parallel on the same day (Fig5.2.2B), results still showed a large amount of variation. No significant difference of raw and normalised fluorescence intensity was found between pH values amongst and within each condition.

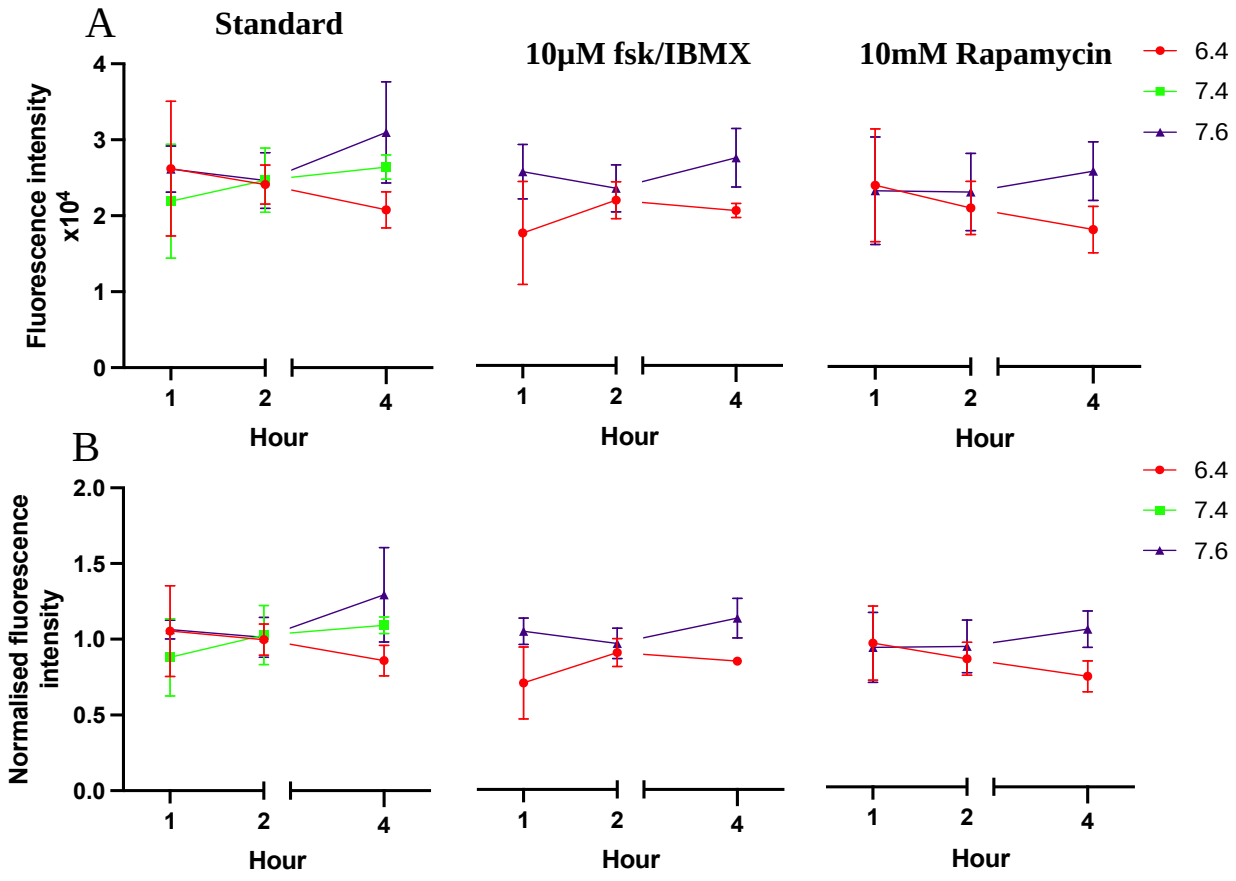


Figure 5.2.2 Quantified fluorescence intensity of anti-GLP-1 from GLUTag cells. Cells were pre-incubated for 1-hour at pHo7.4 in standard secretion media (CO_2/HCO_3^- buffer with 10mM glucose) and either remained in pHo7.4 or exposed to acidic (pHo6.4) or alkali (pHo7.6) conditions and, where labelled, either 10µM fsk/IBMX or 10nM rapamycin. After 1, 2 and 4-hours in respective conditions, cells were fixed, and anti-GLP-1 immunofluorescence measured. A) Raw fluorescence intensity results and B) normalised to the average fluorescence intensity of pHo6.4, 7.4 and 7.6 in 10mM glucose at 2 hours measured in parallel on the same day. Each point represents mean±SEM from **n=3.**

5.3 Discussion

In this chapter I have explored the use of alternative methods to investigate GLP-1 secretory dynamics in GLUTag cells. I have focused specifically on techniques that image GLUTag cells to visualise intracellular GLP-1 with the aim of gaining an insight into the pH-sensitive processes that regulate secretion. However, both tPA-Dendra2 and immunofluorescence visualisation were concluded to be unsuccessful and/or inappropriate techniques to investigate dynamics of intracellular GLP-1 in GLUTag cells.

Considering tPA-Dendra2 first, it is clear GLUTag cells could undergo transfection with high efficacy given the significant amount of green fluorescence visualised (Fig5.2.1A). Furthermore, in live cells, photoconversion of Dendra2 could successfully be achieved with 405nm exposure, shifting green to red fluorescence emission. However, in the presence of known stimulants of GLP-1[40] and tPA[199] (e.g. cAMP-activators and K^+-induced depolarisation) no observations that could represent tPA-Dendra2 secretion were seen.

Thorough troubleshooting during this study confirmed failure of tPA-Dendra2 imaging to visualise GLP-1 secretion was not due to the set up (e.g. incubation media) or imaging parameters (e.g. photobleaching) used with the microscope. Nor was it due to the transfection protocol completely damaging GLUTag cell physiology and GLP-1 secretion, despite a clear impairment as shown in Fig5.1.3. However, other factors can also be considered. Firstly, despite early studies reporting a good degree of co-localisation of tPA and GLP-1[184], here tPA-Dendra2 and GLP-1 did not co-localize, suggesting tPA is not co-loaded with GLP-1 vesicles. Additionally, the success of early studies to visualise fluorescent dynamics of tPA-GFP-expressing vesicles was achieved using TIRF

microscopy. The nature of TIRF microscopy means only thin sections can be imaged, for example, the cell membrane[203]. And, as only the area of acquisition is illuminated and collected, compared to other microscopy techniques such as LSM, TIRF has a higher signal-to-noise ratio and resolution[203]. The Gribble group, who first reported the use of TIRF microscopy to visualise tPA-GFP and GLP-1 exocytosis, found compared to unstimulated controls, 1mM L-ornithine stimulation increased the number of tPA-GFP fusion events (eg. exocytosis of tPA-GFP expressing vesicles) from around 1 to 14 in a 20mins period[184]. Measured with an ELISA kit, the same concentration of L-ornithine was reported to increase GLP-1 secretion around 1.7-fold over a 2-hr period (115pM to 200pM, respectively) [184]. However, whether this amounts to a significant change in intracellular tPA-GFP fluorescence intensity, as measured with confocal microscopy, is unclear. Here, IBMX/fsk was used to stimulate tPA-Dendra2 containing vesicle secretion, which was shown to increase GLP-1 secretion around 4-fold compared to 10mM glucose stimulation over a 2-hr period (Fig5.1.3). Despite this significantly increased detection of extracellular GLP-1, in the immunofluorescence investigations using anti-GLP-1 (Fig5.2.2), limited intracellular fluorescence intensity differences were seen between 10mM glucose or IBMX/fsk stimulation. Thus, it may in fact be that an insufficient number of GLP-1 and tPA-Dendra2 containing vesicles, relative to the store in GLUTag cells, are secreted to detect meaningful changes in green or red Dendra2 fluorescence using a LSCM. Whereas, as TIRF microscopy visualises individual vesicle secretory events, its use is not sensitive nor limited by background tPA-FP fluorescence. Importantly, the use of Dendra2 to track intracellular protein dynamics depends on the use of confocal microscopy to temporally detect changes in fluorescence intensity at different wavelengths[196]. Thus, even if tPA-

Dendra2 did efficiently co-load with GLP-1 vesicles, the microscopic visualisation system required for tPA-Dendra2 may not have been sensitive enough to dissect meaningful data.

For investigations using immunofluorescence, even after normalisation, a significant amount of variation between test repeat results meant robust data representing protein expression could not be obtained. This is further highlighted as between conditions where differences in GLP-1 levels would be expected, for example, after 1-hour exposure of 10uM fsk/IBMX known to cause a 3-fold increase in secretion[154], no obvious change of fluorescence intensity was seen. Suggesting if there are changes in intracellular GLP-1 levels, the technique cannot and/or is not sensitive enough to detect this.

Intracellular immuno-detection requires cell permeabilization and fixation, and due to the nature of enzymatic amplification and measurement methods, immunofluorescence analysis is often considered semi-quantitative. Past studies have demonstrated a quantitative potential of IF[204], however, significant optimisation is required to reduce the signal-to-noise ratio to a level where reproducible data representing protein concentration is obtained from IF images. For example, even subtle differences in the antibody concentration and stability can have significant effects on the readout, jeopardizing reliability[204]. Furthermore, irrespective of plate coatings and cell seeding protocols, GLUTag cells have a tendency to grow in protruding clusters. This causes difficulties focusing cells with confocal microscopy into a two-dimensional image and identifying individual cell area with the matlab code as there is overlapping green fluorescence. Therefore, quantified IF is likely an inappropriate method to detect pH-dependent changes of intracellular GLP-1 retention in GLUTag cells.

In conclusion, the imaging techniques explored here were unsuccessful and/or inappropriate to investigate dynamics of intracellular GLP-1 in GLUTag cells. It appears tPA-Dendra2 is not suitable to visualise secretory dynamics of GLP-1. This may be due to inefficient co-loading of tPA-Dendra2 with GLP-1 vesicles and/or sensitivity limitations of the microscopic system required to track intracellular tPA-Dendra2 in GLUTag cells. For the quantification of GLP-1 using IF detection, although it was interesting to see a trend for pHo7.6 to be higher than pHo6.4 at 4-hour incubation, no meaningful differences between 10mM glucose and IBMX/fsk stimulation were seen contrasting extracellular GLP-1 secretion assay results where over 4-fold differences are reported. It is likely this method is too blunt a tool to dissect meaningful data, mostly attributable to the semi-qualitative nature of the method causing unreliability and a significant amount of variation between test repeat results. Thus, at this stage, other methods, such as protein assays, Western blots and flow cytometry[205], are more reliable approaches to assess GLP-1 expression within GLUTag cells. Recent developments of FP-tagged GLP-1 that have inserted FPs into the middle of the GLP-1 peptide seem promising and, in the future, can be trialled for live-cell imaging of extracellular influences on GLP-1 exocytosis[206].

6 General discussion and conclusion

It is well-recognised in the enteroendocrine L-cell[22] that GLP-1 is secreted in response to direct sensing of nutrients, such as glucose[35]. However, intracellular mechanisms that influence the regulated secretory pathway[105,107] of GLP-1 vesicle exocytosis are still being fully characterised. Accordingly, alterations of luminal pH are known to follow food intake, and reports have emerged of lower average gut pH in obese and diabetic individuals[121] whom have dysregulated GLP-1 secretion responses[26]. Previous results from our laboratory showed acidic pHo inhibits GLP-1 secretion from GLUTag cells, a model enteroendocrine L-cell, suggesting altered luminal pH may have pathological implications in disease with dysregulated energy metabolism.

The main aims of this thesis were to confirm the pH-sensitivity of GLP-1 secretion in a physiological CO_2/HCO_3^- buffer system and to further explore underlying intracellular mechanisms. Results presented in Chapter 3 provide robust evidence to support the first aim, with GLP-1 quantification assay results reporting a significant decrease in secretion when GLUTag cells are exposed to acidic conditions. Alongside these findings, results from Chapter 2 can be used to relate changes in pHo to pHi and the GLP-1 secretion response. For example, incubating cells at pHo6.4 compared to physiological pHo7.4 resulted in a decrease in pHi from 7.2 to ~6.9. This also appeared to cause a loss of glucose-stimulated GLP-1 secretion, where secretion at pHo was comparable to secretion in glucose-free or Ca^{2+} free conditions. Furthermore, in this study a comparable pH-dependence of GLP-1 secretion is reported in physiological CO_2/HCO_3^- buffered and non-physiological HCO_3^--free media, supporting preliminary results from our laboratory which used the latter. Interestingly, despite these similar GLP-1 secretory responses, incubating

GLUTag cells in HCO_3^--free media compared to physiological CO_2/ HCO_3^- buffer caused around a 0.1 pH unit alkalinisation of pHi across the pHo range investigated (pH6.4-7.6). This may suggest the response of GLP-1 secretion to changes in extracellular pH is transduced via surface-expressed H^+ sensors, rather changes in intracellular pH[148]. As such, future work should look to assess the response of GLP-1 secretion to changes in extracellular pH independent of intracellular pH, such as with the use of pharmacological agents that block specific pH-regulators (e.g. amiloride inhibits NHE[207]). Such investigations would further unravel the pH-sensing mechanism that underlies the pH-dependency of GLP-1 secretion in GLUTag cells.

Following from preliminary work, data presented in this thesis has explored potential underlying cellular mechanisms of pH-dependent GLP-1 secretion. However, the multifactorial nature of systems influencing GLP-1 secretion and pH regulation challenges the ability to make robust inferences from observations. For example, in the absence of Ca^{2+}, independent of extracellular pH, GLP-1 secretion is significantly attenuated (Fig3.4). However, as Ca^{2+} plays a crucial role both for action potential generation[40] and exocytosis[115], any alterations to extracellular [Ca^{2+}] will impact on multiple systems in tandem, making the interpretation of these results impossible. Furthermore, preliminary results indicated that GLP-1 secretion is dependent on Cl^-- ions, however, in Chapter 3 it was shown extracellular [Cl^-] has a significant influence on pH regulation in GLUTag cells, likely attributable to the influence of extracellular [Cl^-] on the kinetics of pH regulating Cl^--dependent membrane transporters[4]. Similar findings are in fact reported in pancreatic islets, where whilst incubation in Cl^--free media inhibited insulin secretion, it was also shown to induce an increase in intracellular pH similar to pHo8.3[144]. Nonetheless,

this does not dismiss a role of Ca^{2+} or Cl^- for the pH-dependence of GLP-1 release. It is quite possible that a combination of pH-sensitive pathways collectively contributes to the pH-dependence of GLP-1 secretion, thus, more robust scientific investigations are required to fully dissect and understand underlying mechanisms. For example, for Ca^{2+}, more sophisticated methods (i.e.fluorescent Ca^{2+} imaging) should be adopted to assess the potential effect of pHo on Ca^{2+} signalling in GLUTag. For Cl^-, as currently there are no inhibitors specific to Cl^--dependent transporter currents[208], knock-out models of the ClC-3 transporter, shown not to regulate pHi[134], are likely the best method to validly investigate the pH sensitivity of Cl^--dependent GLP-1 secretion mechanisms.

An interesting finding from this thesis was the significant effect of changes in pHo on GLP-1 secretion rate. It appears rate was more sensitive to extracellular pH than total GLP-1 secretion. This finding corroborates preliminary postulations that intracellular acidification impairs GLP-1 exocytosis, possibly due to alterations of vesicular membrane V-ATPase activity, disrupting luminal pH[136]. Indeed, results from Chapter 3 confirm pHo changes cause parallel pHi changes in GLUTag cells. However, whilst activity of the V-ATPase is regulated by cytoplasmic pH[136], it cannot be assumed changes of pHi induce significant changes in intraorganellar pH. Studying the pH of intracellular compartments is challenging due to subcellular targeting and low acidity[209]. However, approaches are available that can obtain the pH of individual subcellular compartments, such as genetically encoded pH-sensitive fluorophores[210], or nanosensor pH probes[209]. Such approaches can be used to investigate if changes in vesicle pH underlies pH-dependent GLP-1 secretion in GLUTag cells. Alternatively, live imaging is arguably the most robust model of studying protein secretory dynamics in cells[196]. In this study, this was attempted

with the use of a novel GLP-1 surrogate marker, tPA, however, results were unsuccessful. Nonetheless, up-and-coming developments seem promising which in the future may be used to gain insightful observations of the pH dependency of GLP-1 secretion[206].

There are several limitations when correlating GLUTag cell physiology into L-cells within the GI tract. Firstly, despite large fluctuations of pH within the GI lumen[3], the presence of the mucus layer may mean intraluminal pH does not reflect the direct pHo exposure of gut epithelial cells[211]. Though studies found the colonic mucosa pH closely paralleled the lumen pH, the mucosa layer surface tended towards a more alkali pH with smaller fluctuations (between 7.0-7.4)[212,213]. Within the GI tract, goblet cells produce transmembrane mucins which act as luminal protection of the GI tract by covering the apical surface of GI epithelial cells[211]. GLUTag cells lack this 'protective' coating, thus in this study, may have been exposed to pHo conditions that are not physiologically relevant[129,130].

As well, in this study, GLUTag cells were subject to relatively acute (>2 hours) exposures of altered pHo. However, pathologically associated alterations of gut pH likely occur gradually over an extended period[121]. Longer term exposure to pH decreases can alter the expression of acid extruders and loaders as a compensatory mechanism[148], potentially minimising disturbances of intracellular pH. Indeed, chronic acid exposure can be achieved in *in vitro* studies, and is another investigatory line to follow this study.

Furthermore, investigations have specifically focused on glucose-stimulated GLP-1 secretion. However, a wide range of stimuli, including nutrients, hormones and neurotransmitters, and intracellular signalling pathways, such as cAMP-dependent pathways[154], also influence GLP-1 secretion[214]. Changes in pHi likely influence distinct

pathways independently and further investigations assessing the pH-dependence of other secretagogue-stimulated GLP-1 secretion should be conducted.

In conclusion, this thesis has confirmed the pH-dependence of GLP-1 secretion from GLUTag cells in a physiological CO_2/ HCO_3^- buffered system. Furthermore, I have standardised the extra- to intracellular pH relationship in GLUTag cells and demonstrated the importance of understanding influences of experimental conditions on pH regulation. As well, I have shown specifically the rate, rather than total, GLP-1 secretion is significantly implicated in acidic conditions, corroborating previous findings from our laboratory that pH effects GLP-1 exocytosis. Taken together my data supports the proposed model outlined in Fig6.1. However, whilst the pHo-pHi relationship and effect of pHo on GLP-1 release has been characterised, currently there is no direct data directly linking the relationship between pHi and GLP-1 release. To further explore the pH-dependence of GLP-1 secretion rates, alternative approaches will be required to visualize exocytosis events in response to changes to intracellular pH, such as live-cell imaging. Ultimately, the work presented here should be extrapolated to human ex vivo primary gut crypt cultures in Ussing chambers where the integrity of the gut and, by extension, the polarization of the endocrine cells are maintained.

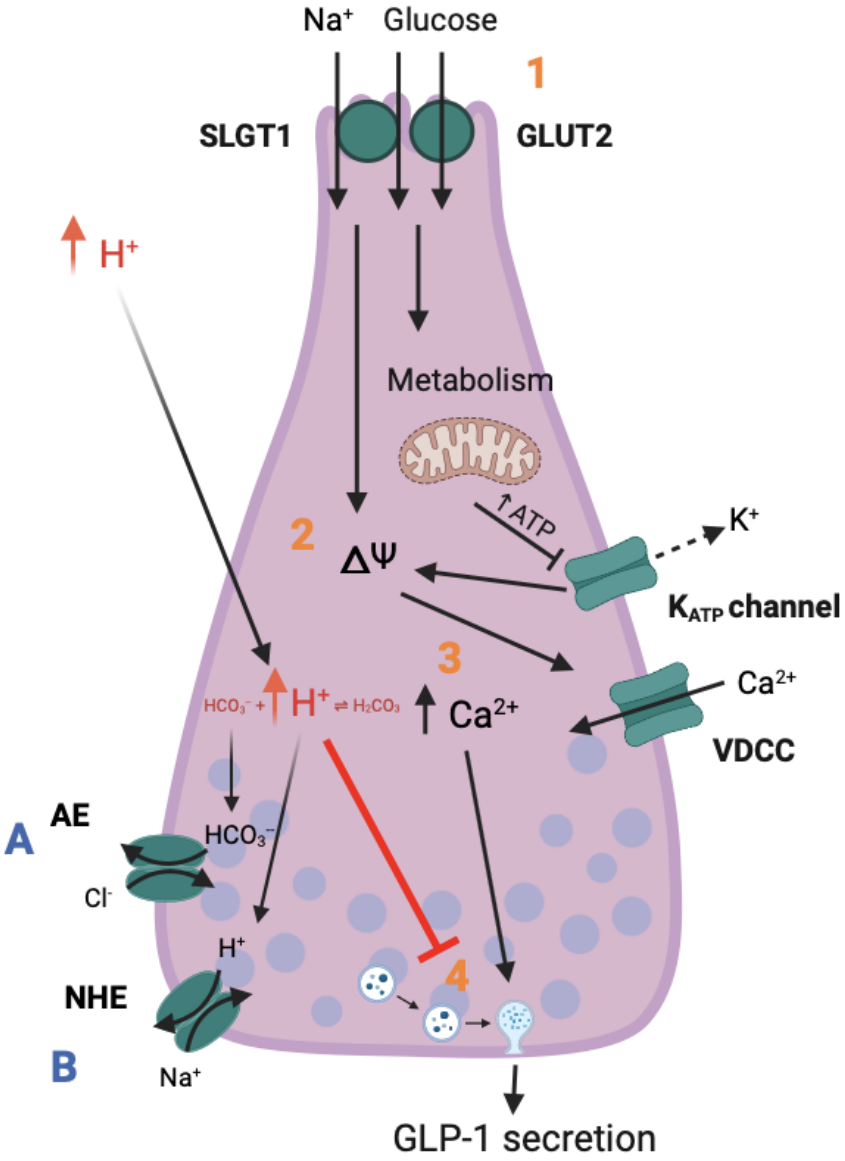


Figure 6.1 Summary of pH sensing mechanisms and glucose-stimulated GLP-1 secretion in L cells.

1. Glucose uptake via the Na^+-coupled glucose co-transporter (SGLT-1) and glucose transporter (GLUT2). 2. Membrane depolarisation via electrogenic uptake of glucose and closure of the ATP-sensitive potassium (K_{ATP}) channel. 3. Activation of voltage dependent Ca^{2+} channel and influx of intracellular Ca^{2+} 4. GLP-1 vesicle exocytosis, involving vesicular docking, priming and Ca^{2+}-triggered fusion. A. Proton-loading anion exchanger (SLC4A2 isoform). B. Proton-extruding Na^+/ H^+ exchanger (SLC9A isoform).

Reference

1. Muller, T.D., *et al.* Glucagon-like peptide 1 (GLP-1). *Mol Metab* **30**, 72-130 (2019).
2. Khutoryanskiy, V.V. Supramolecular materials: Longer and safer gastric residence. *Nat Mater* **14**, 963-964 (2015).
3. Koziolek, M., *et al.* Investigation of pH and Temperature Profiles in the GI Tract of Fasted Human Subjects Using the Intellicap((R)) System. *J Pharm Sci* **104**, 2855-2863 (2015).
4. Casey, J.R., Grinstein, S. & Orlowski, J. Sensors and regulators of intracellular pH. *Nat Rev Mol Cell Biol* **11**, 50-61 (2010).
5. Sternini, C., Anselmi, L. & Rozengurt, E. Enteroendocrine cells: a site of 'taste' in gastrointestinal chemosensing. *Curr Opin Endocrinol Diabetes Obes* **15**, 73-78 (2008).
6. Sjolund, K., Sanden, G., Hakanson, R. & Sundler, F. Endocrine cells in human intestine: an immunocytochemical study. *Gastroenterology* **85**, 1120-1130 (1983).
7. Parikh, A. & Thevenin, C. Physiology, Gastrointestinal Hormonal Control. in *StatPearls* (Treasure Island (FL), 2023).
8. Drucker, D.J. The role of gut hormones in glucose homeostasis. *J Clin Invest* **117**, 24-32 (2007).
9. Gribble, F.M. & Reimann, F. Function and mechanisms of enteroendocrine cells and gut hormones in metabolism. *Nat Rev Endocrinol* **15**, 226-237 (2019).
10. Fukui, H., Xu, X. & Miwa, H. Role of Gut Microbiota-Gut Hormone Axis in the Pathophysiology of Functional Gastrointestinal Disorders. *J Neurogastroenterol Motil* **24**, 367-386 (2018).
11. Nerild, H.H., *et al.* Liraglutide changes postprandial responses of gut hormones involved in the regulation of gallbladder motility. *Diabetes Obes Metab* **25**, 1632-1637 (2023).
12. Latorre, R., Sternini, C., De Giorgio, R. & Greenwood-Van Meerveld, B. Enteroendocrine cells: a review of their role in brain-gut communication. *Neurogastroenterol Motil* **28**, 620-630 (2016).
13. Gribble, F.M. & Reimann, F. Signalling in the gut endocrine axis. *Physiol Behav* **176**, 183-188 (2017).
14. Grant, B., Sandelson, M., Agyemang-Prempeh, B. & Zalin, A. Managing obesity in people with type 2 diabetes. *Clin Med (Lond)* **21**, e327-e231 (2021).
15. Farhadipour, M. & Depoortere, I. The Function of Gastrointestinal Hormones in Obesity-Implications for the Regulation of Energy Intake. *Nutrients* **13**(2021).
16. Ortiz, V.E. & Kwo, J. Obesity: physiologic changes and implications for preoperative management. *BMC Anesthesiol* **15**, 97 (2015).
17. Goyal, R. & Jialal, I. Diabetes Mellitus Type 2. in *StatPearls* (Treasure Island (FL), 2023).
18. Morgan, L. Challenges and Opportunities in Managing Type 2 Diabetes. *Am Health Drug Benefits* **10**, 197-200 (2017).
19. Roder, P.V., Wu, B., Liu, Y. & Han, W. Pancreatic regulation of glucose homeostasis. *Exp Mol Med* **48**, e219 (2016).

20. Ashcroft, S.J. & Ashcroft, F.M. Properties and functions of ATP-sensitive K-channels. *Cell Signal* **2**, 197-214 (1990).
21. Fridlyand, L.E. & Philipson, L.H. Pancreatic Beta Cell G-Protein Coupled Receptors and Second Messenger Interactions: A Systems Biology Computational Analysis. *PLoS One* **11**, e0152869 (2016).
22. Spreckley, E. & Murphy, K.G. The L-Cell in Nutritional Sensing and the Regulation of Appetite. *Front Nutr* **2**, 23 (2015).
23. Nauck, M.A., Bartels, E., Orskov, C., Ebert, R. & Creutzfeldt, W. Additive insulinotropic effects of exogenous synthetic human gastric inhibitory polypeptide and glucagon-like peptide-1-(7-36) amide infused at near-physiological insulinotropic hormone and glucose concentrations. *J Clin Endocrinol Metab* **76**, 912-917 (1993).
24. Kjems, L.L., Holst, J.J., Volund, A. & Madsbad, S. The influence of GLP-1 on glucose-stimulated insulin secretion: effects on beta-cell sensitivity in type 2 and nondiabetic subjects. *Diabetes* **52**, 380-386 (2003).
25. Marzullo, P., *et al.* The relationship between active ghrelin levels and human obesity involves alterations in resting energy expenditure. *J Clin Endocrinol Metab* **89**, 936-939 (2004).
26. Faerch, K., *et al.* GLP-1 Response to Oral Glucose Is Reduced in Prediabetes, Screen-Detected Type 2 Diabetes, and Obesity and Influenced by Sex: The ADDITION-PRO Study. *Diabetes* **64**, 2513-2525 (2015).
27. Hutch, C.R. & Sandoval, D. The Role of GLP-1 in the Metabolic Success of Bariatric Surgery. *Endocrinology* **158**, 4139-4151 (2017).
28. Yeh, T.L., Tsai, M.C., Tsai, W.H., Tu, Y.K. & Chien, K.L. Effect of glucagon-like peptide-1 receptor agonists on glycemic control, and weight reduction in adults: A multivariate meta-analysis. *PLoS One* **18**, e0278685 (2023).
29. Alsafwani, D.M., Alotaibi, H.N., Alzaid, J.A., Alghamdi, A. & Almakhaita, H.M. Liraglutide Effect on Weight, Glycated Hemoglobin, and Blood Pressure: A Single-Center Experience in the Eastern Province of Saudi Arabia. *Cureus* **14**, e23554 (2022).
30. Wilding, J.P.H., Calanna, S. & Kushner, R.F. Once-Weekly Semaglutide in Adults with Overweight or Obesity. Reply. *N Engl J Med* **385**, e4 (2021).
31. Kobalava, Z.D. & Kokhan, E.V. [Semaglutide for the Management of type 2 Diabetes: Clinical Evidence, Cardioprotective Effects, and Guidelines]. *Kardiologiia* **60**, 122-133 (2020).
32. Ryan, D.H., *et al.* Semaglutide Effects on Cardiovascular Outcomes in People With Overweight or Obesity (SELECT) rationale and design. *Am Heart J* **229**, 61-69 (2020).
33. Muller, T.D., Bluher, M., Tschop, M.H. & DiMarchi, R.D. Anti-obesity drug discovery: advances and challenges. *Nat Rev Drug Discov* **21**, 201-223 (2022).
34. Wang, J.Y., *et al.* GLP-1 receptor agonists for the treatment of obesity: Role as a promising approach. *Front Endocrinol (Lausanne)* **14**, 1085799 (2023).
35. Eissele, R., *et al.* Glucagon-like peptide-1 cells in the gastrointestinal tract and pancreas of rat, pig and man. *Eur J Clin Invest* **22**, 283-291 (1992).

36. Anini, Y., Hansotia, T. & Brubaker, P.L. Muscarinic receptors control postprandial release of glucagon-like peptide-1: in vivo and in vitro studies in rats. *Endocrinology* **143**, 2420-2426 (2002).
37. Hansen, L., Deacon, C.F., Orskov, C. & Holst, J.J. Glucagon-like peptide-1-(7-36)amide is transformed to glucagon-like peptide-1-(9-36)amide by dipeptidyl peptidase IV in the capillaries supplying the L cells of the porcine intestine. *Endocrinology* **140**, 5356-5363 (1999).
38. Liddle, R.A. Interactions of Gut Endocrine Cells with Epithelium and Neurons. *Compr Physiol* **8**, 1019-1030 (2018).
39. Bohorquez, D.V., *et al.* An enteroendocrine cell-enteric glia connection revealed by 3D electron microscopy. *PLoS One* **9**, e89881 (2014).
40. Reimann, F., *et al.* Glucose sensing in L cells: a primary cell study. *Cell Metab* **8**, 532-539 (2008).
41. Nauck, M.A., Vardarli, I., Deacon, C.F., Holst, J.J. & Meier, J.J. Secretion of glucagon-like peptide-1 (GLP-1) in type 2 diabetes: what is up, what is down? *Diabetologia* **54**, 10-18 (2011).
42. Elliott, R.M., *et al.* Glucagon-like peptide-1 (7-36)amide and glucose-dependent insulinotropic polypeptide secretion in response to nutrient ingestion in man: acute post-prandial and 24-h secretion patterns. *J Endocrinol* **138**, 159-166 (1993).
43. Nauck, M.A., Siemsgluss, J., Orskov, C. & Holst, J.J. Release of glucagon-like peptide 1 (GLP-1 [7-36 amide]), gastric inhibitory polypeptide (GIP) and insulin in response to oral glucose after upper and lower intestinal resections. *Z Gastroenterol* **34**, 159-166 (1996).
44. Rocca, A.S. & Brubaker, P.L. Role of the vagus nerve in mediating proximal nutrient-induced glucagon-like peptide-1 secretion. *Endocrinology* **140**, 1687-1694 (1999).
45. Theodorakis, M.J., *et al.* Human duodenal enteroendocrine cells: source of both incretin peptides, GLP-1 and GIP. *Am J Physiol Endocrinol Metab* **290**, E550-559 (2006).
46. During, M.J., *et al.* Glucagon-like peptide-1 receptor is involved in learning and neuroprotection. *Nat Med* **9**, 1173-1179 (2003).
47. Anini, Y. & Brubaker, P.L. Muscarinic receptors control glucagon-like peptide 1 secretion by human endocrine L cells. *Endocrinology* **144**, 3244-3250 (2003).
48. Plaisancie, P., Bernard, C., Chayvialle, J.A. & Cuber, J.C. Regulation of glucagon-like peptide-1-(7-36) amide secretion by intestinal neurotransmitters and hormones in the isolated vascularly perfused rat colon. *Endocrinology* **135**, 2398-2403 (1994).
49. Jepsen, S.L., *et al.* Paracrine crosstalk between intestinal L- and D-cells controls secretion of glucagon-like peptide-1 in mice. *Am J Physiol Endocrinol Metab* **317**, E1081-E1093 (2019).
50. Meyer, R.K. & Duca, F.A. RISING STARS: Endocrine regulation of metabolic homeostasis via the intestine and gut microbiome. *J Endocrinol* **258**(2023).
51. Pilichiewicz, A.N., *et al.* Load-dependent effects of duodenal glucose on glycemia, gastrointestinal hormones, antropyloroduodenal motility, and energy intake in healthy men. *Am J Physiol Endocrinol Metab* **293**, E743-753 (2007).

52. Ryan, A.T., *et al.* Intraduodenal protein modulates antropyloroduodenal motility, hormone release, glycemia, appetite, and energy intake in lean men. *Am J Clin Nutr* **96**, 474-482 (2012).
53. Tolhurst, G., Reimann, F. & Gribble, F.M. Nutritional regulation of glucagon-like peptide-1 secretion. *J Physiol* **587**, 27-32 (2009).
54. Reimann, F., Tolhurst, G. & Gribble, F.M. G-protein-coupled receptors in intestinal chemosensation. *Cell Metab* **15**, 421-431 (2012).
55. Husted, A.S., Trauelsen, M., Rudenko, O., Hjorth, S.A. & Schwartz, T.W. GPCR-Mediated Signaling of Metabolites. *Cell Metab* **25**, 777-796 (2017).
56. Hirasawa, A., *et al.* Free fatty acids regulate gut incretin glucagon-like peptide-1 secretion through GPR120. *Nat Med* **11**, 90-94 (2005).
57. Layer, P., Holst, J.J., Grandt, D. & Goebell, H. Ileal release of glucagon-like peptide-1 (GLP-1). Association with inhibition of gastric acid secretion in humans. *Dig Dis Sci* **40**, 1074-1082 (1995).
58. Thomsen, C., *et al.* Differential effects of saturated and monounsaturated fatty acids on postprandial lipemia and incretin responses in healthy subjects. *Am J Clin Nutr* **69**, 1135-1143 (1999).
59. Thomsen, C., Storm, H., Holst, J.J. & Hermansen, K. Differential effects of saturated and monounsaturated fats on postprandial lipemia and glucagon-like peptide 1 responses in patients with type 2 diabetes. *Am J Clin Nutr* **77**, 605-611 (2003).
60. Sidhu, S.S., Thompson, D.G., Warhurst, G., Case, R.M. & Benson, R.S. Fatty acid-induced cholecystokinin secretion and changes in intracellular Ca2+ in two enteroendocrine cell lines, STC-1 and GLUTag. *J Physiol* **528 Pt 1**, 165-176 (2000).
61. Mandoe, M.J., *et al.* The 2-monoacylglycerol moiety of dietary fat appears to be responsible for the fat-induced release of GLP-1 in humans. *Am J Clin Nutr* **102**, 548-555 (2015).
62. Hansen, H.S., Rosenkilde, M.M., Holst, J.J. & Schwartz, T.W. GPR119 as a fat sensor. *Trends Pharmacol Sci* **33**, 374-381 (2012).
63. Reimann, F., Williams, L., da Silva Xavier, G., Rutter, G.A. & Gribble, F.M. Glutamine potently stimulates glucagon-like peptide-1 secretion from GLUTag cells. *Diabetologia* **47**, 1592-1601 (2004).
64. Chen, Q. & Reimer, R.A. Dairy protein and leucine alter GLP-1 release and mRNA of genes involved in intestinal lipid metabolism in vitro. *Nutrition* **25**, 340-349 (2009).
65. Kato, M., Nakanishi, T., Tani, T. & Tsuda, T. Low-molecular fraction of wheat protein hydrolysate stimulates glucagon-like peptide-1 secretion in an enteroendocrine L cell line and improves glucose tolerance in rats. *Nutr Res* **37**, 37-45 (2017).
66. Lejeune, M.P., Westerterp, K.R., Adam, T.C., Luscombe-Marsh, N.D. & Westerterp-Plantenga, M.S. Ghrelin and glucagon-like peptide 1 concentrations, 24-h satiety, and energy and substrate metabolism during a high-protein diet and measured in a respiration chamber. *Am J Clin Nutr* **83**, 89-94 (2006).

67. Mortensen, L.S., *et al.* Differential effects of protein quality on postprandial lipemia in response to a fat-rich meal in type 2 diabetes: comparison of whey, casein, gluten, and cod protein. *Am J Clin Nutr* **90**, 41-48 (2009).
68. Tolhurst, G., *et al.* Glutamine triggers and potentiates glucagon-like peptide-1 secretion by raising cytosolic Ca2+ and cAMP. *Endocrinology* **152**, 405-413 (2011).
69. Gameiro, A., *et al.* The neurotransmitters glycine and GABA stimulate glucagon-like peptide-1 release from the GLUTag cell line. *J Physiol* **569**, 761-772 (2005).
70. Diakogiannaki, E., *et al.* Oligopeptides stimulate glucagon-like peptide-1 secretion in mice through proton-coupled uptake and the calcium-sensing receptor. *Diabetologia* **56**, 2688-2696 (2013).
71. Psichas, A., Reimann, F. & Gribble, F.M. Gut chemosensing mechanisms. *J Clin Invest* **125**, 908-917 (2015).
72. Nakajima, S., Hira, T. & Hara, H. Calcium-sensing receptor mediates dietary peptide-induced CCK secretion in enteroendocrine STC-1 cells. *Mol Nutr Food Res* **56**, 753-760 (2012).
73. Wellendorph, P., *et al.* Deorphanization of GPRC6A: a promiscuous L-alpha-amino acid receptor with preference for basic amino acids. *Mol Pharmacol* **67**, 589-597 (2005).
74. Ding, X., *et al.* Intestinal enteroendocrine L cells in amino acid sensing and diseases. *Front Biosci (Landmark Ed)* **23**, 1740-1753 (2018).
75. Nakamura, T., *et al.* Glutamine-induced signaling pathways via amino acid receptors in enteroendocrine L cell lines. *J Mol Endocrinol* **64**, 133-143 (2020).
76. Hunt, J.E., *et al.* Pharmacological activation of TGR5 promotes intestinal growth via a GLP-2-dependent pathway in mice. *Am J Physiol Gastrointest Liver Physiol* **318**, G980-G987 (2020).
77. Kuhre, R.E., *et al.* Bile acids are important direct and indirect regulators of the secretion of appetite- and metabolism-regulating hormones from the gut and pancreas. *Mol Metab* **11**, 84-95 (2018).
78. Ullmer, C., *et al.* Systemic bile acid sensing by G protein-coupled bile acid receptor 1 (GPBAR1) promotes PYY and GLP-1 release. *Br J Pharmacol* **169**, 671-684 (2013).
79. Hjorne, A.P., Modvig, I.M. & Holst, J.J. The Sensory Mechanisms of Nutrient-Induced GLP-1 Secretion. *Metabolites* **12**(2022).
80. Tomaro-Duchesneau, C., *et al.* Discovery of a bacterial peptide as a modulator of GLP-1 and metabolic disease. *Sci Rep* **10**, 4922 (2020).
81. Allin, K.H., Nielsen, T. & Pedersen, O. Mechanisms in endocrinology: Gut microbiota in patients with type 2 diabetes mellitus. *Eur J Endocrinol* **172**, R167-177 (2015).
82. Madsen, M.S.A., *et al.* Metabolic and gut microbiome changes following GLP-1 or dual GLP-1/GLP-2 receptor agonist treatment in diet-induced obese mice. *Sci Rep* **9**, 15582 (2019).
83. Roberge, J.N. & Brubaker, P.L. Secretion of proglucagon-derived peptides in response to intestinal luminal nutrients. *Endocrinology* **128**, 3169-3174 (1991).
84. Stumpel, F., Burcelin, R., Jungermann, K. & Thorens, B. Normal kinetics of intestinal glucose absorption in the absence of GLUT2: evidence for a transport

pathway requiring glucose phosphorylation and transfer into the endoplasmic reticulum. *Proc Natl Acad Sci U S A* **98**, 11330-11335 (2001).

85. Reimann, F. & Gribble, F.M. Glucose-sensing in glucagon-like peptide-1-secreting cells. *Diabetes* **51**, 2757-2763 (2002).
86. de Bruine, A.P., *et al.* NCI-H716 cells as a model for endocrine differentiation in colorectal cancer. *Virchows Arch B Cell Pathol Incl Mol Pathol* **62**, 311-320 (1992).
87. Drucker, D.J., Jin, T., Asa, S.L., Young, T.A. & Brubaker, P.L. Activation of proglucagon gene transcription by protein kinase-A in a novel mouse enteroendocrine cell line. *Mol Endocrinol* **8**, 1646-1655 (1994).
88. Gribble, F.M., Williams, L., Simpson, A.K. & Reimann, F. A novel glucose-sensing mechanism contributing to glucagon-like peptide-1 secretion from the GLUTag cell line. *Diabetes* **52**, 1147-1154 (2003).
89. Parker, H.E., *et al.* Predominant role of active versus facilitative glucose transport for glucagon-like peptide-1 secretion. *Diabetologia* **55**, 2445-2455 (2012).
90. Kuhre, R.E., Frost, C.R., Svendsen, B. & Holst, J.J. Molecular mechanisms of glucose-stimulated GLP-1 secretion from perfused rat small intestine. *Diabetes* **64**, 370-382 (2015).
91. Roder, P.V., *et al.* The role of SGLT1 and GLUT2 in intestinal glucose transport and sensing. *PLoS One* **9**, e89977 (2014).
92. Sun, E.W., *et al.* Mechanisms Controlling Glucose-Induced GLP-1 Secretion in Human Small Intestine. *Diabetes* **66**, 2144-2149 (2017).
93. Holst, J.J. Glucagon and glucagon-like peptides 1 and 2. *Results Probl Cell Differ* **50**, 121-135 (2010).
94. Jin, T. Mechanisms underlying proglucagon gene expression. *J Endocrinol* **198**, 17-28 (2008).
95. Chepurny, O.G., *et al.* Stimulation of proglucagon gene expression by human GPR119 in enteroendocrine L-cell line GLUTag. *Mol Endocrinol* **27**, 1267-1282 (2013).
96. Zhou, J., *et al.* Peptide YY and proglucagon mRNA expression patterns and regulation in the gut. *Obesity (Silver Spring)* **14**, 683-689 (2006).
97. Yi, F., *et al.* Cross talk between the insulin and Wnt signaling pathways: evidence from intestinal endocrine L cells. *Endocrinology* **149**, 2341-2351 (2008).
98. Lim, G.E., *et al.* Insulin regulates glucagon-like peptide-1 secretion from the enteroendocrine L cell. *Endocrinology* **150**, 580-591 (2009).
99. Drucker, D.J. & Brubaker, P.L. Proglucagon gene expression is regulated by a cyclic AMP-dependent pathway in rat intestine. *Proc Natl Acad Sci U S A* **86**, 3953-3957 (1989).
100. Dhanvantari, S., Izzo, A., Jansen, E. & Brubaker, P.L. Coregulation of glucagon-like peptide-1 synthesis with proglucagon and prohormone convertase 1 gene expression in enteroendocrine GLUTag cells. *Endocrinology* **142**, 37-42 (2001).
101. Dhanvantari, S., Seidah, N.G. & Brubaker, P.L. Role of prohormone convertases in the tissue-specific processing of proglucagon. *Mol Endocrinol* **10**, 342-355 (1996).
102. Ugleholdt, R., *et al.* Impaired intestinal proglucagon processing in mice lacking prohormone convertase 1. *Endocrinology* **145**, 1349-1355 (2004).

103. Brubaker, P.L., Schloos, J. & Drucker, D.J. Regulation of glucagon-like peptide-1 synthesis and secretion in the GLUTag enteroendocrine cell line. *Endocrinology* **139**, 4108-4114 (1998).
104. Dikeakos, J.D., Mercure, C., Lacombe, M.J., Seidah, N.G. & Reudelhuber, T.L. PC1/3, PC2 and PC5/6A are targeted to dense core secretory granules by a common mechanism. *FEBS J* **274**, 4094-4102 (2007).
105. Zhou, A., Webb, G., Zhu, X. & Steiner, D.F. Proteolytic processing in the secretory pathway. *J Biol Chem* **274**, 20745-20748 (1999).
106. Gupta, V. Glucagon-like peptide-1 analogues: An overview. *Indian J Endocrinol Metab* **17**, 413-421 (2013).
107. Seidah, N.G. & Prat, A. Precursor convertases in the secretory pathway, cytosol and extracellular milieu. *Essays Biochem* **38**, 79-94 (2002).
108. Varndell, I.M., *et al.* Localization of glucagon-like peptide (GLP) immunoreactants in human gut and pancreas using light and electron microscopic immunocytochemistry. *J Histochem Cytochem* **33**, 1080-1086 (1985).
109. de Bruine, A.P., *et al.* Extracellular matrix components induce endocrine differentiation in vitro in NCI-H716 cells. *Am J Pathol* **142**, 773-782 (1993).
110. Uehara, S., *et al.* Vesicular storage and secretion of L-glutamate from glucagon-like peptide 1-secreting clonal intestinal L cells. *J Neurochem* **96**, 550-560 (2006).
111. Sun-Wada, G.H., *et al.* The a3 isoform of V-ATPase regulates insulin secretion from pancreatic beta-cells. *J Cell Sci* **119**, 4531-4540 (2006).
112. Paroutis, P., Touret, N. & Grinstein, S. The pH of the secretory pathway: measurement, determinants, and regulation. *Physiology (Bethesda)* **19**, 207-215 (2004).
113. Porte, D., Jr. & Pupo, A.A. Insulin responses to glucose: evidence for a two pool system in man. *J Clin Invest* **48**, 2309-2319 (1969).
114. Li, S.K., Zhu, D., Gaisano, H.Y. & Brubaker, P.L. Role of vesicle-associated membrane protein 2 in exocytosis of glucagon-like peptide-1 from the murine intestinal L cell. *Diabetologia* **57**, 809-818 (2014).
115. Sa, K.J., Park, H., Jang, S.J. & Lee, J.K. Association Mapping of Amylose Content in Maize RIL Population Using SSR and SNP Markers. *Plants (Basel)* **12**(2023).
116. Dolai, S., *et al.* Synaptotagmin-7 Functions to Replenish Insulin Granules for Exocytosis in Human Islet beta-Cells. *Diabetes* **65**, 1962-1976 (2016).
117. Yoshioka, M., Shimomura, Y. & Suzuki, M. Dietary polydextrose affects the large intestine in rats. *J Nutr* **124**, 539-547 (1994).
118. Kohl, K.D., Stengel, A., Samuni-Blank, M. & Dearing, M.D. Effects of anatomy and diet on gastrointestinal pH in rodents. *J Exp Zool A Ecol Genet Physiol* **319**, 225-229 (2013).
119. Sommer, H. & Kasper, H. Effect of long-term administration of dietary fiber on the exocrine pancreas in the rat. *Hepatogastroenterology* **31**, 176-179 (1984).
120. Nugent, S.G., Kumar, D., Rampton, D.S. & Evans, D.F. Intestinal luminal pH in inflammatory bowel disease: possible determinants and implications for therapy with aminosalicylates and other drugs. *Gut* **48**, 571-577 (2001).
121. Steenackers, N., *et al.* Effect of obesity on gastrointestinal transit, pressure and pH using a wireless motility capsule. *Eur J Pharm Biopharm* **167**, 1-8 (2021).

122. Anhe, F.F., Varin, T.V., Schertzer, J.D. & Marette, A. The Gut Microbiota as a Mediator of Metabolic Benefits after Bariatric Surgery. *Can J Diabetes* **41**, 439-447 (2017).
123. Cummings, D.E. & Overduin, J. Gastrointestinal regulation of food intake. *J Clin Invest* **117**, 13-23 (2007).
124. Bayliss, W.M. & Starling, E.H. The mechanism of pancreatic secretion. *J Physiol* **28**, 325-353 (1902).
125. Lucey, M.R., *et al.* Does gastric acid release plasma somatostatin in man? *Gut* **25**, 1217-1220 (1984).
126. Bloom, S.R., *et al.* Release of VIP, secretin and motilin after duodenal acidification in man. *Acta Hepatogastroenterol (Stuttg)* **25**, 365-368 (1978).
127. Mitznegg, P., *et al.* Release of motilin after duodenal acidification. *Lancet* **1**, 888-889 (1976).
128. Miedzybrodzka, E.L., *et al.* Stimulation of motilin secretion by bile, free fatty acids, and acidification in human duodenal organoids. *Mol Metab* **54**, 101356 (2021).
129. Reimann, F., *et al.* Characterization and functional role of voltage gated cation conductances in the glucagon-like peptide-1 secreting GLUTag cell line. *J Physiol* **563**, 161-175 (2005).
130. Rogers, G.J., *et al.* Electrical activity-triggered glucagon-like peptide-1 secretion from primary murine L-cells. *J Physiol* **589**, 1081-1093 (2011).
131. Takata, K. Glucose transporters in the transepithelial transport of glucose. *J Electron Microsc (Tokyo)* **45**, 275-284 (1996).
132. Diez-Sampedro, A., Lostao, M.P., Wright, E.M. & Hirayama, B.A. Glycoside binding and translocation in Na(+)-dependent glucose cotransporters: comparison of SGLT1 and SGLT3. *J Membr Biol* **176**, 111-117 (2000).
133. Sehlin, J. Interrelationship between chloride fluxes in pancreatic islets and insulin release. *Am J Physiol* **235**, E501-508 (1978).
134. Barg, S., *et al.* Priming of insulin granules for exocytosis by granular Cl(-) uptake and acidification. *J Cell Sci* **114**, 2145-2154 (2001).
135. Deriy, L.V., *et al.* The granular chloride channel ClC-3 is permissive for insulin secretion. *Cell Metab* **10**, 316-323 (2009).
136. Huang, C. & Chang, A. pH-dependent cargo sorting from the Golgi. *J Biol Chem* **286**, 10058-10065 (2011).
137. Burgess, T.L. & Kelly, R.B. Constitutive and regulated secretion of proteins. *Annu Rev Cell Biol* **3**, 243-293 (1987).
138. Gil-Lozano, M. & Brubaker, P.L. Murine GLUTag Cells. in *The Impact of Food Bioactives on Health: in vitro and ex vivo models* (eds. Verhoeckx, K., *et al.*) 229-238 (Cham (CH), 2015).
139. Michl, J., Park, K.C. & Swietach, P. Evidence-based guidelines for controlling pH in mammalian live-cell culture systems. *Commun Biol* **2**, 144 (2019).
140. Grapengiesser, E., Gylfe, E. & Hellman, B. Regulation of pH in individual pancreatic beta-cells as evaluated by fluorescence ratio microscopy. *Biochim Biophys Acta* **1014**, 219-224 (1989).
141. Kovbasnjuk, O., *et al.* Human enteroids: preclinical models of non-inflammatory diarrhea. *Stem Cell Res Ther* **4 Suppl 1**, S3 (2013).

142. Bevensee, M.O., Cummins, T.R., Haddad, G.G., Boron, W.F. & Boyarsky, G. pH regulation in single CA1 neurons acutely isolated from the hippocampi of immature and mature rats. *J Physiol* **494 (Pt 2)**, 315-328 (1996).
143. Theparambil, S.M., Naoshin, Z., Thyssen, A. & Deitmer, J.W. Reversed electrogenic sodium bicarbonate cotransporter 1 is the major acid loader during recovery from cytosolic alkalosis in mouse cortical astrocytes. *J Physiol* **593**, 3533-3547 (2015).
144. Gunawardana, S.C., Rocheleau, J.V., Head, W.S. & Piston, D.W. Nutrient-stimulated insulin secretion in mouse islets is critically dependent on intracellular pH. *BMC Endocr Disord* **4**, 1 (2004).
145. Cyranka, M., *et al.* NMDA Receptor Antagonists Increase the Release of GLP-1 From Gut Endocrine Cells. *Front Pharmacol* **13**, 861311 (2022).
146. Buckler, K.J. & Vaughan-Jones, R.D. Application of a new pH-sensitive fluoroprobe (carboxy-SNARF-1) for intracellular pH measurement in small, isolated cells. *Pflugers Arch* **417**, 234-239 (1990).
147. Michl, J., *et al.* Acid-adapted cancer cells alkalinize their cytoplasm by degrading the acid-loading membrane transporter anion exchanger 2, SLC4A2. *Cell Rep* **42**, 112601 (2023).
148. Ruffin, V.A., Salameh, A.I., Boron, W.F. & Parker, M.D. Intracellular pH regulation by acid-base transporters in mammalian neurons. *Front Physiol* **5**, 43 (2014).
149. Dechant, R., *et al.* Cytosolic pH is a second messenger for glucose and regulates the PKA pathway through V-ATPase. *EMBO J* **29**, 2515-2526 (2010).
150. Lindstrom, P. & Sehlin, J. Effect of glucose on the intracellular pH of pancreatic islet cells. *Biochem J* **218**, 887-892 (1984).
151. Verdich, C., *et al.* The role of postprandial releases of insulin and incretin hormones in meal-induced satiety--effect of obesity and weight reduction. *Int J Obes Relat Metab Disord* **25**, 1206-1214 (2001).
152. Madsbad, S. The role of glucagon-like peptide-1 impairment in obesity and potential therapeutic implications. *Diabetes Obes Metab* **16**, 9-21 (2014).
153. Wang, Z. & Thurmond, D.C. Mechanisms of biphasic insulin-granule exocytosis - roles of the cytoskeleton, small GTPases and SNARE proteins. *J Cell Sci* **122**, 893-903 (2009).
154. Simpson, A.K., *et al.* Cyclic AMP triggers glucagon-like peptide-1 secretion from the GLUTag enteroendocrine cell line. *Diabetologia* **50**, 2181-2189 (2007).
155. Pouyssegur, J., Franchi, A., L'Allemain, G. & Paris, S. Cytoplasmic pH, a key determinant of growth factor-induced DNA synthesis in quiescent fibroblasts. *FEBS Lett* **190**, 115-119 (1985).
156. Chiche, J., *et al.* Hypoxia-inducible carbonic anhydrase IX and XII promote tumor cell growth by counteracting acidosis through the regulation of the intracellular pH. *Cancer Res* **69**, 358-368 (2009).
157. Balgi, A.D., *et al.* Regulation of mTORC1 signaling by pH. *PLoS One* **6**, e21549 (2011).
158. Lei, G., *et al.* Stat3-mTOR signaling mediates the stimulation of GLP-1 production induced by IL-27. *J Mol Endocrinol* **63**, 215-226 (2019).

159. Barovsky, K., Pedone, C. & Brooker, G. Distinct mechanisms of forskolin-stimulated cyclic AMP accumulation and forskolin-potentiated hormone responses in C6-2B cells. *Mol Pharmacol* **25**, 256-260 (1984).
160. Zou, X., *et al.* The Phosphodiesterase Inhibitor IBMX Blocks the Potassium Channel THIK-1 from the Extracellular Side. *Mol Pharmacol* **98**, 143-155 (2020).
161. Elebring, E., Casselbrant, A., Persson, S.M.T., Fandriks, L. & Wallenius, V. betaHB inhibits glucose-induced GLP-1 secretion in GLUTag and human jejunal enteroids. *J Mol Endocrinol* **70**(2023).
162. Parihar, A., *et al.* Cryopreservation: A Comprehensive Overview, Challenges, and Future Perspectives. *Adv Biol (Weinh)* **7**, e2200285 (2023).
163. Huebinger, J. Modification of cellular membranes conveys cryoprotection to cells during rapid, non-equilibrium cryopreservation. *PLoS One* **13**, e0205520 (2018).
164. Gil-Lozano, M., Mingomataj, E.L., Wu, W.K., Ridout, S.A. & Brubaker, P.L. Circadian secretion of the intestinal hormone GLP-1 by the rodent L cell. *Diabetes* **63**, 3674-3685 (2014).
165. Kuhre, R.E., Deacon, C.F., Holst, J.J. & Petersen, N. What Is an L-Cell and How Do We Study the Secretory Mechanisms of the L-Cell? *Front Endocrinol (Lausanne)* **12**, 694284 (2021).
166. Kamakura, R., Raza, G.S., Prasannan, A., Walkowiak, J. & Herzig, K.H. Dipeptidyl peptidase-4 and GLP-1 interplay in STC-1 and GLUTag cell lines. *Peptides* **134**, 170419 (2020).
167. Yoshimoto, T., Fischl, M., Orlowski, R.C. & Walter, R. Post-proline cleaving enzyme and post-proline dipeptidyl aminopeptidase. Comparison of two peptidases with high specificity for proline residues. *J Biol Chem* **253**, 3708-3716 (1978).
168. Orskov, C., Wettergren, A. & Holst, J.J. Biological effects and metabolic rates of glucagonlike peptide-1 7-36 amide and glucagonlike peptide-1 7-37 in healthy subjects are indistinguishable. *Diabetes* **42**, 658-661 (1993).
169. Wettergren, A., Pridal, L., Wojdemann, M. & Holst, J.J. Amidated and non-amidated glucagon-like peptide-1 (GLP-1): non-pancreatic effects (cephalic phase acid secretion) and stability in plasma in humans. *Regul Pept* **77**, 83-87 (1998).
170. Kuhre, R.E., *et al.* GLP-1 amidation efficiency along the length of the intestine in mice, rats and pigs and in GLP-1 secreting cell lines. *Peptides* **55**, 52-57 (2014).
171. Lagadic-Gossmann, D., Huc, L. & Lecureur, V. Alterations of intracellular pH homeostasis in apoptosis: origins and roles. *Cell Death Differ* **11**, 953-961 (2004).
172. Sharma, V., Kaur, R., Bhatnagar, A. & Kaur, J. Low-pH-induced apoptosis: role of endoplasmic reticulum stress-induced calcium permeability and mitochondria-dependent signaling. *Cell Stress Chaperones* **20**, 431-440 (2015).
173. Saxton, R.A. & Sabatini, D.M. mTOR Signaling in Growth, Metabolism, and Disease. *Cell* **169**, 361-371 (2017).
174. Xu, G., *et al.* Intestinal mTOR regulates GLP-1 production in mouse L cells. *Diabetologia* **58**, 1887-1897 (2015).
175. Carnell, L. & Moore, H.P. Transport via the regulated secretory pathway in semi-intact PC12 cells: role of intra-cisternal calcium and pH in the transport and sorting of secretogranin II. *J Cell Biol* **127**, 693-705 (1994).

176. Schmidt, W.K. & Moore, H.P. Ionic milieu controls the compartment-specific activation of pro-opiomelanocortin processing in AtT-20 cells. *Mol Biol Cell* **6**, 1271-1285 (1995).
177. Girsch, J.H., Walters, K., Jackson, W. & Grose, C. Progeny Varicella-Zoster Virus Capsids Exit the Nucleus but Never Undergo Secondary Envelopment during Autophagic Flux Inhibition by Bafilomycin A1. *J Virol* **93**(2019).
178. Lang, S., *et al.* Glucagon receptor antagonist upregulates circulating GLP-1 level by promoting intestinal L-cell proliferation and GLP-1 production in type 2 diabetes. *BMJ Open Diabetes Res Care* **8**(2020).
179. Kappe, C., Zhang, Q., Holst, J.J., Nystrom, T. & Sjoholm, A. Evidence for paracrine/autocrine regulation of GLP-1-producing cells. *Am J Physiol Cell Physiol* **305**, C1041-1049 (2013).
180. Gembal, M., Gilon, P. & Henquin, J.C. Evidence that glucose can control insulin release independently from its action on ATP-sensitive K+ channels in mouse B cells. *J Clin Invest* **89**, 1288-1295 (1992).
181. Juntti-Berggren, L., Arkhammar, P., Nilsson, T., Rorsman, P. & Berggren, P.O. Glucose-induced increase in cytoplasmic pH in pancreatic beta-cells is mediated by Na+/H+ exchange, an effect not dependent on protein kinase C. *J Biol Chem* **266**, 23537-23541 (1991).
182. Postic, S., *et al.* pH-Dependence of Glucose-Dependent Activity of Beta Cell Networks in Acute Mouse Pancreatic Tissue Slice. *Front Endocrinol (Lausanne)* **13**, 916688 (2022).
183. Chen, Z., Truong, T.M. & Ai, H.W. Illuminating Brain Activities with Fluorescent Protein-Based Biosensors. *Chemosensors (Basel)* **5**(2017).
184. Oya, M., *et al.* The G protein-coupled receptor family C group 6 subtype A (GPRC6A) receptor is involved in amino acid-induced glucagon-like peptide-1 secretion from GLUTag cells. *J Biol Chem* **288**, 4513-4521 (2013).
185. Harada, K., Takashima, M., Kitaguchi, T. & Tsuboi, T. F-actin determines the time-dependent shift in docking dynamics of glucagon-like peptide-1 granules upon stimulation of secretion. *FEBS Lett* **597**, 657-671 (2023).
186. Jilani, T.N. & Siddiqui, A.H. Tissue Plasminogen Activator. in *StatPearls* (Treasure Island (FL), 2023).
187. Kristensen, P., *et al.* Immunocytochemical demonstration of tissue-type plasminogen activator in endocrine cells of the rat pituitary gland. *J Cell Biol* **101**, 305-311 (1985).
188. Kristensen, P., Nielsen, J.H., Larsson, L.I. & Dano, K. Tissue-type plasminogen activator in somatostatin cells of rat pancreas and hypothalamus. *Endocrinology* **121**, 2238-2244 (1987).
189. Kristensen, P., Hougaard, D.M., Nielsen, L.S. & Dano, K. Tissue-type plasminogen activator in rat adrenal medulla. *Histochemistry* **85**, 431-436 (1986).
190. Hebert, M., Lesept, F., Vivien, D. & Macrez, R. The story of an exceptional serine protease, tissue-type plasminogen activator (tPA). *Rev Neurol (Paris)* **172**, 186-197 (2016).
191. Parmer, R.J., *et al.* Tissue plasminogen activator (t-PA) is targeted to the regulated secretory pathway. Catecholamine storage vesicles as a reservoir for the rapid release of t-PA. *J Biol Chem* **272**, 1976-1982 (1997).

192. Parmer, R.J. & Miles, L.A. Targeting of tissue plasminogen activator to the regulated pathway of secretion. *Trends Cardiovasc Med* **8**, 306-312 (1998).
193. Lenoir, S., *et al.* Post-synaptic Release of the Neuronal Tissue-Type Plasminogen Activator (tPA). *Front Cell Neurosci* **13**, 164 (2019).
194. Gualandris, A., Jones, T.E., Strickland, S. & Tsirka, S.E. Membrane depolarization induces calcium-dependent secretion of tissue plasminogen activator. *J Neurosci* **16**, 2220-2225 (1996).
195. Gurskaya, N.G., *et al.* Engineering of a monomeric green-to-red photoactivatable fluorescent protein induced by blue light. *Nat Biotechnol* **24**, 461-465 (2006).
196. Chudakov, D.M., Lukyanov, S. & Lukyanov, K.A. Using photoactivatable fluorescent protein Dendra2 to track protein movement. *Biotechniques* **42**, 553, 555, 557 passim (2007).
197. Woods, E., Courtney, J., Scholz, D., Hall, W.W. & Gautier, V.W. Tracking protein dynamics with photoconvertible Dendra2 on spinning disk confocal systems. *J Microsc* **256**, 197-207 (2014).
198. Klak, M., *et al.* Irradiation with 365 nm and 405 nm wavelength shows differences in DNA damage of swine pancreatic islets. *PLoS One* **15**, e0235052 (2020).
199. Baranes, D., *et al.* Tissue plasminogen activator contributes to the late phase of LTP and to synaptic growth in the hippocampal mossy fiber pathway. *Neuron* **21**, 813-825 (1998).
200. Kuhre, R.E., *et al.* Peptide production and secretion in GLUTag, NCI-H716, and STC-1 cells: a comparison to native L-cells. *J Mol Endocrinol* **56**, 201-211 (2016).
201. Shipitsin, M., *et al.* Automated quantitative multiplex immunofluorescence in situ imaging identifies phospho-S6 and phospho-PRAS40 as predictive protein biomarkers for prostate cancer lethality. *Proteome Sci* **12**, 40 (2014).
202. Elliott, A.D. Confocal Microscopy: Principles and Modern Practices. *Curr Protoc Cytom* **92**, e68 (2020).
203. Fish, K.N. Total internal reflection fluorescence (TIRF) microscopy. *Curr Protoc Cytom* **Chapter 12**, Unit12 18 (2009).
204. Toki, M.I., Cecchi, F., Hembrough, T., Syrigos, K.N. & Rimm, D.L. Proof of the quantitative potential of immunofluorescence by mass spectrometry. *Lab Invest* **97**, 329-334 (2017).
205. Shihan, M.H., Novo, S.G., Le Marchand, S.J., Wang, Y. & Duncan, M.K. A simple method for quantitating confocal fluorescent images. *Biochem Biophys Rep* **25**, 100916 (2021).
206. Tsuzuki, A., *et al.* Direct visualization of glucagon-like peptide-1 secretion by fluorescent fusion proteins. *J Diabetes Investig* **13**, 1134-1139 (2022).
207. Masereel, B., Pochet, L. & Laeckmann, D. An overview of inhibitors of Na(+)/H(+) exchanger. *Eur J Med Chem* **38**, 547-554 (2003).
208. Habela, C.W., Olsen, M.L. & Sontheimer, H. ClC3 is a critical regulator of the cell cycle in normal and malignant glial cells. *J Neurosci* **28**, 9205-9217 (2008).
209. Wang, C., *et al.* Investigation of endosome and lysosome biology by ultra pH-sensitive nanoprobes. *Adv Drug Deliv Rev* **113**, 87-96 (2017).
210. Bencina, M. Illumination of the spatial order of intracellular pH by genetically encoded pH-sensitive sensors. *Sensors (Basel)* **13**, 16736-16758 (2013).

211. Johansson, M.E., Sjovall, H. & Hansson, G.C. The gastrointestinal mucus system in health and disease. *Nat Rev Gastroenterol Hepatol* **10**, 352-361 (2013).
212. McDougall, C.J., Wong, R., Scudera, P., Lesser, M. & DeCosse, J.J. Colonic mucosal pH in humans. *Dig Dis Sci* **38**, 542-545 (1993).
213. McNeil, N.I., Ling, K.L. & Wager, J. Mucosal surface pH of the large intestine of the rat and of normal and inflamed large intestine in man. *Gut* **28**, 707-713 (1987).
214. Deacon, C.F. What do we know about the secretion and degradation of incretin hormones? *Regul Pept* **128**, 117-124 (2005).

Appendix

tPA-Dendra2 sequence

Alignment of Sequence_1: [addgene tPA-linker-Dendra2] with Sequence_2: [plasmid]

```
Similarity : 2368/2530 (93.60 %)

                                                          M  K  G  E
Seq_1  1     ----------------------------------------------ATGAAGGGAGAG  12
             ##############################################|||||||||||
Seq_2  1     TTCGGGTCTCCCAGGTCCAACTGCACCTCGGTTCTATCGATTGCCACCATGAAGGGAGAG  60
             F  G  S  P  R  S  N  C  T  S  V  L  S  I  A  T  M  K  G  E


             L  L  C  V  L  L  L  C  G  V  A  F  T  L  P  D  Q  G  I  H
Seq_1  13    CTGTTGTGCGTCCTGCTGCTTTGTGGAGTGGCGTTCACGTTGCCTGACCAGGGAATACAC  72
             ||||||||||||||||||||||||||||||||||||||||||||||||||||||||||||
Seq_2  61    CTGTTGTGCGTCCTGCTGCTTTGTGGAGTGGCGTTCACGTTGCCTGACCAGGGAATACAC  120
             L  L  C  V  L  L  L  C  G  V  A  F  T  L  P  D  Q  G  I  H


             R  R  F  R  R  G  A  R  S  Y  R  A  T  C  R  D  E  Q  T  Q
Seq_1  73    AGGAGGTTCAGAAGAGGAGCTCGGTCCTACAGAGCGACCTGCAGAGATGAACAGACTCAG  132
             ||||||||||||||||||||||||||||||||||||||||||||||||||||||||||||
Seq_2  121   AGGAGGTTCAGAAGAGGAGCTCGGTCCTACAGAGCGACCTGCAGAGATGAACAGACTCAG  180
             R  R  F  R  R  G  A  R  S  Y  R  A  T  C  R  D  E  Q  T  Q


             T  T  Y  Q  Q  H  Q  S  W  L  R  P  M  L  R  G  N  R  V  E
Seq_1  133   ACAACTTACCAACAGCATCAGTCATGGCTACGTCCCATGCTCAGAGGCAATCGGGTGGAA  192
             ||||||||||||||||||||||||||||||||||||||||||||||||||||||||||||
Seq_2  181   ACAACTTACCAACAGCATCAGTCATGGCTACGTCCCATGCTCAGAGGCAATCGGGTGGAA  240
             T  T  Y  Q  Q  H  Q  S  W  L  R  P  M  L  R  G  N  R  V  E


             Y  C  R  C  N  S  G  L  A  Q  C  H  S  V  P  V  R  S  C  S
Seq_1  193   TACTGCCGGTGCAACAGCGGCCTGGCACAGTGCCACTCGGTGCCCGTCCGAAGTTGCAGT  252
             ||||||||||||||||||||||||||||||||||||||||||||||||||||||||||||
Seq_2  241   TACTGCCGGTGCAACAGCGGCCTGGCACAGTGCCACTCGGTGCCCGTCCGAAGTTGCAGT  300
             Y  C  R  C  N  S  G  L  A  Q  C  H  S  V  P  V  R  S  C  S
```

```
            E  P  R  C  F  N  G  G  T  C  Q  Q  A  L  Y  F  S  D  F  V
Seq_1  253   GAACCGAGATGCTTCAATGGGGGTACGTGTCAGCAGGCCCTGTATTTCTCTGACTTCGTC  312
              ||||||||||||||||||||||||||||||||||||||||||||||||||||||||||
Seq_2  301   GAACCGAGATGCTTCAATGGGGGTACGTGTCAGCAGGCCCTGTATTTCTCTGACTTCGTC  360
            E  P  R  C  F  N  G  G  T  C  Q  Q  A  L  Y  F  S  D  F  V

            C  Q  C  P  D  G  F  V  G  K  R  C  D  I  D  T  R  A  T  C
Seq_1  313   TGCCAGTGCCCTGACGGATTTGTTGGGAAACGCTGTGATATAGATACCAGAGCAACCTGC  372
              ||||||||||||||||||||||||||||||||||||||||||||||||||||||||||
Seq_2  361   TGCCAGTGCCCTGACGGATTTGTTGGGAAACGCTGTGATATAGATACCAGAGCAACCTGC  420
            C  Q  C  P  D  G  F  V  G  K  R  C  D  I  D  T  R  A  T  C

            F  E  G  Q  G  I  T  Y  R  G  T  W  S  T  A  E  N  G  A  E
Seq_1  373   TTCGAGGGCCAGGGCATCACCTACAGAGGCACATGGAGCACAGCAGAAAATGGGGCTGAA  432
              ||||||||||||||||||||||||||||||||||||||||||||||||||||||||||
Seq_2  421   TTCGAGGGCCAGGGCATCACCTACAGAGGCACATGGAGCACAGCAGAAAATGGGGCTGAA  480
            F  E  G  Q  G  I  T  Y  R  G  T  W  S  T  A  E  N  G  A  E

            C  I  N  W  N  S  S  A  L  S  Q  K  P  Y  S  A  R  R  P  N
Seq_1  433   TGCATCAACTGGAATAGCAGTGCCCTGTCCCAGAAGCCCTACAGTGCAAGGAGGCCAAAT  492
              ||||||||||||||||||||||||||||||||||||||||||||||||||||||||||
Seq_2  481   TGCATCAACTGGAATAGCAGTGCCCTGTCCCAGAAGCCCTACAGTGCAAGGAGGCCAAAT  540
            C  I  N  W  N  S  S  A  L  S  Q  K  P  Y  S  A  R  R  P  N

            A  I  K  L  G  L  G  N  H  N  Y  C  R  N  P  D  R  D  V  K
Seq_1  493   GCCATCAAGCTGGGCCTTGGGAACCACAATTACTGCAGAAACCCAGACCGAGACGTGAAG  552
              ||||||||||||||||||||||||||||||||||||||||||||||||||||||||||
Seq_2  541   GCCATCAAGCTGGGCCTTGGGAACCACAATTACTGCAGAAACCCAGACCGAGACGTGAAG  600
            A  I  K  L  G  L  G  N  H  N  Y  C  R  N  P  D  R  D  V  K

            P  W  C  Y  V  F  K  A  G  K  Y  T  T  E  F  C  S  T  P  A
Seq_1  553   CCCTGGTGCTATGTCTTTAAGGCAGGGAAGTATACCACGGAGTTCTGCAGCACGCCGGCT  612
              ||||||||||||||||||||||||||||||||||||||||||||||||||||||||||
Seq_2  601   CCCTGGTGCTATGTCTTTAAGGCAGGGAAGTATACCACGGAGTTCTGCAGCACGCCGGCT  660
            P  W  C  Y  V  F  K  A  G  K  Y  T  T  E  F  C  S  T  P  A

            C  P  K  G  P  T  E  D  C  Y  V  G  K  G  V  T  Y  R  G  T
Seq_1  613   TGCCCTAAGGGACCAACTGAGGACTGCTATGTTGGAAAAGGTGTGACTTACCGTGGCACC  672
              ||||||||||||||||||||||||||||||||||||||||||||||||||||||||||
Seq_2  661   TGCCCTAAGGGACCAACTGAGGACTGCTATGTTGGAAAAGGTGTGACTTACCGTGGCACC  720
            C  P  K  G  P  T  E  D  C  Y  V  G  K  G  V  T  Y  R  G  T
```

```
            H  S  F  T  T  S  K  A  S  C  L  P  W  N  S  M  I  L  I  G
Seq_1  673   CACAGCTTTACCACATCCAAGGCCTCCTGCCTCCCATGGAATTCCATGATCCTGATAGGC  732
              ||||||||||||||||||||||||||||||||||||||||||||||||||||||||||||
Seq_2  721   CACAGCTTTACCACATCCAAGGCCTCCTGCCTCCCATGGAATTCCATGATCCTGATAGGC  780
            H  S  F  T  T  S  K  A  S  C  L  P  W  N  S  M  I  L  I  G

            K  T  Y  T  A  W  R  A  N  S  Q  A  L  G  L  G  R  H  N  Y
Seq_1  733   AAGACTTACACAGCGTGGAGGGCCAACTCCCAGGCACTTGGCCTGGGCAGACACAATTAT  792
              ||||||||||||||||||||||||||||||||||||||||#||||||||||||||||||
Seq_2  781   AAGACTTACACAGCGTGGAGGGCCAACTCCCAGGCACTTGGTCTGGGCAGACACAATTAT  840
            K  T  Y  T  A  W  R  A  N  S  Q  A  L  G  L  G  R  H  N  Y

            C  R  N  P  D  G  D  A  K  P  W  C  H  V  M  K  D  R  K  L
Seq_1  793   TGCCGGAACCCAGATGGGGATGCCAAACCTTGGTGCCACGTGATGAAGGACCGAAAGCTG  852
              ||||||||||||||||||||||||#||||||||||||||||||||||#|||||||||
Seq_2  841   TGCCGGAACCCAGATGGGGATGCCAGACCTTGGTGCCACGTGATGAAGGATCGAAAGCTG  900
            C  R  N  P  D  G  D  A  R  P  W  C  H  V  M  K  D  R  K  L

            T  W  E  Y  C  D  M  S  P  C  S  T  C  G  L  R  Q  Y  K  Q
Seq_1  853   ACATGGGAATATTGCGACATGTCCCCATGCTCCACCTGCGGCCTGAGGCAATACAAACAG  912
              ||||||||||||||||||||||||||||||||||||||||||||||||||||||||||||
Seq_2  901   ACATGGGAATATTGCGACATGTCCCCATGCTCCACCTGCGGCCTGAGGCAATACAAACAG  960
            T  W  E  Y  C  D  M  S  P  C  S  T  C  G  L  R  Q  Y  K  Q

            P  Q  F  R  I  K  G  G  L  F  T  D  I  T  S  H  P  W  Q  A
Seq_1  913   CCTCAGTTTCGAATTAAAGGAGGACTCTTCACAGACATCACCTCACACCCTTGGCAGGCC  972
              ||||||||||||||||||||||||||||||||||||||||||||||||||||||||||||
Seq_2  961   CCTCAGTTTCGAATTAAAGGAGGACTCTTCACAGACATCACCTCACACCCTTGGCAGGCC  1020
            P  Q  F  R  I  K  G  G  L  F  T  D  I  T  S  H  P  W  Q  A

            A  I  F  V  K  N  K  R  S  P  G  E  R  F  L  C  G  G  V  L
Seq_1  973   GCCATCTTTGTCAAGAACAAGAGGTCTCCAGGAGAGAGATTCCTGTGTGGAGGGGTGCTG  1032
              ||||||||||||||||||||||||||||||||||||||||||||||||||||||||||||
Seq_2  1021  GCCATCTTTGTCAAGAACAAGAGGTCTCCAGGAGAGAGATTCCTGTGTGGAGGGGTGCTG  1080
            A  I  F  V  K  N  K  R  S  P  G  E  R  F  L  C  G  G  V  L

            I  S  S  C  W  V  L  S  A  A  H  C  F  V  E  R  F  P  P  H
Seq_1  1033  ATCAGTTCCTGCTGGGTGCTATCTGCCGCCCACTGCTTTGTAGAGAGGTTTCCACCCCAT  1092
              ||||||||||||||||||||||||||||||||||||||||||||||||||||||||||||
Seq_2  1081  ATCAGTTCCTGCTGGGTGCTATCTGCCGCCCACTGCTTTGTAGAGAGGTTTCCACCCCAT  1140
            I  S  S  C  W  V  L  S  A  A  H  C  F  V  E  R  F  P  P  H

            H  L  K  V  V  L  G  R  T  Y  R  V  V  P  G  K  E  E  Q  T
Seq_1  1093  CATCTTAAAGTGGTCTTGGGCAGAACATACAGAGTGGTCCCTGGAAAGGAGGAGCAGACA  1152
              ||||||||||||||||||||||||||||||||||||||||||||||||||||||||||||
Seq_2  1141  CATCTTAAAGTGGTCTTGGGCAGAACATACAGAGTGGTCCCTGGAAAGGAGGAGCAGACA  1200
            H  L  K  V  V  L  G  R  T  Y  R  V  V  P  G  K  E  E  Q  T
```

```
            F  E  I  E  K  Y  I  V  H  K  E  F  D  D  D  T  Y  D  N  D
Seq_1  1153 TTCGAGATCGAAAAGTACATAGTCCATAAGGAATTTGATGACGACACTTATGACAATGAC 1212
            ||||||||||||||||||||||||||||||||||||||||||||||||||||||||||||
Seq_2  1201 TTCGAGATCGAAAAGTACATAGTCCATAAGGAATTTGATGACGACACTTATGACAATGAC 1260
            F  E  I  E  K  Y  I  V  H  K  E  F  D  D  D  T  Y  D  N  D

            I  A  L  L  Q  L  R  S  D  S  S  Q  C  A  Q  E  S  S  S  V
Seq_1  1213 ATCGCATTACTGCAGCTGAGGTCAGATTCCAGTCAGTGTGCCCAGGAGAGCAGTTCTGTC 1272
            ||||||||||||||||||||||||||||||||||||||||||||||||||||||||||||
Seq_2  1261 ATCGCATTACTGCAGCTGAGGTCAGATTCCAGTCAGTGTGCCCAGGAGAGCAGTTCTGTC 1320
            I  A  L  L  Q  L  R  S  D  S  S  Q  C  A  Q  E  S  S  S  V

            G  T  A  C  L  P  D  P  D  V  Q  L  P  D  W  T  E  C  E  L
Seq_1  1273 GGCACTGCCTGCCTCCCTGACCCCGACGTACAGCTTCCTGACTGGACAGAGTGTGAGCTT 1332
            ||||||||||||||||||||||||||||||||||||||||||||||||||||||||||||
Seq_2  1321 GGCACTGCCTGCCTCCCTGACCCCGACGTACAGCTTCCTGACTGGACAGAGTGTGAGCTT 1380
            G  T  A  C  L  P  D  P  D  V  Q  L  P  D  W  T  E  C  E  L

            S  G  Y  G  K  H  E  A  S  S  P  F  F  S  D  R  L  K  E  A
Seq_1  1333 TCTGGCTACGGCAAGCATGAGGCATCCTCTCCTTTCTTCTCTGACCGGCTGAAGGAGGCT 1392
            ||||||||||||||||||||||||||||||||||||||||||||||||||||||||||||
Seq_2  1381 TCTGGCTACGGCAAGCATGAGGCATCCTCTCCTTTCTTCTCTGACCGGCTGAAGGAGGCT 1440
            S  G  Y  G  K  H  E  A  S  S  P  F  F  S  D  R  L  K  E  A

            H  V  R  L  Y  P  S  S  R  C  T  S  Q  H  L  F  N  K  T  I
Seq_1  1393 CACGTCAGACTGTATCCGTCCAGCCGCTGTACCTCACAGCATCTGTTTAACAAAACCATC 1452
            ||||||||||||||||||||||||||||||||||||||||||||||||||||||||||||
Seq_2  1441 CACGTCAGACTGTATCCGTCCAGCCGCTGTACCTCACAGCATCTGTTTAACAAAACCATC 1500
            H  V  R  L  Y  P  S  S  R  C  T  S  Q  H  L  F  N  K  T  I

            T  S  N  M  L  C  A  G  D  T  R  T  G  G  N  Q  D  V  H  D
Seq_1  1453 ACGAGCAACATGCTGTGTGCAGGAGACACCCGAACTGGGGGCAACCAAGACGTCCATGAC 1512
            ||||||||||||||||||||||||||||||||||||||||||||||||||||||||||||
Seq_2  1501 ACGAGCAACATGCTGTGTGCAGGAGACACCCGAACTGGGGGCAACCAAGACGTCCATGAC 1560
            T  S  N  M  L  C  A  G  D  T  R  T  G  G  N  Q  D  V  H  D

            A  C  Q  G  D  S  G  G  P  L  V  C  M  I  D  K  R  M  T  L
Seq_1  1513 GCGTGCCAGGGTGACTCAGGAGGCCCTCTGGTGTGCATGATCGATAAGCGGATGACTTTA 1572
            ||||||||||||||||||||||||||||||||||||||||||||||||||||||||||||
Seq_2  1561 GCGTGCCAGGGTGACTCAGGAGGCCCTCTGGTGTGCATGATCGATAAGCGGATGACTTTA 1620
            A  C  Q  G  D  S  G  G  P  L  V  C  M  I  D  K  R  M  T  L

            L  G  I  I  S  W  G  L  G  C  G  Q  K  D  V  P  G  I  Y  T
Seq_1  1573 CTGGGCATCATCAGCTGGGGCCTCGGCTGTGGGCAGAAGGACGTGCCAGGGATATACACA 1632
            ||||||||||||||||||||||||||||||||||||||||||||||||||||||||||||
Seq_2  1621 CTGGGCATCATCAGCTGGGGCCTCGGCTGTGGGCAGAAGGACGTGCCAGGGATATACACA 1680
            L  G  I  I  S  W  G  L  G  C  G  Q  K  D  V  P  G  I  Y  T
```

```
            K  V  T  N  Y  L  N  W  I  Q  D  N  M  K  Q  G  G  G  S  G
Seq_1  1633  AAGGTCACTAATTACCTGAACTGGATCCAAGACAACATGAAGCAAGGAGGAGGAAGTGGA  1692
              ||||||||||||||||||||||||||||||||||||||||||||||||||||||||||||
Seq_2  1681  AAGGTCACTAATTACCTGAACTGGATCCAAGACAACATGAAGCAAGGAGGAGGAAGTGGA  1740
            K  V  T  N  Y  L  N  W  I  Q  D  N  M  K  Q  G  G  G  S  G

            G  G  S  R  G  N  L  I  K  E  D  M  R  V  K  V  H  M  E  G
Seq_1  1693  GGAGGATCCCGGGGTAACCTGATCAAGGAGGACATGCGCGTGAAGGTGCACATGGAGGGC  1752
              ||||||||||||||||||||||||||||||||||||||||||||||||||||||||||||
Seq_2  1741  GGAGGATCCCGGGGTAACCTGATCAAGGAGGACATGCGCGTGAAGGTGCACATGGAGGGC  1800
            G  G  S  R  G  N  L  I  K  E  D  M  R  V  K  V  H  M  E  G

            N  V  N  G  H  A  F  V  I  E  G  E  G  K  G  K  P  Y  E  G
Seq_1  1753  AACGTGAACGGCCACGCCTTCGTGATCGAGGGCGAGGGCAAGGGCAAGCCCTACGAGGGC  1812
              ||||||||||||||||||||||||||||||||##||||||||||#|||||||||||||||
Seq_2  1801  AACGTGAACGGCCACGCCTTCGTGATCGAGGG--AGGGCAAGGGC-AGCCCTACGAGGGC  1857
            N  V  N  G  H  A  F  V  I  E  G    G  Q  G  Q    P  Y  E  G

            T  Q  T  A  N  L  T  V  K  E  G  A  P  L  P  F  S  Y  D  I
Seq_1  1813  ACCCAGACCGCCAACCTGACCGTGAAGGAGGGCGCCCCCCTGCCCTTCAGCTACGACATC  1872
              ||||||||||||||||||||||||||||||#||||#|||||||||||||||||||||||||
Seq_2  1858  ACCCAGACCGCCAACCTGACCGTGAAGGAAGGCGGCCCCCTGCCCTTCAGCTACGACATC  1917
            T  Q  T  A  N  L  T  V  K  E  G  G  P  L  P  F  S  Y  D  I

            L  T  T  A  V  H  Y  G  N  R  V  F  T  K  Y  P  E  D  I  P
Seq_1  1873  CTGACCACCGCCGTGCACTACGGCAACCGGGTGTTCACCAAGTACCCCGAGGACATCCCC  1932
              ||||||#|||||||||||||||#|||||||#|#|||||||||||||||||||||||||||
Seq_2  1918  CTGACC-CCGCCGTGCACTACGG-AACCGGGGG-TCACCAAGTACCCCGAGGACATCCCC  1974
            L  T   P  P  C  T  T  E   P  G  V   T  K  Y  P  E  D  I  P

            D  Y  F  K  Q  S  F  P  E  G  Y  S  W  E  R  T  M  T  F  E
Seq_1  1933  GACTACTTCAAGCAGAGCTTCCCCGAGGGCTACAGCTGGGAGCGCACCATGACCTTCGAG  1992
              ||||||||||||||||||||||||||||||||||||||||||||||||||||||||||||
Seq_2  1975  GACTACTTCAAGCAGAGCTTCCCCGAGGGCTACAGCTGGGAGCGCACCATGACCTTCGAG  2034
            D  Y  F  K  Q  S  F  P  E  G  Y  S  W  E  R  T  M  T  F  E

            D  K  G  I  C  T  I  R  S  D  I  S  L  E  G  D  C  F  F  Q
Seq_1  1993  GACAAGGGCATCTGCACCATCCGCAGCGACATCAGCCTGGAGGGCGACTGCTTCTTCCAG  2052
              ||||||||||||||||||||||||||||||||||||||||||||||||||||||||||||
Seq_2  2035  GACAAGGGCATCTGCACCATCCGCAGCGACATCAGCCTGGAGGGCGACTGCTTCTTCCAG  2094
            D  K  G  I  C  T  I  R  S  D  I  S  L  E  G  D  C  F  F  Q

            N  V  R  F  K  G  T  N  F  P  P  N  G  P  V  M  Q  K  K  T
Seq_1  2053  AACGTGCGCTTCAAGGGCACCAACTTCCCCCCCAACGGCCCCGTGATGCAGAAGAAGACC  2112
              ||||||||||||||||||||||||||||||||||||||||||||||||||||||||||||
Seq_2  2095  AACGTGCGCTTCAAGGGCACCAACTTCCCCCCCAACGGCCCCGTGATGCAGAAGAAGACC  2154
            N  V  R  F  K  G  T  N  F  P  P  N  G  P  V  M  Q  K  K  T
```

```
            L  K  W  E  P  S  T  E  K  L  H  V  R  D  G  L  L  V  G  N
Seq_1  2113  CTGAAGTGGGAGCCCAGCACCGAGAAGCTGCACGTGCGCGACGGCCTGCTGGTGGGCAAC  2172
              ||||||||||||||||||||||||||||||||||||||||||||||||||||||||||||
Seq_2  2155  CTGAAGTGGGAGCCCAGCACCGAGAAGCTGCACGTGCGCGACGGCCTGCTGGTGGGCAAC  2214
            L  K  W  E  P  S  T  E  K  L  H  V  R  D  G  L  L  V  G  N

            I  N  M  A  L  L  L  E  G  G  G  H  Y  L  C  D  F  K  T  T
Seq_1  2173  ATCAACATGGCCCTGCTGCTGGAGGGCGGCGGCCACTACCTGTGCGACTTCAAGACCACC  2232
              ||||||||||||||||||||||||||||||||||||||||||||||||||||||||||||
Seq_2  2215  ATCAACATGGCCCTGCTGCTGGAGGGCGGCGGCCACTACCTGTGCGACTTCAAGACCACC  2274
            I  N  M  A  L  L  L  E  G  G  G  H  Y  L  C  D  F  K  T  T

            Y  K  A  K  K  V  V  Q  L  P  D  A  H  F  V  D  H  R  I  E
Seq_1  2233  TACAAGGCCAAGAAGGTGGTGCAGCTGCCCGACGCCCACTTCGTGGACCACCGCATCGAG  2292
              ||||||||||||||||||||||||||||||||||||||||||||||||||||||||||||
Seq_2  2275  TACAAGGCCAAGAAGGTGGTGCAGCTGCCCGACGCCCACTTCGTGGACCACCGCATCGAG  2334
            Y  K  A  K  K  V  V  Q  L  P  D  A  H  F  V  D  H  R  I  E

            I  L  G  N  D  S  D  Y  N  K  V  K  L  Y  E  H  A  V  A  R
Seq_1  2293  ATCCTGGGCAACGACAGCGACTACAACAAGGTGAAGCTGTACGAGCACGCCGTGGCCCGC  2352
              ||||||||||||||||||||||||||||||||||||||||||||||||||||||||||||
Seq_2  2335  ATCCTGGGCAACGACAGCGACTACAACAAGGTGAAGCTGTACGAGCACGCCGTGGCCCGC  2394
            I  L  G  N  D  S  D  Y  N  K  V  K  L  Y  E  H  A  V  A  R

            Y  S  P  L  P  S  Q  V  W  X
Seq_1  2353  TACAGCCCCCTGCCCAGCCAGGTGTGGT--------------------------------  2380
              ||||||||||||||||||||||||||################################
Seq_2  2395  TACAGCCCCCTGCCCAGCCAGGTGTGGTTGATCTAGAGTCGACCTGCAGAAGCTTGGCCG  2454
            Y  S  P  L  P  S  Q  V  W  L  I  *  S  R  P  A  E  A  W  P


Seq_1  2381  ------------------------------------------------------------  2380
              ############################################################
Seq_2  2455  CCATGGCCCAACTTGTTTATTGCAGCTTATAATGGTTACAAATAAAGCAATAGCATCACA  2514
            P  W  P  N  L  F  I  A  A  Y  N  G  Y  K  *  S  N  S  I  T


                        X
Seq_1  2381  ----------------  2380
              ################
Seq_2  2515  AATTCACAAATAAAGC  2530
            N  S  Q  I  K  X
```

Supplementary Code 1:

```
clear
cond={'glu'};
pH=[6.3 7.4 7.6];

k=zeros(3,3);

for icond=1:length(cond),
   for ipH=1:length(pH),
      files=dir(strcat(cond{icond},num2str(pH(ipH)),'*.lsm'));
      for ifile=1:length(files),
         im=imread(files(ifile).name);
         imG=im(:,:,2);
         im_nuc=imbinarize(imgaussfilt(im(:,:,1),2));im_nuc=imfill(im_nuc,'holes');

         pdist=bwdist(im_nuc);
         for j=1:150,
           if length(find(pdist>j-1 & pdist<=j))>50
              rS(j)=nanmean(imG(find(pdist>j-1 & pdist<=j)));
           else
              rS(j)=NaN;
           end
         end
         thres=min(rS)+0.1*(max(rS)-min(rS));
```

```
im_cyt=imbinarize(imgaussfilt(im(:,:,2),2),thres*2^-16);im_cyt=imfill(im_cyt,'holes');
im_cell=im_cyt;
im_cell(find(im_nuc==1))=1;
%segmenting nuclei
D=-bwdist(~im_nuc);
Dmask = imextendedmin(D,2);
D2 = imimposemin(D,Dmask);
Ld2 = watershed(D2);
im_nuc2 = im_nuc;
im_nuc2 = bwareaopen(im_nuc2,100);
im_nuc2(Ld2 == 0) = 0;
pdist=bwdist(im_nuc2);
stats=regionprops(im_nuc2,"PixelIdxList","Area");
segmRGB(:,:,:)=uint16(zeros(1024,1024,3));
%ROIs
for iroi=1:length(stats)
  mask=0*im_nuc2;
  mask(stats(iroi).PixelIdxList)=1;
  if length(find(bwdist(mask)==pdist & im_cyt==1))<12000 &
length(find(bwdist(mask)==pdist & im_cyt==1))>500,
    k(icond,ipH)=k(icond,ipH)+1;
    nuc_area{icond,ipH}(k(icond,ipH))=stats(iroi).Area;
    %nuclear
    nuc_gfp{icond,ipH}(k(icond,ipH))=mean(double(imG(stats(iroi).PixelIdxList)));

    %cytoplasmic
    ix_cyt=find(bwdist(mask)==pdist & im_cyt.*(1-im_nuc)==1);
    cyt_gfp{icond,ipH}(k(icond,ipH))=mean(double(imG(ix_cyt)));

    %whole-cell
    ix_wc=find(bwdist(mask)==pdist & im_cyt==1);
```

```
            wc_gfp{icond,ipH}(k(icond,ipH))=mean(double(imG(ix_wc)));
            wc_area{icond,ipH}(k(icond,ipH))=length(ix_wc);

            roi_nuc=0*im_cyt;roi_nuc(stats(iroi).PixelIdxList)=1;
            roi_cyt=0*im_cyt;roi_cyt(ix_cyt)=1;
            roi_cell=0*im_cyt;roi_cell(ix_wc)=1;
            outline=boundarymask(roi_cell);

            %segmented RGB
            segmRGB(:,:,2)=segmRGB(:,:,2)+uint16(roi_nuc*nuc_gfp{icond,ipH}(k(icond,ipH)));
            segmRGB(:,:,2)=segmRGB(:,:,2)+uint16(roi_cyt*cyt_gfp{icond,ipH}(k(icond,ipH)));
            %segmRGB(:,:,3)=segmRGB(:,:,3)+double(outline);
          end
        end
        temp=segmRGB(:,:,3);
        temp(find(temp>0))=2^16;
        segmRGB(:,:,3)=temp;
        rgb(:,:,1,ifile)=uint16(segmRGB(:,:,1));
        rgb(:,:,2,ifile)=uint16(segmRGB(:,:,2));
        rgb(:,:,3,ifile)=uint16(segmRGB(:,:,3));
      end
      figure;
      montage(rgb,'Bordersize',2,'BackgroundColor','w');
      pause(1)

exportgraphics(gcf,strcat('montage_',cond{icond},'_pH_',num2str(pH(ipH)),'.tif'),'Resolution',300)
      close
      clear rgb
    end
end
```

```
col={'r' 'g' 'b'};
figure(1);movegui('center')
for icond=1:length(cond),
   for ipH=1:length(pH),
      subplot(3,1,1);hold on;swarmchart((4*(icond-
1)+ipH)*ones(1,k(icond,ipH)),cyt_gfp{icond,ipH},5,col{ipH});
      errorbar((4*(icond-
1)+ipH),nanmean(cyt_gfp{icond,ipH}),sqrt(nanvar(cyt_gfp{icond,ipH})),'o','color',col{ipH});
      title('Cytoplasmic GFP');xticks([2  6 10]);xticklabels(cond);ylabel('Fluorescence')
      set(gca,'linewidth',1,'Fontsize',18,'Fontname','Arial');
      subplot(3,1,2);hold on;swarmchart((4*(icond-
1)+ipH)*ones(1,k(icond,ipH)),nuc_gfp{icond,ipH},5,col{ipH});
      errorbar((4*(icond-
1)+ipH),nanmean(nuc_gfp{icond,ipH}),sqrt(nanvar(nuc_gfp{icond,ipH})),'o','color',col{ipH});
      title('Nuclear GFP');xticks([2  6 10]);xticklabels(cond);ylabel('Fluorescence')
      set(gca,'linewidth',1,'Fontsize',18,'Fontname','Arial');
      subplot(3,1,3);hold on;swarmchart((4*(icond-
1)+ipH)*ones(1,k(icond,ipH)),wc_area{icond,ipH},5,col{ipH});
      errorbar((4*(icond-
1)+ipH),nanmean(wc_area{icond,ipH}),sqrt(nanvar(wc_area{icond,ipH})),'o','color',col{ipH});
      title('Cell area');xticks([2  6 10]);xticklabels(cond);ylabel('Area')
      set(gca,'linewidth',1,'Fontsize',18,'Fontname','Arial');
   end
end
set(gcf, 'Position', get(0, 'Screensize'));
exportgraphics(gcf,'summary.tif','Resolution',300)
```